THE ROLE OF NITRIC OXIDE AND ITS REDOX VARIANTS IN THE REGULATION OF VASCULAR SMOOTH MUSCLE TONE

Thesis submitted for the degree of

Doctor of Philosophy

in the

University of Oxford

Alice M H Pinkney

New College

Supervisors:

Professor Christopher J Garland

Professor Kim A Dora

Michaelmas Term 2017

Abstract

The role of nitric oxide and its redox variants in the regulation of vascular smooth muscle tone

Alice M H Pinkney New College, University of Oxford

Doctor of Philosophy Michaelmas Term 2017

The role of nitric oxide (NO) and its redox variant nitroxyl (HNO) in the regulation of vascular smooth muscle tone was investigated in isolated rat mesenteric arteries, using a combination of wire myography, electrophysiology and immunohistochemistry.

The suitability of the HNO donor isopropylamine NONOate (IPA/NO) as an alternative to Angeli's (AS) salt in organ bath studies was examined. Previous studies of IPA/NO have been primarily *in vivo* in nature. IPA/NO had a similar profile to AS for both vasorelaxation and hyperpolarization of rat mesenteric arteries and was therefore a suitable alternative to AS. In addition, the presence of a sGC/cGMP-independent pathway, through which HNO exerted a significant vasorelaxatory action, was confirmed together with the importance of K^+ channels as the main component of this secondary pathway. Repeated applications of either AS or IPA/NO did not effect relaxation produced by these donors, but the hyperpolarization was significantly reduced.

Following the characterization of IPA/NO, the potential role of the HNO-TRPA1-CGRP pathway was investigated in isolated rat mesenteric arteries. The presence of TRPA1 was confirmed in perivascular nerves' using immunohistochemistry and a role in hyperpolarization of vascular smooth muscle cells was demonstrated. However, neither the TRPA1 antagonist

HC030031 (50 μM), nor depletion of CGRP affected vasorelaxation, suggesting the HNO-TRPA1-CGRP pathway may not be physiologically important.

Finally, the role of HNO and NO in the regulation of vasomotion was examined. Addition of the NO synthase inhibitor L-NAME (100 μM) unveiled rapid, depolarizing spikes in the membrane potential of vascular smooth muscle cells. However, the complexity of membrane potential recordings in constricted arteries prevented a conclusive determination of which redox variant of NO is responsible for supressing these spikes. Tension studies suggest that the dominant redox variant involved in regulation of vasomotion is NO, but this remains to be confirmed.

Together these data confirm a role for NO and HNO as important regulators of vascular tone and as such they both provide potential as therapeutic agents in the treatment of cardiovascular disorders such as hypertension.

Acknowledgements

At the outset of my DPhil, the path to the submission of this thesis was described to me as a rollercoaster. This has certainly been the case with many uphill struggles, but many moments of joy when new discoveries were made.

It is for certain that I would not have made it this far without the unwavering support of my supervisors Professor Christopher Garland and Professor Kim Dora. Without their well-timed nudges and reassurances, I would probably still be writing!

I also wish to thank the members of my lab, both past and present, for their friendship and guidance. In particular I would like to thank Hamish Lemmey who's (eternal) upbeat demeanour made even the hardest day's fun, as well as, Chloe Powell and Harrison Davis who, despite moving on after completing their DPhils, remain life-long friends.

Finally, I would like to thank my family and in-laws for their continued support in all my endeavours. Credit must be given to my father for finishing every phone call in the final months with 'finish your thesis' and my mother who reminded me it was OK to take a break. The greatest thanks should, however, go to my fiancé, Matthew Holden, without his unrelenting support I never would have made it this far.

Publications from the work in this thesis

Pinkney AMH, Lemmey HAL, Dora KA, Garland CJ (2017). Vasorelaxation to the nitroxyl donor Isopropylamine NONOate in resistance arteries does not require perivascular calcitonin gene-related peptide. Hypertension, 70:587-593

The above paper is formed from aspects of chapters 3 and 4.

Table of contents

Abstract II

Acknowledgements IV

Publications from the work in this thesis V

Table of contents 1

Table of figures 4

Abbreviations 5

Chapter 1

Introduction 8

1.1 The cardiovascular system 9

1.2 Structure of resistance arteries and arterioles 9

1.3 The influence of perivascular nerves on vascular tone 11

1.4 Endothelial control of vascular function 12

1.4.I Endothelium-derived relaxing factor(s) 13

1.4.II Endothelium-derived hyperpolarization 14

1.5 Redox Variants of NO and their role in the vasculature 16

1.5.I $NO^{\bullet}$ 17

1.5.II NO^{-} 21

1.5.III NO^{+} 25

1.6 General Aim 25

Chapter 2

Methods & Materials 26

2.1 Tissue isolation 27

2.2 Wire myography 29

2.2.I Mounting arteries for wire myography 29

2.2.II Analysis of wire myography data 30

2.3 Sharp microelectrode intracellular recording 33

2.3.I Preparation of arteries 33

2.3.II Preparation of microelectrodes 33

2.3.III Determination of successful intracellular recordings 34

2.4 Immunohistochemistry 36

2.4.I Preparation of pressurized arteries 36

2.4.II Preparation of pinned arteries 36

2.4.III Immunohistochemistry protocol 37

2.4.III.i Luminal application 38

2.4.III.ii Imaging 38

2.5 Solutions and drugs 38

2.6 Statistical analysis and curve fitting 41

Chapter 3

A comparative characterisation of the HNO donor Isopropylamine NONOate 42

3.1 Introduction 43
3.1.I Donors of HNO 44
3.1.II Limitations of Angeli's salt as a donor of HNO 45
3.1.III Isopropylamine NONOate 46
3.1.III Aims 47
3.2 Methods & Materials 48
3.2.I Wire myography 48
3.2.II Sharp microelectrode studies of membrane potential 48
3.2.III Isopropylamine NONOate 49
3.3 Results 50
3.4 Discussion and future work 61
3.5 Conclusion 65

Chapter 4

Neurovascular Involvement in the response to HNO 66

4.1 Introduction 67
4.1.I Transient receptor potential A1 (TRPA1) channels 67
4.1.II TRPA1 channel expression 70
4.1.III Aims 70
4.2 Materials & Methods 71
4.2.I Wire myography 71
4.2.II Sharp microelectrode studies of membrane potential 71
4.2.III Immunohistochemistry 72
4.3 Results 73
4.4 Discussion and future work 83
4.5 Conclusion 86

Chapter 5

An examination into the role of NO and HNO in vasomotion 87

5.1 Introduction 88
5.1.I Mechanisms of vasomotion 89
5.1.II Alteration of vasomotion in disease 92
5.1.III Aims 93
5.2 Methods & Materials 94
5.2.I Wire myography 94
5.2.II Sharp microelectrode studies of membrane potential 94
5.3 Results 95
5.4 Discussion and future work 102
5.5 Conclusion 106

Chapter 6

Summary and future directions.....107

References 113

Table of figures

Figure 1.2.1: Structure of a resistance artery. 10
Figure 1.5.1: The generation and vascular signaling pathways of nitric oxide (NO). 19
Figure 1.5.2: Proposed pathways of nitroxyl (HNO) induced relaxation of vascular smooth muscle cells. 23
Figure 2.1.1: Dissection of rat mesenteric arteries 28
Figure 2.2.1: Wire myograph setup 32
Figure 2.3.1: Setup for sharp microelectrode intracellular recording 35
Table 2.4.1: Details of antibodies used in thesis 38
Table 2.5.1: Details of drugs and chemicals used in this thesis 41
Figure 3.3.1: Concentration-responses to HNO donors in unstimulated mesenteric arteries. 51
Figure 3.3.2: Concentration-responses to HNO donors in mesenteric arteries pre-constricted with phenylephrine. 52
Figure 3.3.3: The effect of HNO and NO scavengers on the hyperpolarization and relaxation of rat mesenteric arteries in response to cumulative addition of HNO donors 54
Figure 3.3.4: Examination of the role of sGC and K^+ channels in the response to HNO 56
Figure 3.3.5: The effect of high concentrations of IPA/NO 58
Figure 3.3.6: The effect of repeated exposure to HNO donors on relaxation and hyperpolarization in rat mesenteric arteries 60
Figure 4.1.1: Structure of a single TPRA1 subunit. 69
Figure 4.3.1: TRPA1 labelling in rat mesenteric arteries 74
Figure 4.3.2: The presence of TRPA1 and neurofilament light chain in adventitia. 75
Figure 4.3.3: Identifying TRPA1 in the endothelium of mesenteric arteries. 76
Figure 4.3.4: Examination into the effect of AITC in mesenteric arteries. 78
Figure 4.3.5: The role of TRPA1 in the response to HNO donors 80
Figure 4.3.6: The effect of CGRP on mesenteric arteries. 82
Figure 5.3.1: Simultaneous recording of membrane potential (Em) and tension 96
Figure 5.3.2: Generation of spikes at increasing concentrations of PE 97
Figure 5.3.3: The effect of HNO and NO on the response to phenylephrine in rat mesenteric arteries. 100
Figure 5.3.4: The effect of increasing constriction and concentration of PE on amplitude of vasomotion 101
Figure 6.1: Summary schematic detailing the signaling pathways confirmed in this study. 112

Abbreviations

AC	adenylyl cyclase
ACh	acetylcholine
AITC	allyl isothiocyanate
Akt	protein kinase B
AS	Angeli's salt
ATP	adenosine 5'-triphosphate
BH_4	(6R)-5,6,7,8-tetrahydrobiopterin
BK_{Ca}	large conductance calcium-activated potassium channel
CaM	calmodulin
cAMP	cyclic adenosine monophosphate
cGMP	cyclic guanosine monophosphate
CGRP	calcitinin gene-related peptide
COX	cyclooxygenase
Cx	connexin
DRG	dorsal root ganglion
EC	endothelial cell
EDH	endothelium-derived hyperpolarization
EDHF	endothelium-derived hyperpolarizing factor
EDRF	endothelium-derived relaxing factor
Em	membrane potential
eNOS	endothelial nitric oxide synthase
ER	endoplasmic reticulum
GPCR	G-protein coupled receptor

GTP	guanosine triphosphate
H_2S	hydrogen sulphide
HNO	nitroxyl
HXC	hydroxocobalamin
IEL	internal elastic lamina
IK_{Ca}	intermediate conductance calcium-activated potassium channel
iNOS	inducible nitirc oxide synthase
IP_3	inositol triphosphate
IP_3R	inositol triphosphate receptor
IPA/NO	isopropylamine NONOate
K_{ATP}	ATP-sensitive potassium channels
K_{Ca}	calcium-activated potassium channel
K_{ir}	inwardly rectifying potassium channel
K_v	voltage gated potassium channels
MEJ	myoendothelial junction
NA	noradrenaline
nNOS	neuronal nitric oxide synthase
NO	nitric oxide
NO^-	nitroxide ion
NO^+	nitrosonium ion
NOS	nitric oxide synthase
PE	phenylephrine
PKA	protein kinase A
PKG	protein kinase G

PLC	phospholipase C
sGC	soluble guanylyl cyclase
SK_{Ca}	small conductance calcium-activated potassium channel
SMC	smooth muscle cell
SNP	sodium nitroprusside
SOD	superoxide dismutase
SR	sarcoplasmic reticulum
TRP	transient receptor potential
TRPA1	transient receptor potential ankyrin 1 channel

Chapter 1

Introduction

1.1 The cardiovascular system

The cardiovascular system is a complex network consisting of the heart and blood vessels, allowing for the delivery of essential nutrients and oxygen and the removal of waste products from our bodies' tissues. The focus of this thesis is that of the small resistance arteries of the mesenteric vasculature and for this reason the small resistance arteries and arterioles are described below.

1.2 Structure of resistance arteries and arterioles

Resistance arteries consist of three layers called: the tunica intima, tunica media and tunica adventitia (**Figure 1.2.1**; reviewed by Tennant and McGeachie (1990)). The tunica intima comprises of a monolayer of endothelial cells (EC) arranged such that a single EC spans several smooth muscle cells (SMC), of the tunica media, which wrap around the tube-like structure formed by the endothelium (Haas & Duling, 1997). The intima and media are separated by a sheet of elastin called the internal elastic lamina (IEL), which has multiple fenestrations allowing for the transfer of signals between adjoining ECs and SMCs, where myoendothelial junctions (MEJ) occur (reviewed by Heberlein et al. (2009)). Surrounding the SMCs, the tunica adventitia is comprised of many different cell types including fibroblasts, connective tissue and perivascular nerves. The adventitial layer has been implicated in a variety of mechanisms of vascular function including neural regulation of vascular tone (reviewed by Gutterman (1999)).

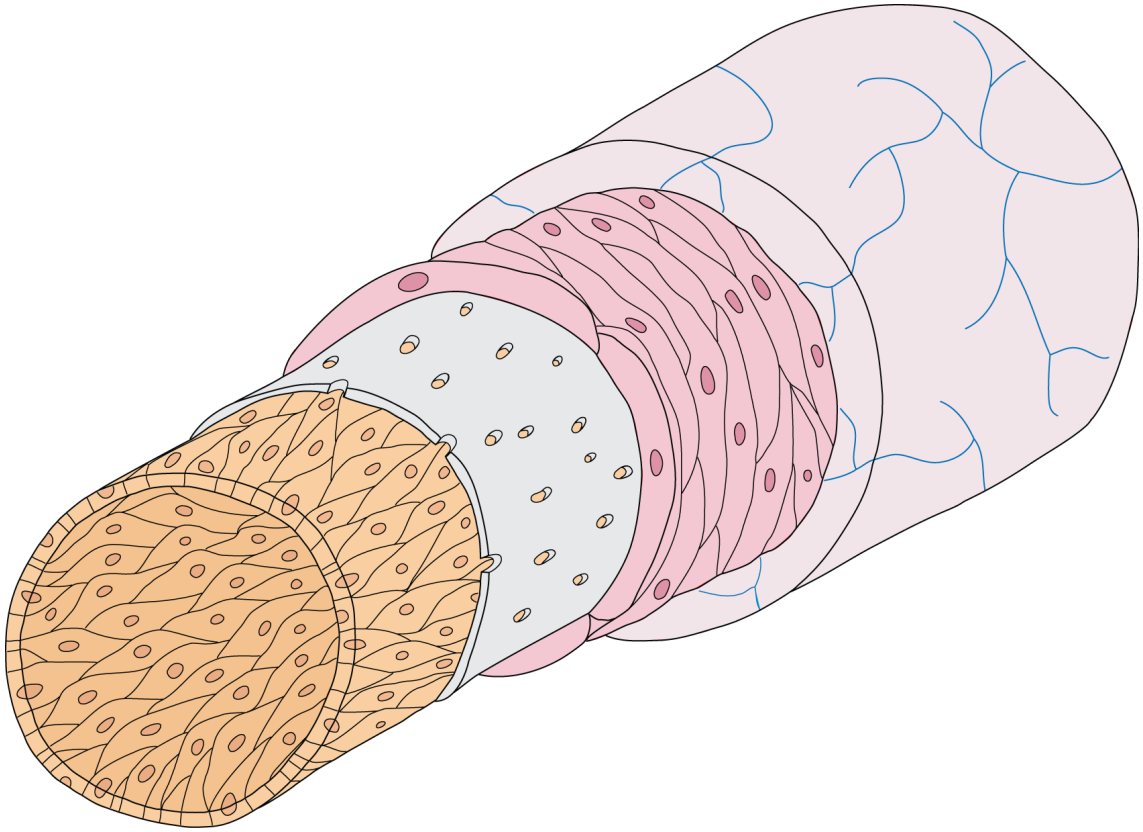


Figure 1.2.1: Structure of a resistance artery.

A stylised schematic depicting the arrangement of cells in an intact artery. The intima, innermost layer, consists of endothelial cells arranged longitudinally through the vessel. The second layer is the internal elastic lamina, which allows direct contact between endothelial and smooth muscle cells. The media (third layer) consists of smooth muscle cells, which are wrapped around the vessel. Finally, the adventitia (outermost layer) consists primarily of elastin and collagen, in addition to the perivascular nerves which innervate the vessel.

1.3 The influence of perivascular nerves on vascular tone

Sympathetic, parasympathetic and sensory-motor nerves have all been identified within the adventitia of blood vessels and have been shown to release a variety of vasoactive substances (Hill et al., 2001).

Sympathetic nerves are known to release neurotransmitters that produce vasoconstriction: noradrenaline (NA), which binds to and activates α_1- and α_2-adrenoreceptors on arterial SMC (Guimaraes & Moura, 2001); adenosine 5'-triphosphate (ATP), which binds to P2 receptors (mainly $P2X_1$ receptors) on SMC (reviewed by Burnstock (2009)) and neuropeptide Y, which activates Y_1 receptors inducing direct vasoconstriction, but also potentiating the response to NA and ATP (Edvinsson et al., 1984; Racchi et al., 1999).

Parasympathetic nerves are able to release acetylcholine (ACh), vasoactive intestinal peptide, ATP and nitric oxide (NO), however parasympathetic innervation of resistance arteries is limited so shall not be discussed further (Storkebaum & Carmeliet, 2011).

The sensory nerves, when activated by a variety of physical or chemical stimuli, are known to release a number of neurotransmitters that elicit vasodilation, including calcitonin gene-related peptide (CGRP), substance P, ATP (reviewed by Rubino and Burnstock (1996)) and NO (Zheng et al., 1997). Unlike NA and ACh, there is no reuptake mechanism for CGRP and substance P meaning that repeated or prolonged exposure to a stimulant of sensory nerves can deplete

supply of these neurotransmitters and thus ‘desensitise’ the nerve (Storkebaum & Carmeliet, 2011).

1.4 Endothelial control of vascular function

The vascular endothelium was initially thought to be an inert barrier, but a variety of evidence generated over the last three decades suggests otherwise. The endothelial barrier is formed by tight junctions and adherens junctions between ECs, which act to reduce the permeability of the endothelial layer, creating a semi-permeable structure. The permeability of the endothelial layer is dependent on the number and therefore ‘tightness’ of the cell-cell connections. As the tightness of the barrier increases, the size of the molecules able to pass through the endothelial layer reduces (reviewed by Komarova and Malik (2010)).

Additionally, the presence of homocellular gap junctions allows the passage of small water-soluble molecules between neighbouring ECs. The gap junctions present in the endothelium consist of at least three different proteins: connexion (Cx)37, Cx40 and Cx43 (Yeh et al., 1998). Homocellular gap junctions, formed of Cx40, Cx45 and low levels of Cx43 (Kruger et al., 2000; Little et al., 1995), also exist between SMCs, whilst heterocellular gap junctions can occur between ECs and SMCs at the MEJ. An in vitro study by Isakson and Duling (2005) suggests that the gap junctions at the MEJ are formed by combinations of Cx40 and Cx43, with Cx40 the predominant protein on the endothelial side. This coupling between ECs and SMCs allows for not only the movement of small molecules between the different cells, but also for the spread of current allowing

changes in membrane potential (Em) to pass between neighbouring cells, thus allowing for a coordinated, synchronised response to spread throughout the artery in response to a stimulus (reviewed by Dora (2001)).

The assumption that the endothelial layer was simply an inert barrier was altered by the publication of work carried out by Furchgott and Zawadzki (1980), who demonstrated that the presence of an intact endothelium was essential for ACh induced vasorelaxation. They termed the unidentified factor endothelium-derived relaxing factor (EDRF), which is explored further in **section 1.4.I**. A second distinct, endothelium-derived pathway for vasorelaxation has also been described in the literature as endothelium-derived hyperpolarization (EDH)(Garland et al., 2011) and is examined in **section 1.4.II**. In addition to the vasorelaxant pathways described, the endothelium has also been shown to secrete a variety of other factors including vasoconstrictors, inflammatory mediators and antithrombotic factors (reviewed by Galley and Webster (2004)).

1.4.I Endothelium-derived relaxing factor(s)

As stated above, Furchgott and Zawadzki first described EDRF in 1980. Subsequent work by Ignarro *et al.* (1987a; 1987b) determined EDRF to possess identical chemical and biological properties to NO and therefore declared that EDRF was NO. For their work examining '*nitric oxide as a signalling molecule in the cardiovascular system'* Furchgott, Ignarro and Murad were awarded the Nobel Prize in Physiology and Medicine in 1998; testament to the milestone that the discovery of NO represented.

NO is generated through the conversion of L-arginine and molecular oxygen by the enzyme NO synthase (NOS); a co-product L-citrulline is also formed. There are three known isoforms of NOS: isoform 1, neuronal-NOS (nNOS), was first identified in the brain (Bredt & Snyder, 1990); isoform 2, inducible-NOS (iNOS), is not constitutively expressed, but can be induced by the addition of bacterial lipopolysaccharide and cytokines (Stuehr et al., 1991); isoform 3, endothelial-NOS (eNOS), is expressed in ECs (reviewed by Forstermann et al. (1994)).

In addition to NO, the endothelium also produces prostacyclin, which was discovered to relax blood vessels (Moncada et al., 1976; Moncada et al., 1977) prior to the identification of EDRF by Furchgott. Prostacyclin is produced by the initial conversion of arachidonic acid to prostaglandin H_2 by cyclooxygenase (COX), and a subsequent conversion of prostaglandin H_2 by prostacyclin synthase to prostacyclin (reviewed by Luo et al. (2016)).

1.4.II Endothelium-derived hyperpolarization

The term endothelium-derived hyperpolarizing factor (EDHF) was first coined by Arthur Weston and others (reviewed by Taylor and Weston (1988)) and was the result of a number of studies which suggested the existence of an additional endothelium-derived relaxing factor, besides EDRF, with hyperpolarizing properties.

Bolton et al. (1984), building on observations that ACh could contract rabbit mesenteric arteries, whilst also producing hyperpolarization of vascular SMCs (Kuriyama & Suzuki, 1978), was the first to suggest that the hyperpolarization

produced in response to muscarinic stimulation may originate in the endothelium. This work was further built on by Chen et al. (1988) who demonstrated that EDH occurred in response to ACh and was unaffected by the addition of indomethacin (an inhibitor of prostacyclin receptor-mediated responses), methylene blue or haemoglobin (both NO scavengers), thus differentiating the observed response and EDRF. The authors of the study also showed that $^{86}Rb^{+}$ efflux (a marker of K^{+}) was increased by the addition of ACh. Like the observed hyperpolarization, this effect was resistant to the actions of indomethacin, methylene blue and haemoglobin.

The identification of K^{+} as an ion of interest in EDH lead to the study of various potassium channels in the EDHF pathway and development of the 'classical' EDHF pathway (reviewed by Edwards et al. (2010)). Studies by Waldron & Garland (1994) and Zygmunt & Hogestatt (1996) demonstrated the importance of calcium-activated potassium channels (K_{Ca}) in the EDH response. Both studies showed that the combined addition of apamin (a blocker of small conductance (S)K_{Ca} channels) and charybdotoxin (a blocker of intermediate conductance (I)K_{Ca} channels and large conductance (B)K_{Ca} channels) could abolish hyperpolarization to ACh. Zygmunt and Hogestatt (1996) also showed that iberiotoxin (a blocker of BK_{Ca}), both alone and in combination with apamin was unable to prevent ACh induced hyperpolarization, thus demonstrating that BK_{Ca} is not involved in EDH. Further examination of SK_{Ca} and IK_{Ca} by Edwards et al. (1998) showed that both channels were located on the endothelium and activated by ACh. The activation of SK_{Ca} and IK_{Ca} lead to an increase in K^{+} in the myoendothelial space which promoted the activation of Na^{+}/K^{+}-ATPases and inwardly rectifying K^{+} channels (K_{IR}) located on SMCs, thus generating

hyperpolarization in the SMC concomitant with the expected EDHF response. K^+ was therefore identified as a possible EDHF. Additional studies in rat and other species have demonstrated the importance of K^+ in EDH (Beny & Schaad, 2000; Dora & Garland, 2001; Edwards et al., 2001; Nelli et al., 2003). More recent evidence has suggested that myoendothelial gap junctions may allow the direct passage of hyperpolarization between EC and SMC (Dora et al., 2003).

In addition to the classical EDH pathway, a non-classical EDHF pathway has been described. The non-classical pathway relies on an increase in endothelial intracellular calcium, generated by local hormones or through shear stress, leading to the generation of EDH in adjacent SMCs (Edwards et al., 2010). Various molecules from the endothelium have been identified as potential EDHFs, including the EDRF NO and its reduced and protonated sibling nitroxyl (HNO), which will be discussed further in **section 1.5**. Other suggested EDHF candidates include prostacyclin (reviewed by Parkington et al. (2004)) and epoxyeicosatrienoic acids (reviewed by Campbell and Fleming (2010)). A more comprehensive list of potential EDHFs has been compiled by Edwards et al. (2010).

1.5 Redox Variants of NO and their role in the vasculature

As mentioned in **section 1.4.2**, NO can exist in different redox states, the most well studied form of which is $NO^{\bullet}$, referred to interchangeably with NO in the literature. Throughout this text $NO^{\bullet}$ will be referred to as NO. The loss of an electron results in the formation of nitrosonium ions (NO^+) and the gain of an

electron produces nitroxide ions (NO^-) (Stamler et al., 1992). The roles in the vasculature of these ions are discussed below.

1.5.I $NO^\bullet$

As discussed in **section 1.4.I** NO is generated through the conversion of L-arginine to L-citrulline by NOS, of which the most important isoform in the vasculature is eNOS (Li & Forstermann, 2000). In order to convert L-arginine NOS requires a number of co-factors including (6R)-5,6,7,8-tetrahydrobiopterin (BH_4), the absence of which affects the production of NO (Wever et al., 1997).

A multitude of endogenously produced substances can activate eNOS through various pathways. For a detailed review refer to Dudzinski et al. (2006). One of the major pathways of NOS activation is though the increase of intracellular calcium via the activation of G-protein coupled receptors (GPCR), which activate phospholipase-C (PLC). The increase in intracellular calcium causes calmodulin to bind to NOS, thus initiating the generation of NO (Bredt & Snyder, 1990; Forstermann et al., 1990). Phosphorylation of two different serine residues (1177 and 635) on eNOS, by protein kinase A (PKA), protein kinase B (Akt), or shear stress (in a PKA-dependent manner), can also lead to eNOS activation and generation of NO (reviewed by Zhao et al. (2015)).

Vasorelaxation in response to NO is primarily mediated through the activation of the soluble guanylyl clyclase (sGC)-cyclic guanosine monophosphate (cGMP) pathway (reviewed by Friebe and Koesling (2003)) in SMCs. The sGC-cGMP signalling pathway is initiated when sGC is activated by the presence of NO. Activated sGC then converts guanosine triphosphate (GTP) to cGMP, a type of intracellular messenger, which has the ability to activate a variety of

downstream pathways, ultimately producing relaxation of SMCs and vasodilation (reviewed by Murad (1986)). Additionally, there is evidence that NO can also activate a variety of potassium channels both directly and indirectly, which results in hyperpolarization and/or vasodilation (Bolotina et al., 1994; Lin et al., 2004; Mistry & Garland, 1998; Murphy & Brayden, 1995; Sampson et al., 2001). The generation and signalling mechanisms of NO are detailed in **Figure 1.5.1**.

The actions of NO are not limited to the activation of sGC and potassium channels, a multitude of biological processes such as apoptosis, ion channel activity and various pathological conditions can be modulated through S-nitrosylation (Qian & Fulton, 2013). S-nitrosylation refers to the ability of NO to modify protein cysteine residues to generate S-nitrothiols (reviewed by Lima et al. (2010)).

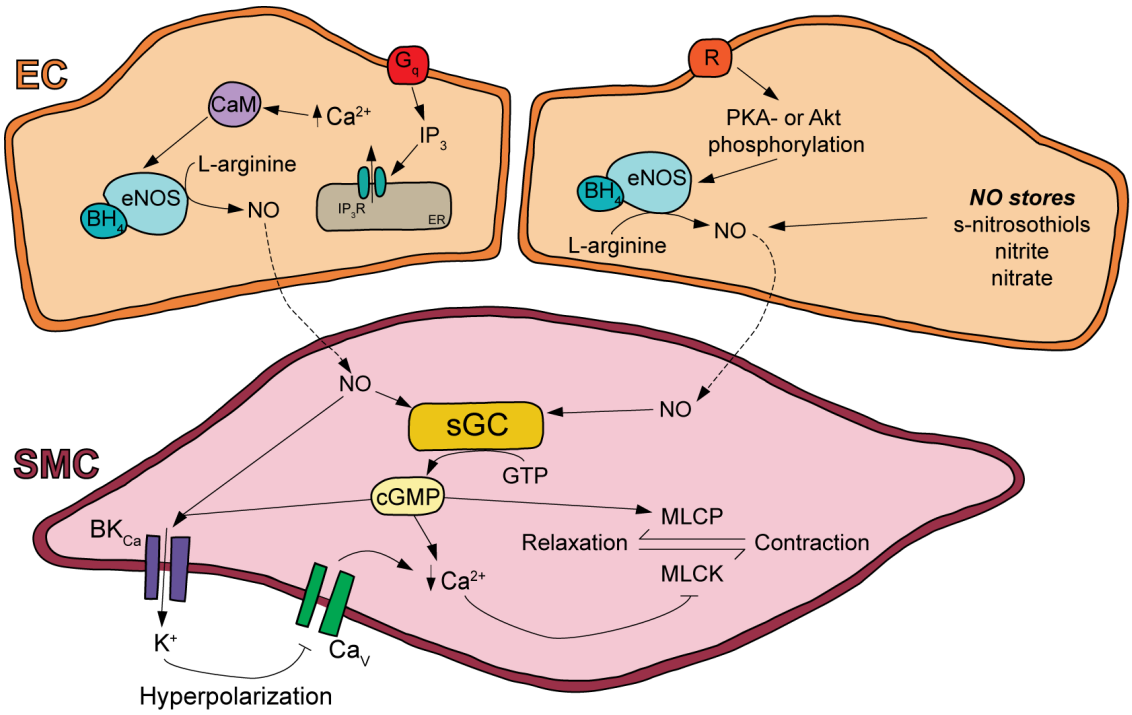


Figure 1.5.1: The generation and vascular signaling pathways of nitric oxide (NO).

Activation of Gq protein coupled receptors by agonists, such as acetylcholine, leads to the generation of inositol triphosphate (IP_3) and subsequent activation of IP_3 receptors (IP_3R). Activated IP_3R release Ca^{2+} stored in the endoplasmic reticulum (ER) of endothelial cells (EC), thus increasing levels of intracellular Ca^{2+}. This increase in Ca^{2+} activates calmodulin (CaM), which in turn activates endothelial nitric oxide synthase (eNOS). Alternatively, eNOS can be activated through phosphorylation by protein kinase A (PKA) or protein kinase B (Akt), which are themselves activated by shear stress on the endothelium, hormones or growth factor. S-nitrosothiols, nitrite and nitrate can all be converted to NO and therefore act as a form of storage for NO. NO freely diffuses from the endothelium to smooth muscle cells (SMC) and activates soluble guanylyl cyclase (sGC). Activated sGC converts guanosine triphosphate (GTP) to cyclic guanosine monophosphate (cGMP), which leads to a decrease in intracellular Ca^{2+}. The decrease in intracellular Ca^{2+} reduces the activity of myosin light chain kinase (MLCK). It has been suggested that cGMP may also indirectly activate myosin

light chain phosphatase (MLCP) via protein kinase G (Huang et al. (2004)). Activation of MLCP dephosphorylates myosin light chain, eliciting a conformational change in the myosin, which results in muscle relaxation. There is also evidence that NO can activate large conductance Ca^{2+}-activated potassium channels (BK_{Ca}) either directly, or through the activation of sGC. The efflux of K^+ hyperpolarizes the SMC inhibiting L-type voltage gated Ca^{2+} channels, thus helping to reduce intracellular Ca^{2+} levels that, in turn, reduce the activity of MLCK.

1.5.II NO^-

The formation of NO^-, known as HNO in its protonated form, has been examined through a variety of *in vitro* studies. It transpires that HNO may be generated via several different mechanisms. Adak et al. (2000) and Hobbs et al. (1994) demonstrated that HNO could be formed by eNOS, especially in the absence of or with reduced influence from BH_4. Intermediates in the conversion of L-arginine to NO by NOS may also lead to the generation of HNO (Fukuto et al., 2005). Other studies have demonstrated generation of HNO independent to NOS. Many of these studies focus on the reduction of NO to HNO, which is mediated by ubiquinol (Poderoso et al., 1999), manganese superoxide dismutase (SOD)(Niketic et al., 1999), cytochrome c (Sharpe & Cooper, 1998) and xanthine oxidase (Saleem & Ohshima, 2004). Interestingly, it has been suggested that SOD or other biological oxidants may convert HNO to NO (Fukuto et al., 1993), however, due to the distinct biological effects of HNO and NO this view is disputed (Irvine et al., 2008). The reaction between S-nitrosothiols and other thiol species may also produce HNO (Arnelle & Stamler, 1995; Wong et al., 1998). More recent work has shown, for the first time, endogenous HNO generation in cultured cells using a HNO selective electrode and a HNO-selective fluorescent sensor. The generation of HNO was attributed to a reaction between hydrogen sulphide (H_2S) and NO (Eberhardt et al., 2014).

Like NO, HNO has been shown to relax pre-constricted small mesenteric arteries (Favaloro & Kemp-Harper, 2009). It has also been demonstrated that HNO can hyperpolarize SMCs at resting Em (Yuill et al., 2011) and is partially

responsible for the hyperpolarization produced by ACh (Andrews et al., 2009). HNO has also been associated with the activation of potassium channels, namely voltage gated potassium channels (K_v), ATP-sensitive potassium channels (K_{ATP}) and BK_{Ca} channels (Favaloro & Kemp-Harper, 2007; Favaloro & Kemp-Harper, 2009; Irvine et al., 2003; Yuill et al., 2011).

In addition to activation of potassium channels, HNO has been implicated in the activation of sGC (downstream pathway described in **section 1.5.I**) leading to vasorelaxation (Miller et al., 2009). It has, however, been suggested that HNO may undergo conversion to NO before activating sGC (Fukuto et al., 1993). More recently, neuronal stimulation by HNO has been proposed, which will be discussed in greater detail in **Chapter 4**. In brief, Eberhardt et al. (2014) has proposed that HNO may activate transient receptor potential A1 channels (TRPA1) on sensory nerve endings present in the adventitial layer. The activation of TRPA1 leads to the release of CGRP, which activates CGRP receptors on vascular SMCs and consequently activates the adenylyl cyclase (AC) pathway. The generation and signalling pathways of HNO are detailed in **Figure 1.5.2**.

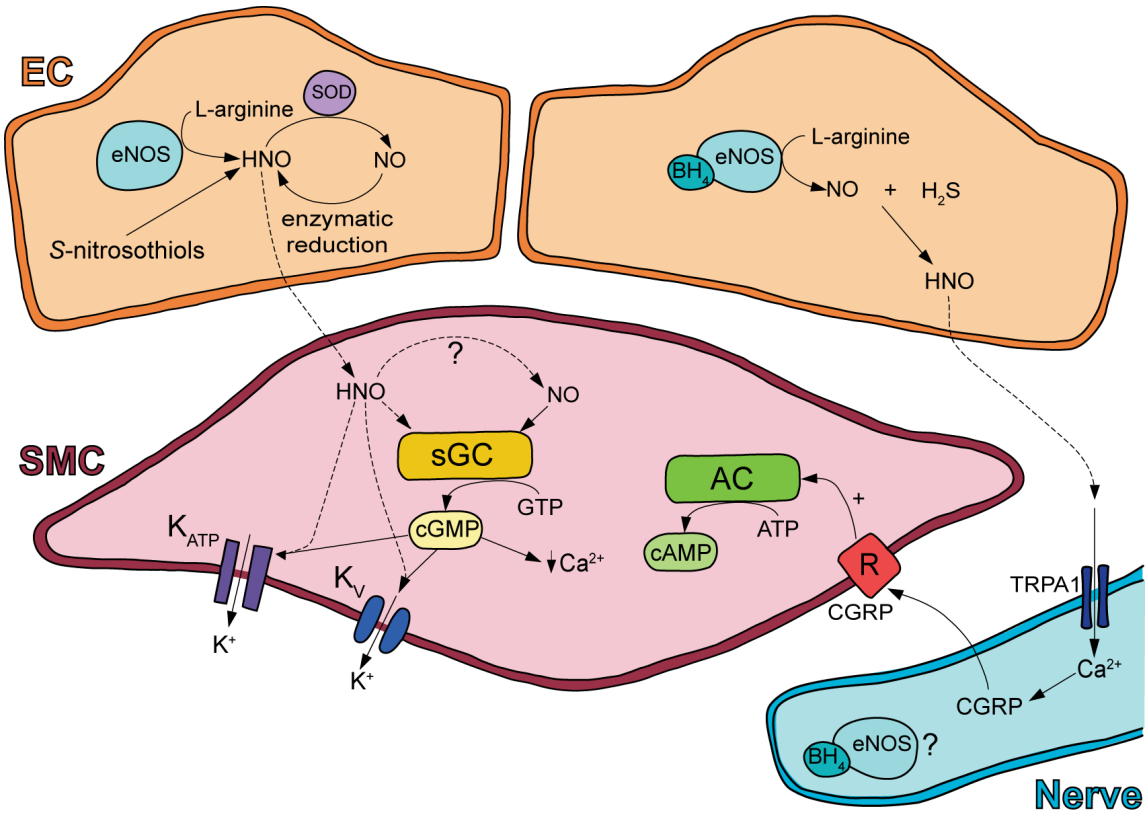


Figure 1.5.2: Proposed pathways of nitroxyl (HNO) induced relaxation of vascular smooth muscle cells.

HNO can be formed directly by NO synthase (NOS) in endothelial cells (EC) when the influence of tetrahydrobiopterin (BH_4) is reduced, or from the NOS intermediates N_ω-hydroxy-L-arginine and hydroxylamine. Non-NOS sources can also contribute to HNO formation. Nitric oxide (NO) can be reduced to HNO by mitochondrial cyctochrome c, xanthine oxidase, ubiquinol and manganese superoxide dismutase (SOD). HNO can also be formed by reaction of S-nitrosothiols with other thiol species. $NO^{\bullet}$ is generated by NOS in the presence of BH_4, it can then react with hydrogen sulphide (H_2S) to form HNO. Both NO and HNO are proposed to diffuse into vascular smooth muscle cells (SMC) and interact with soluble guanylyl cyclase (sGC), although HNO may require prior oxidation to NO. Activated sGC converts guanosine triphosphate (GTP) to cyclic guanosine monophosphate (cGMP), which (primarily via protein kinase G (PKG)) leads to a decrease in intracellular calcium and SMC relaxation as detailed in **Figure 1.5.1**. cGMP can activate ATP-sensitive potassium

channels (K_{ATP}) and voltage-gated potassium channels (K_v) and HNO may also activate these channels directly dependent on vascular bed. The subsequent hyperpolarization causes SMCs to relax as detailed in Figure 1.5.1. HNO may also activate transient receptor potential A1 (TRPA1) channels, which triggers the release of calcitonin gene-related peptide (CGRP) from sensory nerves. CGRP activates CGRP receptors (R) on SMC, promoting the activation of adenylyl cyclase (AC) and subsequent increase in cyclic adenosine monophosphate (cAMP). There is also potential for the generation of NO in the sensory nerves, which could then react with H_2S, providing an additional reservoir of HNO.

1.5.III NO^+

As mentioned in **section 1.5**, the oxidation of $NO^{\bullet}$ results in the formation of NO^+. Chemical evidence suggests the existence of NO^+ in aqueous media under acidic conditions (Stamler et al., 1992). At physiological pH its formation is thought to occur through heterolytic fission of N_2O_4, however, it is then rapidly converted to nitrite though its reaction with water (van Faassen & Vanin, 2007). The biological relevance of the NO^+ ion, under physiological conditions, is therefore disputed (Stamler et al., 1992). It has, however, been suggested that NO^+ in the form of nitrite, can act as an intravascular store of NO (Webb et al., 2008).

Nitrite can be converted to NO in the acidic conditions of the stomach, with the intermediate formation of nitrous acid (Benjamin et al., 1994; Lundberg et al., 1994). NO can also be generated from nitrite by bacterial metabolism (reviewed by Lundberg et al. (2004)) Thus, the effects of nitrite on the vasculature are probably attributable to NO.

1.6 General Aim

Current NO donors are of limited use as medicines primarily due to tolerance development. Therefore, it was decided to investigate the role of HNO as an improved molecule for future medical use.

Chapter 2

Methods & Materials

2.1 Tissue isolation

Animal use was approved by the University of Oxford Ethical Committee and complied with the Animals (Scientific Procedures) Act 1986, United Kingdom. Animals were housed in a temperature-controlled environment with a 24-hour light-dark cycle and food and water ad libitum.

Male Wistar rats (225-250 g, Charles River, UK) were killed by cervical dislocation followed by exsanguination, as defined by Schedule 1 of the Animals (Scientific Procedures) Act 1986, UK. The mesentery was removed from the rat and placed in ice-cold MOPS-buffered solution (see **section 2.5** for composition) before transferral to the laboratory. Tissue was subsequently pinned out in a re-usable Sylgard coated Petri dish, filled with ice-cold MOPS-buffered solution within 1 hour of removal.

Third order branches (170 μm – 361 μm, mean = 265 μm ± 1.73 μm; n=284 arteries) of the superior mesenteric artery were dissected away from the neighbouring vein and cleared of surrounding adipose and connective tissue (**Figure 2.1.1**). For wire myography and electrophysiology experiments, arterial segments were cut to 2 mm in length. For other experiments, arteries were cut into segments ≥ 2 mm. Where the protocol required pressurization of arteries, extra care was taken to avoid small side branches. Tissue was kept at 4 °C in the Petri dish so further arteries could be dissected if required. After use, the dissection dish was cleaned using 70 % ethanol followed by Milli-Q distilled water.

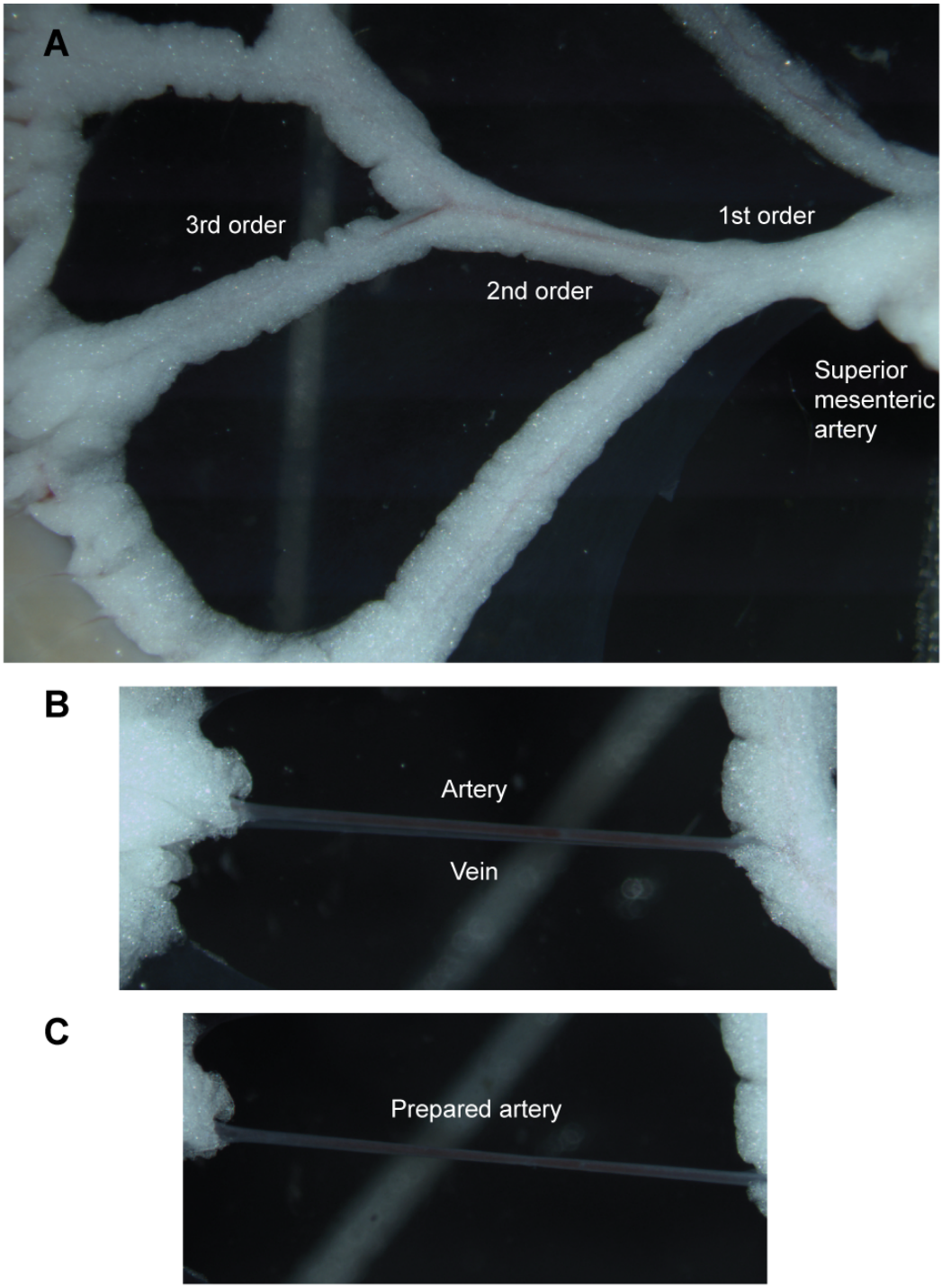


Figure 2.1.1: Dissection of rat mesenteric arteries

A Pinned rat mesenteric artery detailing the location of the superior mesenteric artery and first, second, and third order arteries. **B** Third order artery and vein after removal of surrounding adipose and connective tissue. The vein in this instance is positioned under the artery. **C** Fully dissected artery cleaned of all remaining connective tissue, ready for experimentation.

2.2 Wire myography

Initially described by Bevan and Osher (1972), wire myography was refined by Mulvany and Halpern (1977) in order to study the contractile properties of small resistance arteries. Wires are inserted through the lumen of an artery and secured onto two parallel specimen supports attached to a transducer and micrometer (**Figure 2.2.1**). This configuration allows for the measurement of contraction under isometric conditions. Before experimentation can proceed, vessels are stretched in stages and tension readings recorded and fitted to an exponential curve. This allows for the optimal resting tension of the vessel to be calculated. Mulvany and Halpern (1977) determined the optimal resting tension to be equivalent to 0.8 x the internal diameter of the vessel at 100 mmHg. They found that at values greater than this there was the potential for active wall tension recordings to be masked by the resting wall tension of the vessel.

2.2.I Mounting arteries for wire myography

Segments of third order mesenteric artery, prepared as described in **section 2.1**, were mounted luminally using two 25 μm diameter gold-plated tungsten wires, in the chamber of a Mulvany-Halpern myograph (model 400A, 10 ml chamber, for single recordings; or model 610M, 5 ml chamber, for multiple recordings; DMT Denmark) in cold Krebs solution (see **section 2.5** for composition). An equilibration period of ~30 min was allowed whilst the chamber was warmed to 37°C. Following this, arteries were normalized by constructing a passive diameter-tension curve, as described by Mulvany and

Halpern (1977), to a resting tension equivalent to that generated at 0.9 x the diameter of the vessel at 70 mmHg.

Arteries were left to equilibrate, at their optimal resting tension, for a minimum of 20 min before their viability was assessed. Contractility was assessed using phenylephrine (PE), an α_1-adrenergic vasoconstrictor, and endothelial health was determined using acetylcholine (ACh), a muscarinic M_3 receptor vasodilator. Only arteries that contracted by more than 8 mN to PE (1-10 μM) and then achieved ≥ 95% relaxation to ACh (0.1-1 μM), following constriction to PE, were considered to be viable and used for experimentation. Bath temperature was maintained at 37°C throughout the experiment and the Krebs solution was replaced approximately every 30 min to reduce the chance of Ca^{2+} precipitation.

2.2.II Analysis of wire myography data

Relaxation is expressed as a % of the maximal level of tension achieved immediately prior to the addition of the test compound according to the following calculation:

$$\frac{recorded\ tension - resting\ tension}{maximum\ tension - \ resting\ tension}\ x\ 100$$

The level of pre-constriction, to be used in relaxation experiments, was determined by first constructing a PE concentration-response curve (1-10 μM). 70% of the maximal constriction achieved in the concentration-response curve was then calculated. Where pre-constriction was required in experiments an agonist was used to approximately reach the pre-determined 70% value. The

maximum tension used in the calculation refers to the maximum tension achieved at any point in the concentration-response experiment.

Where experiments did not require pre-constriction, for example constriction concentration-response curves, maximum tension was determined by applying 45 mM KCl (using 2 M stock solution) to the bath. The same calculation, as used for constructing relaxation concentration-response curves, was used for the construction of constriction concentration-response curves.

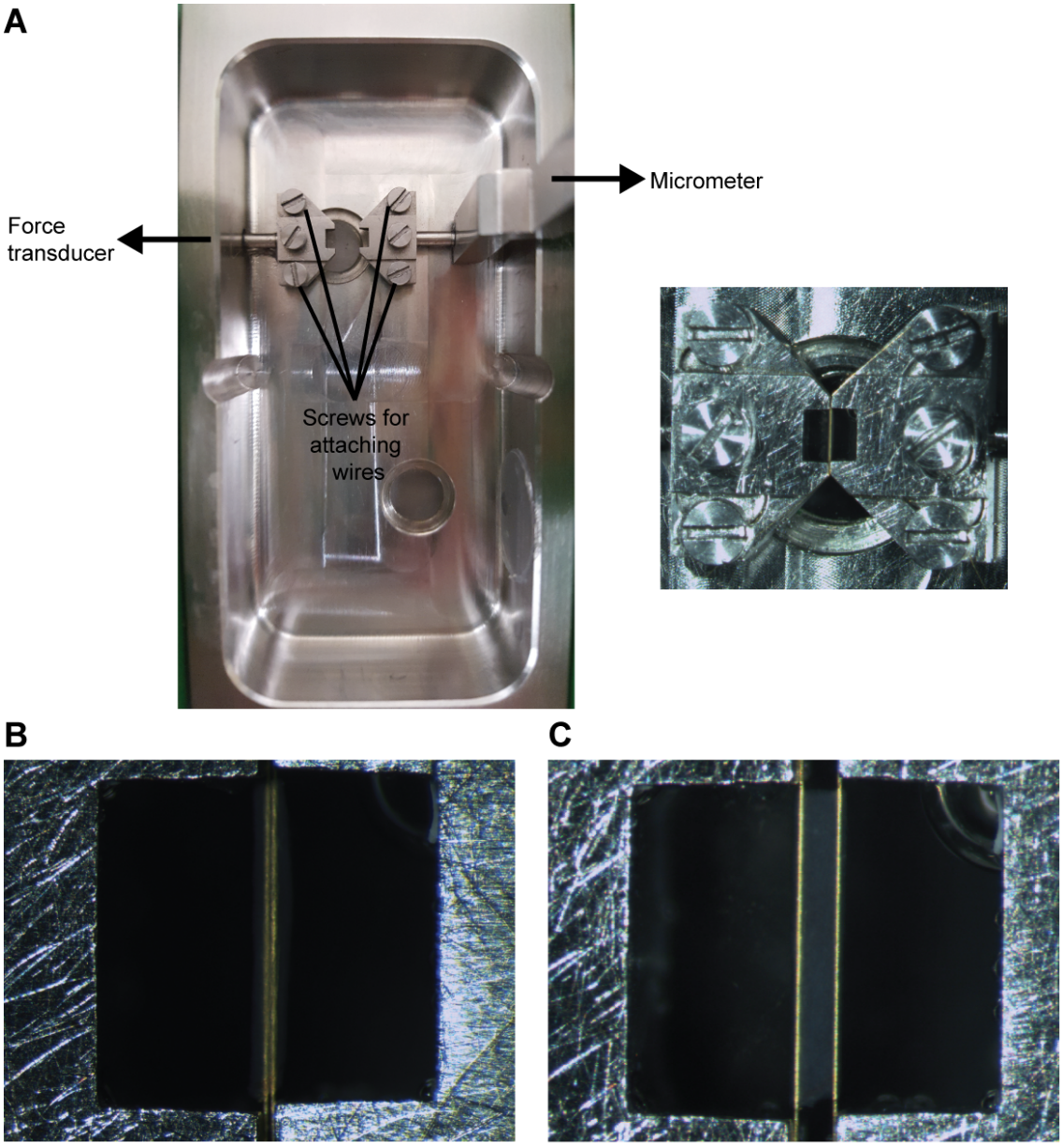


Figure 2.2.1: Wire myograph setup

A 10 mL chamber of a two channel myograph (model 400A, DMT) with force transducer, micrometer and screws required to secure the mounting wires labelled. **Right** Close-up of the myograph specimen supports with a mounted vessel. **B** Close up of artery mounted using two 25 µm gold-plated tungsten wires, without applied tension. **C** Close up of artery with tension applied as would be seen after the normalization protocol. Artery is approximately 2 mm in length.

2.3 Sharp microelectrode intracellular recording

The use of sharp microelectrodes to make intracellular recordings of smooth muscle cells in intact arteries has previously been described by Garland and McPherson (1992). By using a wire myograph to mount the artery, a simultaneous recording of both tension and membrane potential can be made. This allows for intracellular events and sustained changes in membrane potential to be directly compared to whole artery relaxation or constriction.

2.3.I Preparation of arteries

Arteries were prepared and mounted, as above (**Sections 2.1 & 2.2**), in a two channel 10 ml myograph. Extra care was taken, when dissecting, to ensure that all connective tissue was removed. Excess connective tissue can impair the ability to gain a stable recording.

2.3.II Preparation of microelectrodes

The sharp microelectrodes were made on the day of use. Borosilicate glass capillaries with an internal filament (30-0044; Harvard Apparatus, MA, USA) were pulled using a pre-defined programme on a pipette puller (model P-1000; Sutter Instrument, CA, USA). The electrodes were then backfilled with 2 M KCl and inserted into an electrode holder and attached to the headstage of the electrophysiology rig (**Figure 2.3.1**). The electrode was tested to ensure that the tip resistance was between 60-100 MΩ. If the tip resistance was not suitable the parameters on the pipette puller were adjusted and a new electrode was pulled and filled.

2.3.III Determination of successful intracellular recordings

To gain an intracellular recording of a single smooth muscle cell, the electrode was advanced in 1 μm increments towards the mounted artery using a Burleigh Inchworm motor and 6000 series controller (Burleigh, USA). An impalement was considered successful if the resting membrane potential was *circa* -50 mV and remained stable for a minimum of 30 seconds. Smooth muscle membrane potential was recorded through a pre-amplifier (Neurolog system, Digitimer Ltd., U.K.) linked to a MacLab data acquisition system (AD Instruments Model 4e, usually at 100 Hz). A HumBug noise eliminator (Digitimer Ltd., U.K.) was used to eliminate 50 Hz/60 Hz noise.

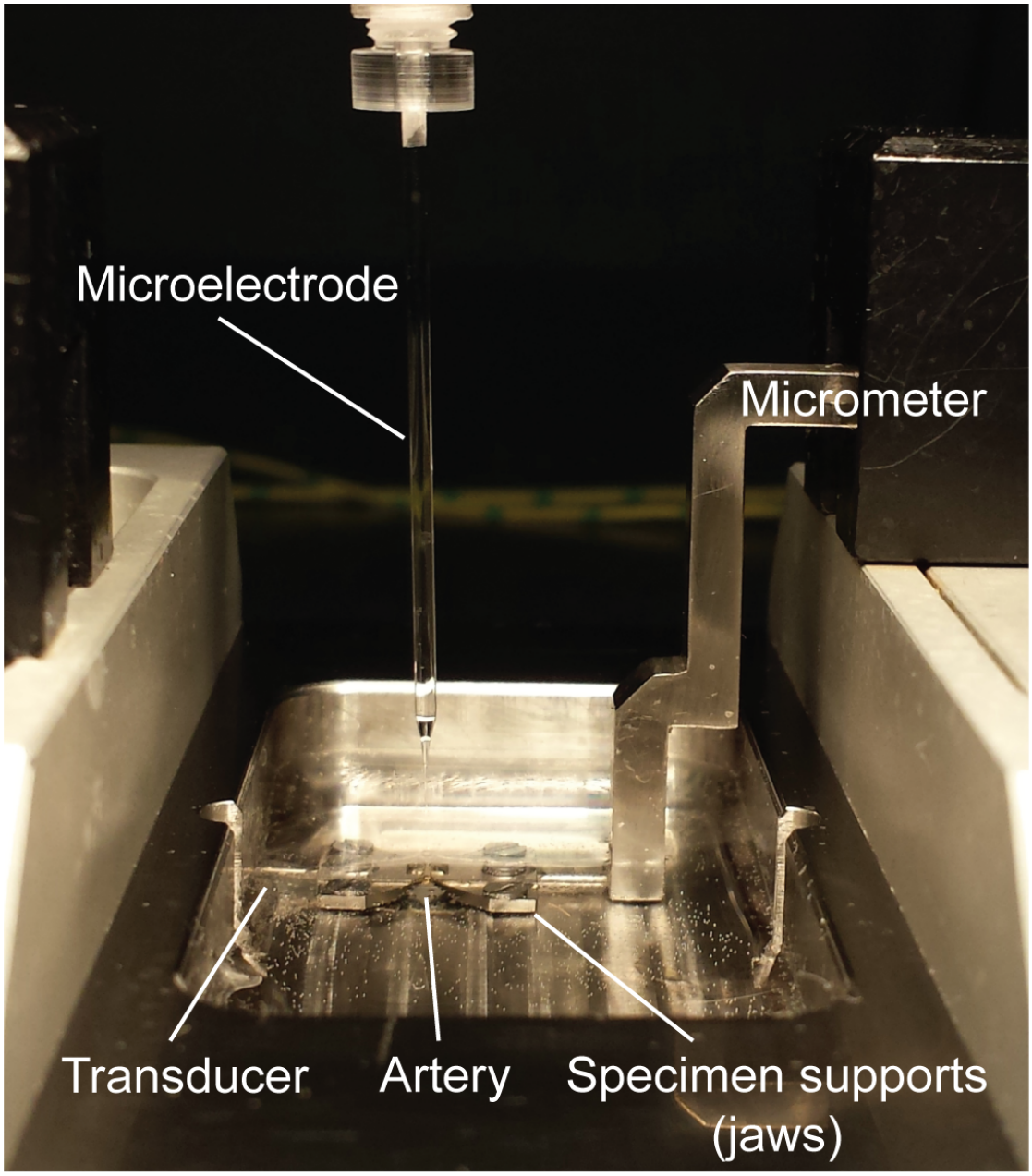


Figure 2.3.1: Setup for sharp microelectrode intracellular recording

10 mL chamber of a two channel myograph (model 400A, DMT) with force transducer, micrometer, specimen supports, artery and microelectrode labelled. The microelectrode is filled with a 2 M KCl solution.

2.4 Immunohistochemistry

2.4.I Preparation of pressurized arteries

A section of rat third order mesenteric artery was dissected as above (see **section 2.1**), cannulated at each end with polished glass pipettes (external diameter 190-200 μm) and secured with sutures (Ethilon polyamide 10-0; Ethicon, USA) in a 2 mL temperature regulated chamber (RC-27 chamber and PH-6 heating platform; Warner Instruments, CT, USA) filled with a MOPS-buffered solution. The artery was superfused for 30 minutes at 37°C (flow rate 2 mL/min), before the pressure was raised to 70 mmHg and the artery checked for leaks. A leak was determined as present if the external diameter of the artery decreased when a three-way tap connecting the artery to the pressure system was closed. Where the leak was the result of a loose suture, the suture was retied and the artery tested again. If this failed to fix the leak, or a side branch was noted, a new artery was mounted and tested.

Health of the artery was assessed by the addition of 1-3 μM PE, followed by up to 1 μM Ach. Only vessels that relaxed by ≥ 95%, confirming that the endothelium was undamaged, were used.

2.4.II Preparation of pinned arteries

Sections of rat third order mesenteric artery were dissected as described in **section 2.1**. The arteries were then either left intact or carefully cut longitudinally to reveal the endothelium (*en-face* preparation). The prepared arteries were then pinned into a Sylgard-lined 24-well plate, ensuring that the endothelium of the *en-face* arteries was facing up.

Following the immunohistochemistry protocol (**section 2.4.III**), the artery sections were mounted on microscope slides in VectaShield Mounting Medium for Fluorescene H-1000 (Vector Laboratories Inc., USA) and then sealed under a 10 mm diameter glass coverslip, using clear nail varnish.

2.4.III Immunohistochemistry protocol

Once prepared, the arteries were fixed in a 2% paraformaldehyde (PFA) solution for 10 minutes at 37°C and subsequently washed with phosphate-buffered saline (PBS, 0.01 M). Arteries were then pre-incubated in blocking buffer (1% bovine serum albumen (BSA) and 0.1% Tween20 in PBS) for 1 hour at 37°C. Pressurized arteries were maintained at 70 mmHg. Primary antibodies, dissolved in blocking buffer at room temperature, were added to the bath (pressurized vessels were luminally perfused) and incubated overnight at 4°C (not pressurized). Arteries were then washed with PBS before secondary antibodies, dissolved in blocking buffer (1% BSA and 0.01% Tween20 in PBS), were incubated at room temperature for 2 hours. The arteries were then washed with PBS before imaging. Depending on the primary antibody used, in pressurized arteries, the secondary antibody was applied luminally, abluminally, or both. Propidium iodide (7.5 μM) and Alexa Flour 633 hydrazide (1 μM) were added abluminally to stain nuclei and the internal elastic laminar (IEL) respectively. Phalloidin (2 μM), used to identify smooth muscle cells, was added with the primary antibodies and incubated overnight. All primary and secondary antibodies used are detailed in **Table 2.4.1**.

2.4.III.i Luminal application

Where luminal application of a solution was required, a LKB peristaltic pump was used (~4 μL min^{-1}).

2.4.III.ii Imaging

Fluorescence was excited in the arteries at 405 nm, 488 nm, 543 nm and 633 nm and the emitted fluorescence was acquired at either 1024 x 768 pixels or 1024 x 1024 pixels through a 40x water immersion objective using a confocal microscope (Olympus, FluoView software). Z-stacks of the artery, from the adventitia to the endothelium, were acquired in increments of 0.25 or 0.5 μm and reconstructed in Imaris Software (Version 7.7.1; Bitplane).

Protein	Primary Antibody	Immunogen	Secondary Antibody
TRPA1	• 1:500 • ACC-037 • Rabbit polyclonal • Alomone	• (C)NSTGIINETSDHSE, corresponding to amino acid residues 747-760 of human TRPA1 • 86% homology with rat	• 1:1000 • A11008 • Goat anti-rabbit • Life Technologies (UK)
NF-L	• 1:200 • MA1-2010 • Mouse monoclonal • Thermo Scientific	• Enzymatically dephosphorylated porcine neurofilaments	• 1:200 • A31553 • Goat anti-mouse • Life Technologies (UK)

Table 2.4.1: **Details of antibodies used in thesis**

2.5 Solutions and drugs

All wire myography and sharp microelectrode experiments were performed using a Krebs solution containing (mM): NaCl, 118; KCl, 3.6; $MgSO_4.7H_2O$, 1.2; KH_2PO_4, 1.2; D-glucose, 11; $NaHCO_3$, 25; CaCl, 2.5; at 37°C; continuously bubbled with 5% CO_2/21% O_2/balance Nitrogen. All dissection and

pressurization prior to immunohistochemistry was conducted in a MOPS-buffered solution containing (mM):NaCl, 145;KCl, 4.7; $CaCl_2$ 2; $MgSO_4.7H_2O$, 1.17; MOPS, 2; NaH_2PO_4, 1.2; D-glucose, 5; pyruvate, 2; EDTA, 0.02; NaOH, 2.75; at 37°C (on ice for dissection); pH = 7.4 ± 0.02 adjusted using 1 M or 4 M NaOH.

High K^+ Krebs solution, used as a vasoconstrictor in some experiments, contained (mM): KCl, 123; $MgSO_4.7H_2O$, 1.2; KH_2PO_4, 1.2; D-glucose, 11; $NaHCO_3$, 25; CaCl, 2.5; at 37°C; continuously bubbled with 5% CO_2/21% O_2/balance Nitrogen.

Details of suppliers of drugs and chemicals are given in **Table 2.5.**

Drug/Chemical	Product code	Supplier	Stock conc	Stock solvent
Acetylcholine (Ach)	A6625	Sigma-Aldrich (UK)	10 mM	Milli-Q
AITC	377430	sigma-Aldrich (UK)	100 mM	DMSO
Alexa Fluor 633 hydrazide	A30634	Invitrogen	1 mM	
Angeli's salt (AS)	176695	Calbiochem	100 mM	10 mM NaOH
Bovine Serum Albumin (BSA)	A7906	Sigma-Aldrich (UK)	NA	NA
CaCl2	E506	VWR	1 M	distilled water
Calcitonin gene related peptide (CGRP)	1161	Tocris	100 µM	Milli-Q
Capsaicin	M-2028	Sigma-Aldrich (UK)	10 mM	EtOH
D-Glucose	G/0500/60	Fisher	NA	NA
EDTA	E9884	Sigma-Aldrich (UK)	NA	NA
HC030031	2896	Tocris	100 mM	DMSO
Hydroxocobalamin (HXC)	H1428000	Sigma-Aldrich (UK)	100 mM	Milli-Q
Isopropylamine NONOate (IPA/NO)	custom-made	Gift from K.M. Miranda, University of Arizona	10 mM	10 mM NaOH
KCl	P/4240/53	Fisher	2 M	Milli-Q
KH2PO4	26936.236	VWR	NA	NA
L-cysteine	C1276	sigma-Aldrich (UK)	500 mM	Milli-Q
L-NAME	N5751	Sigma-Aldrich (UK)	100 mM	Milli-Q
MgSO4.7H2O	25165.26	VWR	NA	NA
MOPS	M5162	Sigma-Aldrich (UK)	NA	NA
N-acetyl-l-cysteine (NAC)	A7250	Sigma-Aldrich (UK)	100 mM	Milli-Q
NaCl	194090010	Acros Organics	NA	NA
NaH2PO4	102454R	VWR	NA	NA
NaHCO3	14707	Alfa Aesar	NA	NA
NaOH	28244.262	VWR	NA	NA

ODQ	880	Tocris	20 mM	DMSO
Paraformaldehyde (PFA)	custom-made	Electron Microscopy Sciences (UK)	2%	Distilled water
Phalloidin	P1951	Sigma-Aldrich (UK)	1 mg/ml	DMSO
Phenylephrine (PE)	P6126	Sigma-Aldrich (UK)	10 mM	Milli-Q
Phosphate-buffered saline (PBS)	P3813	Sigma-Aldrich (UK)	NA	Milli-Q
Propidium iodide (PI)	P4170	Sigma-Aldrich (UK)	4.5 mM	Milli-Q
Pyruvate	P2256	Sigma-Aldrich (UK)	NA	NA
Tween20	P2287	Sigma-Aldrich (UK)	NA	NA
U46619	16450	Cayman Chemical (USA)	10 mM	DMSO

Table 2.5.1: **Details of drugs and chemicals used in this thesis**

2.6 Statistical analysis and curve fitting

All data are expressed as mean ± SEM, analysed using Microsoft Excel and GraphPad Prism 5.0. *n* values refer to the number of animals used. Depending on the data sets to be analysed, either a 2way ANOVA was performed, followed by a Bonferroni post-test to analyse individual points, or a two-tailed Student's *t*-test was performed. Statistical significance was defined by $P < 0.05$.

Curves were fitted using GraphPad Prism 5.0, as either log(agonist) vs. response (three parameters) defined by the equation:

Y=Bottom + (Top-Bottom)/(1+10^((LogEC50-X)))

Or, log(agonist) vs response – variable slope (4 parameters) defined by the equation:

Y=Bottom + (Top-Bottom)/(1+10^((LogEC50-x)*HillSlope)).

Chapter 3

A comparative characterisation of the HNO donor Isopropylamine NONOate

3.1 Introduction

In 2014, 27% of deaths in the UK were attributed to cardiovascular disease, of which 54% were associated with vascular disease, hypertension or coronary heart disease (Townsend et al., 2015).

There are a number of different treatment options available to treat hypertension and angina, some of which harness the vasodilatory effects of NO (Thomson & Loudon, 2014). For example, NO gas may be used therapeutically by direct inhalation to treat pulmonary hypertension, where it has been shown to be a selective vasodilator (Griffiths & Evans, 2005; Pepke-Zaba et al., 1991) Sodium nitroprusside (SNP) preparations may also be used to rapidly lower blood pressure in hypertensive crises, although concern has been raised about the potential for release of cyanide during the decomposition of SNP (Bates et al., 1991; Miller & Megson, 2007) Organic nitrates such as glyceryl trinitrate are the most commonly used NO donor drugs (Miller & Megson, 2007). As discussed in **section 1.5** nitrate and nitrite can be converted to NO and therefore increase its bioavailability. The released NO is effective in treating heart failure, as the relaxation of arteries reduces afterload on the damaged ventricle, leading to an increase in stroke volume and ejection fraction. In addition, venous dilation occurs which reduces the preload on the heart and helps to reduce edema. Organic nitrates are also used to treat angina, due to their ability to reduce preload on the heart, through venous dilation, and dilate coronary arteries which both reduces myocardial oxygen demand and increases the oxygen supply to the heart, therefore reducing the symptoms of angina (Klabunde, 2012; Piper & McDonagh, 2014). There are however a

number of issues associated with the use of nitrates as vasodilators, namely tolerance development, potential cytotoxic effects and loss of effectiveness under conditions of oxidative stress (Irvine et al., 2008). For this reason, attention has turned to HNO and its donor compounds as an alternative treatment.

3.1.I Donors of HNO

There are many HNO donor compounds available for use in biological systems. Unlike donors of NO, HNO donors are resistant to scavenging by superoxide (Miranda et al., 2002) and do not develop vascular tolerance (Irvine et al., 2007; Irvine et al., 2011). Paolocci et al. (2003) has also reported positive inotropic and lusitropic effects in dogs with cardiac failure, thus donors of HNO may present an alternative therapeutic avenue with which to treat cardiovascular disease.

The most commonly used donors of HNO, as defined by Irvine et al. (2008) are cyanamide, Piloty's acid, Angeli's salt (AS), isopropylamine NONOate (IPA/NO), and acyloxy nitroso compounds. Of these, AS is the most well studied HNO donor and shall be discussed further in **section 3.1.II**.

Currently no HNO donors are in use clinically for the treatment of cardiovascular diseases. Cyanamide is, however, approved for the treatment of alcohol dependence, whereby HNO is generated by the enzymatic conversion of cyanamide and subsequent decomposition of the intermediary *N*-hyroxycyanamide (Nagasawa et al., 1990; Shirota et al., 1996). HNO then acts as an inhibitor of aldehyde dehydrogenase (Nagasawa et al., 1990), which

leads to adverse physiological effects when alcohol is consumed, thus encouraging alcohol avoidance (Brien et al., 1978).

More recently Cardioxyl Pharmaceuticals, now owned by Bristol-Myers Squibb, began the development of HNO donors for the treatment of heart failure. Their initial compound CXL-1020, a congener of Piloty's acid, reached phase II trials and was successful in improving inotropy in patients with decompensated heart failure (Arcaro et al., 2014; Sabbah et al., 2013). A second generation of nitroxyl prodrugs have now been developed, with CXL-1427 currently progressing through clinical trials (Singh et al., 2017). These developments provide further evidence that HNO donors present a viable alternative to traditional NO releasing agents in the treatment of various cardiovascular diseases (reviewed by Kemp-Harper et al. (2016)).

3.1.II Limitations of Angeli's salt as a donor of HNO

As mentioned previously (**Section 3.1.1**), AS is the most commonly utilised of the HNO donors in biological studies (Paolocci et al., 2007). Sodium trioxodinitrate, now more commonly known as AS, was first synthesised in 1896 by Angelo Angeli (DuMond & King, 2011). In aqueous solution, at pH levels greater than 4, AS decomposes to release HNO and nitrite (Bonner & Ravid, 1975). This is the first limitation of AS as a HNO donor, as an increasing body of evidence suggests an important role for nitrite as an endogenous store of NO and potential signalling molecule in its own right (reviewed by Gladwin et al. (2005)). All studies employing the use of AS should therefore carry out control experiments, in which degraded AS is used, to account for any effects of nitrite.

The second limitation of AS is the compounds short half-life of ~2.5 minutes (κ= 4-5 x $10^{-3}s^{-1}$) (Irvine et al., 2008; Maragos et al., 1991) at physiological pH and temperature (pH 7.4; 37°C). HNO can also undergo dimerization with itself, resulting in the transient formation of hyponitrous acid, which itself decomposes to produce nitrous oxide and water, thus reducing the availability of HNO released from AS (Miranda, 2005). Therefore experiments, examining the longer-term effects of HNO, must take the potential loss of HNO into account or consider a longer lasting donor of HNO. The short half-life of AS also limits the storage of AS. Short-term storage is possible in alkaline solution, as the rate of decomposition decreases at pH levels >8 (Miranda, 2005).

3.1.III Isopropylamine NONOate

Given the various limitations of AS, newer HNO donors have been developed, one of which is IPA/NO. IPA/NO belongs to the diazeniumdiolates class of NO donors, which are commonly referred to as NONOates and have shown promise as a treatment for various disorders in animal models (reviewed by Keefer (2003)). NONOates are generated through the exposure of amines to high pressures of NO; which, when dissolved in a non-alkaline solution, fragment into the parent compound and two NO containing molecules (Miranda et al., 2005b). AS also falls within the NONOate class of NO donors, with oxide in place of the amine group (Miranda et al., 2005b), but as discussed in **section 3.1.II** generates HNO instead of NO, which is the typical product of NONOates.

Like AS, IPA/NO has a short half-life (~2.3 min; κ= 5.1 x $10^{-3}s^{-1}$ at pH 7.4; 37°C) (Irvine et al., 2008; Maragos et al., 1991) and requires storage in a highly

alkaline solution to prevent decomposition. Whilst AS only release NO at pH<4 (Bonner & Ravid, 1975), there is evidence that IPA/NO may act as a dual donor of HNO and NO at physiological pH, with HNO the primary product (Miranda et al., 2005b). Unlike AS, there is no co-production of nitrite, however a nitrosamine is formed as a by-product and may have toxicological properties (Miranda et al., 2005a; Paolocci et al., 2007).

IPA/NO is not suitable for use clinically due to its short half-life, however, it is currently used as a template for newer generations of organic HNO donors such as AcOM-IPA-NO which has a half-life of 41 minutes (Andrei et al., 2010). It is therefore essential that a fuller understanding of the mechanisms underlying the observed functional responses to IPA/NO is gained (Kemp-Harper et al., 2016).

3.1.III Aims

The HNO donor AS has been well characterised in a variety of studies but has various limitations, as discussed above. IPA/NO has been developed as an alternative donor of HNO and is used as a template molecule for newer generations of HNO donors, which may show potential for therapeutic use. However, IPA/NO has undergone limited characterisation and as yet the electrophysiological characteristics of IPA/NO as a donor of HNO has not been investigated. Therefore, the aim of this study was to undertake a comparative assessment of the effectiveness of IPA/NO, as a donor of HNO in rat mesenteric arteries, to AS; particularly focusing on its electrophysiological properties.

3.2 Methods & Materials

3.2.I Wire myography

Rat third order mesenteric arteries were pre-constricted with a sub-maximal concentration of phenylephrine (PE) or U46619 (~70% maximal tone). Except for L-cysteine and L-NAME, all drugs were added directly to the bath and inhibitors were pre-incubated for a minimum of 30 minutes before dose response experiments were carried out. Previous experiments showed that addition of L-cysteine directly to the bath produced a sharp drop in pH and took approximately 20 minutes to buffer back to physiological pH and therefore working-concentration solutions containing L-cysteine were made in advance and allowed to buffer before addition to the myograph bath. L-NAME (100 μM) was present throughout to prevent the basal and agonist-mediated release of nitric oxide (Dora et al., 2000).

For full details on the set up for wire myography studies please refer to **Methods & Materials section 2.2**.

3.2.II Sharp microelectrode studies of membrane potential

Rat third order mesenteric arteries were mounted and normalised to resting tension in an isometric wire myograph as previously described (**Methods & Materials section 2.1 & 2.2**). The resting membrane potential (Em) of a single smooth muscle cell was examined by impalement with a sharp microelectrode back-filled with a 2M KCl solution. Inhibitors were added 30 minutes prior to impalement of the cell. Once a smooth muscle cell impalement had been

successfully achieved (**Materials & Methods section 2.3.III**) increasing concentrations of IPA/NO or AS were carefully added so as not to disturb the recording. All drugs were mixed through bubbling in the chamber. In common with the wire myography experiments L-NAME (100 μM) was present throughout all experiments.

For full details on the set up for sharp microelectrode studies please refer to **Methods & Materials section 2.3**.

3.2.III Isopropylamine NONOate

IPA/NO was kindly synthesised and gifted by K. Miranda (University of Arizona). The recommended preparative method is disclosed in the paper 'HNO and NO release from primary amine-based diazeniumdiolate as a function of pH' - Salmon et al. (2011).

3.3 Results

Smooth muscle hyperpolarization and relaxation to IPA/NO and AS

Both AS and IPA/NO hyperpolarized rat mesenteric resistance arteries, in a concentration dependent manner. At the highest concentration of both IPA/NO and AS (10 μM) membrane potential decreased from resting membrane potential (-49.3 ± 1.0 mV; n=7) by 13.9 ± 1.8 mV (n=7) and 13.2 ± 3.1 mV (n=9), respectively (**Figure 3.3.1**). No difference was found between the hyperpolarization response to IPA/NO and Angeli's salt, where the pEC50 values were calculated as 5.93 and 5.31 respectively.

In rat mesenteric arteries pre-constricted (~ 70% maximal tone) with PE (100 nM–1 μM), IPA/NO produced near full relaxation at concentrations of 1 μM (n=10; **Figure 3.3.2A**), whilst AS fully relaxed all arteries at this concentration (n=6; **Figure 3.3.2B**). A 2way ANOVA with Bonferroni multiple comparisons showed that whilst the pEC50 values were similar (IPA/NO = 6.68 Vs AS = 7.176), at 100 nM there was a significant difference between the relaxation to IPA/NO and AS.

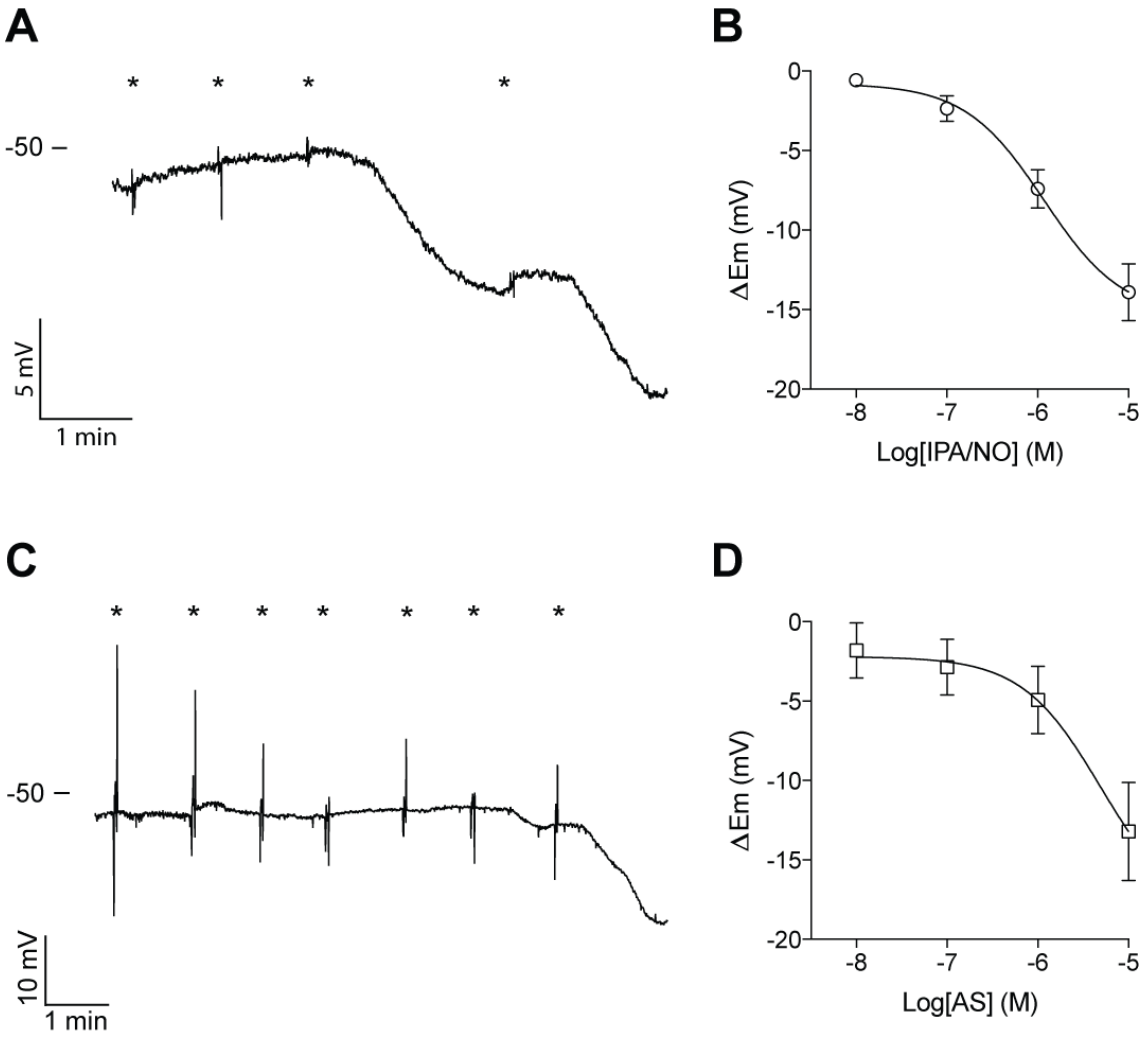


Figure 3.3.1: Concentration-responses to HNO donors in unstimulated mesenteric arteries.

Summarised data for change in membrane potential of smooth muscle cells, from resting, to cumulative addition of (B) IPA/NO (n=7) and (D) Angeli's salt (AS; n=9). Original traces for (A) IPA/NO and (C) AS are shown, demonstrating the hyperpolarization produced in response to HNO. * indicates increasing concentrations of IPA/NO (10 nM, 100 nM, 1 μM, 10 μM) or AS (10 nM, 30 nM, 100 nM, 300 nM, 1 μM, 3 μM, 10 μM). L-NAME was present throughout. Curves were fitted using the three-parameter equation and a 2way ANOVA with Bonferroni multiple comparisons test demonstrated no significant difference between IPA/NO and AS.

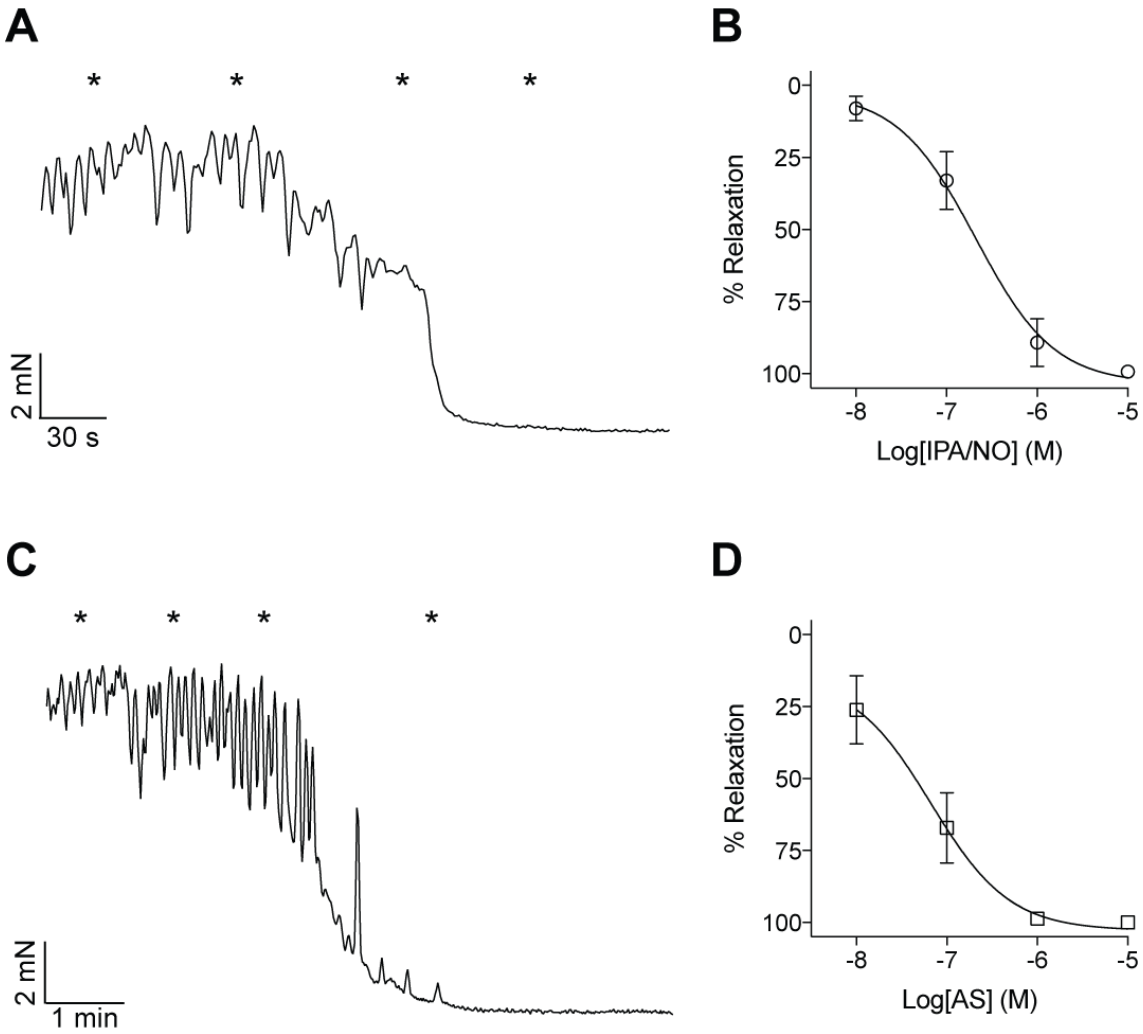


Figure 3.3.2: Concentration-responses to HNO donors in mesenteric arteries pre-constricted with phenylephrine.

Summarised data for relaxation in response to cumulative addition of (B) IPA/NO (n=10) and (D) Angeli's salt (AS; n=6). Original traces for (A) IPA/NO and (C) AS are shown, demonstrating the relaxation produced by HNO. * indicates increasing concentrations of IPA/NO (10 nM, 100 nM, 1 μM, 10 μM) or AS (10 nM, 100 nM, 300 nM, 1 μM). L-NAME was present throughout. Curves were fitted using the three-parameter equation and a 2way ANOVA with Bonferroni multiple comparison analysis showed that IPA/NO and AS were different at 100 nM.

The effects of scavengers of HNO and NO

To assess the extent to which HNO and NO are responsible for the responses attributed to IPA/NO and AS, the HNO scavenger, L-cysteine (3 mM; pEC50 = 5.62), and NO scavenger, hydroxocobalamin (HXC; 100 μM; pEC50 = 6.60), were applied to the myograph baths. L-cysteine significantly reduced the hyperpolarization to IPA/NO (pEC50 = 5.93) at 10 μM (**Figure 3.3.3**). In contrast, the presence of L-cysteine significantly reduced the relaxation in response to 100 nM AS and IPA/NO, but had no effect at higher concentrations of these two donors. The pEC50 values were calculated as follows: for AS (pEC50 = 7.07) vs L-cysteine pEC50 = 6.456, vs HXC pEC50 = 7.20; for IPA/NO (pEC50 = 7.50) vs L-cysteine pEC50 = 6.73, vs HXC pEC50 = 7.35. HXC had no effect on hyperpolarization to IPA/NO or relaxation to either of the HNO donors.

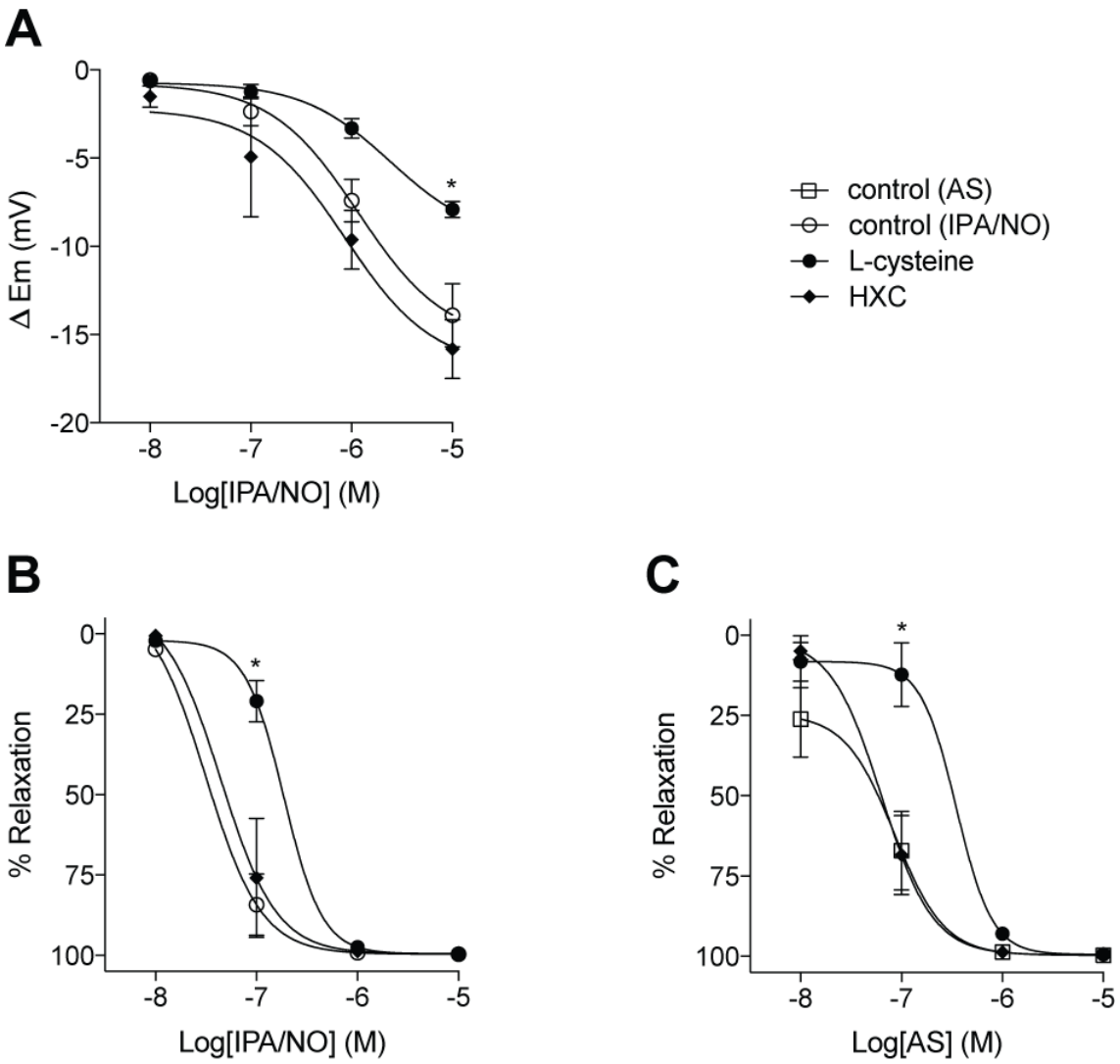


Figure 3.3.3: The effect of HNO and NO scavengers on the hyperpolarization and relaxation of rat mesenteric arteries in response to cumulative addition of HNO donors.

(A) L-cysteine (3 mM; n=4) significantly reduced the hyperpolarization of smooth muscle cells in response to IPA/NO compared to IPA/NO alone (n=7) in unstimulated arteries. Hydroxocobalamin (HXC; 100 μM; n=4) had no effect. Curves were fitted using the three-parameter equation. (B & C) The addition of L-cysteine (n=4) significantly reduced the response to 100 nM of both HNO donors, whilst HXC (n=4), had no effect on relaxation. Curves were fitted using the four-parameter equation. L-NAME was present throughout all experiments. *P<0.05 using a 2way ANOVA with Bonferroni multiple comparisons test.

Examination of the role of K^+ channels and sGC in HNO induced relaxation

The sGC inhibitor ODQ (10 μM) significantly reduced the response to both IPA/NO and AS. The addition of high extracellular K^+ (123 mM K^+ Krebs, exchanged for the standard bath solution) attenuated and shifted the relaxation to both IPA/NO and AS to the right (**Figure 3.3.4**). The mean maximal response to IPA/NO in the presence of high K^+ was reduced to 75.29 ± 1.63% and the response to AS was reduced to 55.19 ± 7.09%.

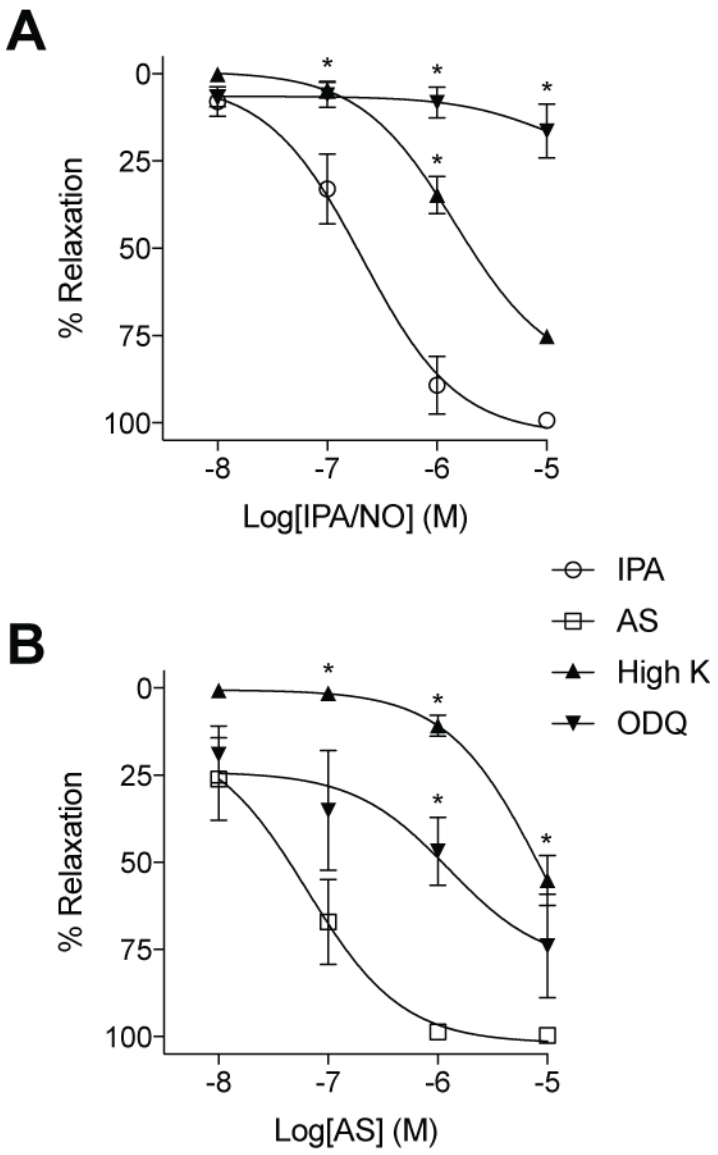


Figure 3.3.4: Examination of the role of sGC and K^+ channels in the response to HNO.

(A) The relaxation of arteries, pre-constricted with phenylephrine to IPA/NO (n=10; pEC50 = 6.68) was significantly inhibited by the sGC inhibitor ODQ (10μM; n=5; pEC50 = 4.94). Pre-constriction by a high K^+ solution (123 mM) significantly inhibited the response to IPA/NO at all but the highest concentration (n=4; pEC50 = 5.83). (B) The response to Angeli's salt (n=6; pEC50 = 7.19) was also significantly inhibited by ODQ (n=4; pEC50 = 5.90) and high K^+ solution (n=4; pEC50 = 5.04). L-NAME was present throughout. *P<0.05 Vs control using a 2way ANOVA with Bonferroni multiple comparisons test. Curves were fitted using the three-parameter equation.

Examination of high concentrations of IPA/NO

Full relaxation to IPA/NO is achieved between 1 and 10 μM (**Figure 3.3.2A**), however, in experiments examining the hyperpolarization to IPA/NO from resting membrane potential the response still does not plateau even at the highest concentration of IPA/NO (100 μM; **Figure 3.3.5A**). Given that the relaxation to IPA/NO at 10 μM, in the presence of 10 μM ODQ, was not fully inhibited, high concentrations of IPA/NO were examined further. It was found that at 100 μM IPA/NO, in the presence of ODQ, near maximal relaxation was achieved (95.77 ± 1.45%). High K^+ (123 mM K^+ Krebs) was then applied in combination with ODQ, to examine the involvement of K^+ channels at high concentrations of IPA/NO, resulting in complete inhibition of relaxation to IPA/NO (**Figure 3.3.5B**).

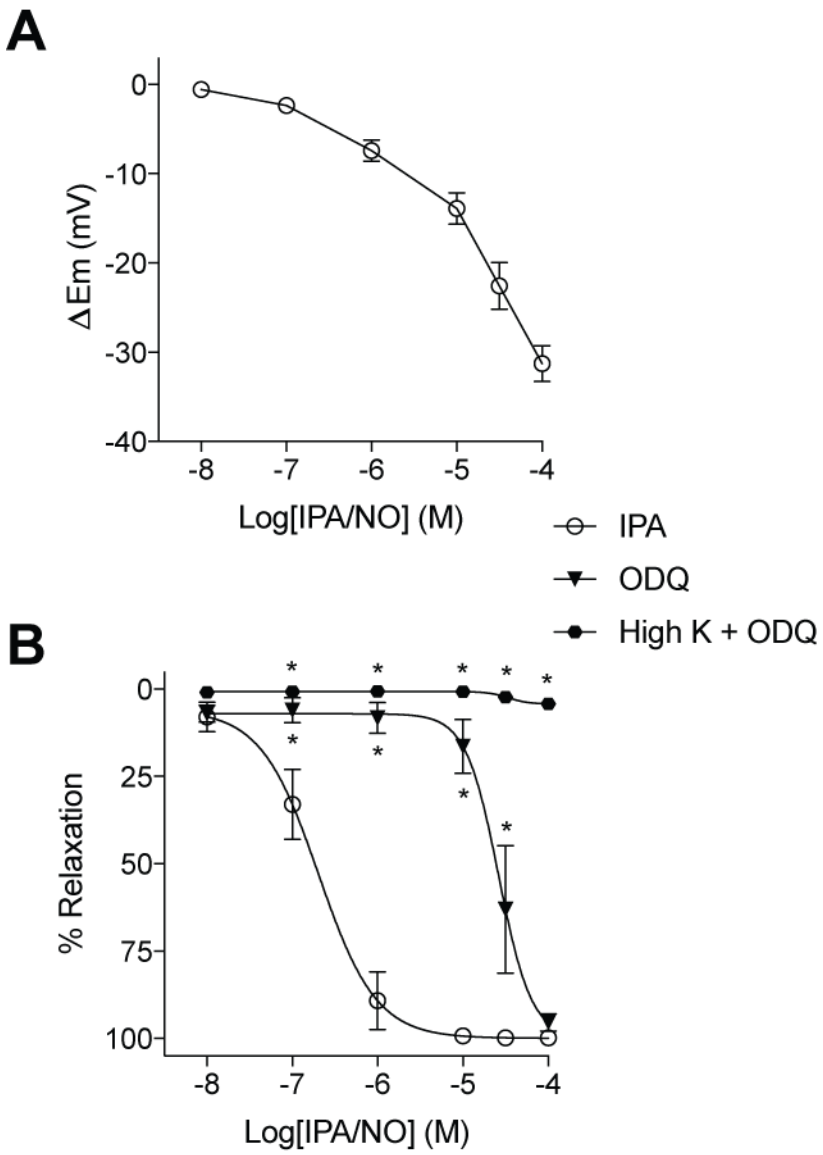


Figure 3.3.5: The effect of high concentrations of IPA/NO.

(A) The hyperpolarization of mesenteric artery smooth muscle cells does not reach a plateau (n=7). (B) High concentrations of IPA/NO (10 - 100 μM; n=10; pEC50 = 6.69) overcome the inhibition of relaxation caused by ODQ (10 μM; n=5; pEC50 = 4.58). The combination of ODQ and pre-constriction with a high K^+ solution (123 mM; n=4; pEC50 = 4.47) significantly inhibits the relaxation to IPA/NO and inhibits the relaxation observed at higher concentrations of IPA/NO in the presence of ODQ. L-NAME present throughout. *P<0.05 Vs control using a 2way ANOVA with Bonferroni multiple comparisons test.

Repeated exposure to IPA/NO and Angeli's salt

Finally, the possibility of using repeated exposures of the two HNO donors was examined. A full cumulative concentration-response experiment was carried out for each artery, regardless of whether a smooth muscle Em recording could be maintained in examinations of hyperpolarization from resting Em. Arteries were then washed and left to rest for a minimum of 20 minutes, before a second cumulative concentration-response experiment was carried out. It was found that the maximal hyperpolarization of membrane potential from resting was attenuated for both IPA/NO (exposure 1: -31.26 ± 2.02 mV, n=4; exposure 2: -21.63 ± 1.97 mV, n=3) and AS (exposure 1: -20.16 ± 4.21 mV, n=4; exposure 2: -11.40 ± 8.21 mV, n=3). Pre-constriction in the AS experiments was provided by U46619, as the experiments were conducted whilst undertaking a different body of work where U46619 pre-constriction was required. In contrast, no significant difference was observed between the two exposures of IPA/NO and AS in experiments examining the relaxation in response to the HNO donors (**Figure 3.3.6**).

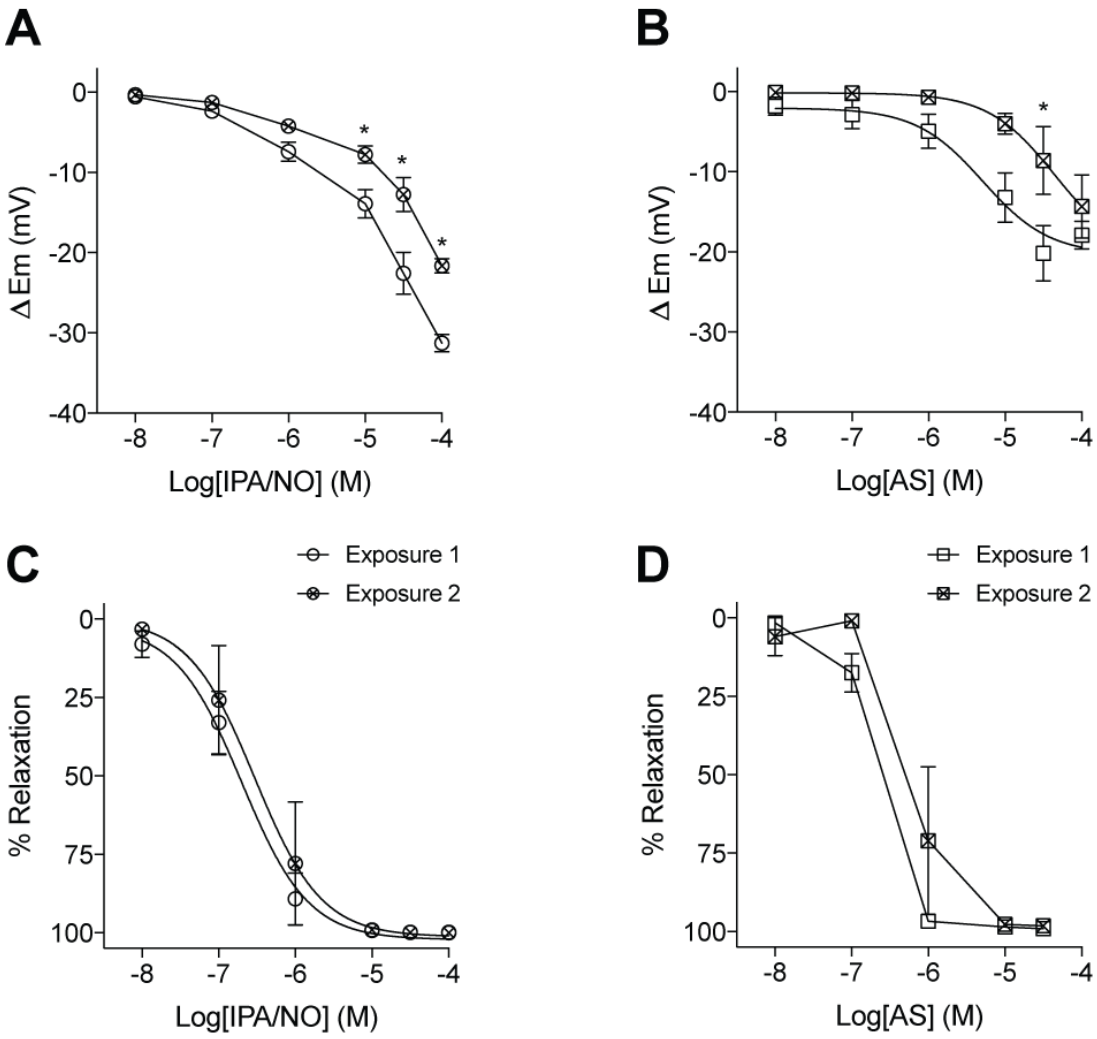


Figure 3.3.6: The effect of repeated exposure to HNO donors on relaxation and hyperpolarization in rat mesenteric arteries.

Hyperpolarization from resting membrane potential was significantly decreased by repeat exposure to both (A) IPA/NO (Exposure 1 n=7; Exposure 2 n=6) and (B) Angeli's salt (AS; Exposure 1 n=9, pEC50 = 5.29; Exposure 2 n=4, pEC50 = 4.35). No difference in relaxation was observed between repeated exposures to (C) IPA/NO (Arteries pre-constricted using PE; Exposure 1 n=10, pEC50 = 6.70; Exposure 2 n=5, pEC50 = 6.53) or (D) AS (Arteries pre-constricted using U46619; Exposure 1 and 2 n=2). L-NAME was present throughout. * P<0.05 using a 2way ANOVA with Bonferroni multiple comparisons test. Differences between exposures in relaxation experiments were assessed using a two-tailed t-test. Where applicable, curves were fitted using the three-parameter equation.

3.4 Discussion and future work

This chapter provides a direct comparison between IPA/NO and AS. More importantly it provides the first exploration of the changes in membrane potential, in non-constricted arteries, in response to IPA/NO. Currently most investigations into the action of HNO in the vasculature employ the use of AS as the donor compound (Andrews et al., 2009; Favaloro & Kemp-Harper, 2007; Favaloro & Kemp-Harper, 2009; Irvine et al., 2003; Yuill et al., 2011).

Examination of both hyperpolarization, from resting membrane potential, and relaxation in response to both HNO donors demonstrated that there were only minor differences between the two when all data sets were included. However, later batches of IPA/NO stock were more potent with near full relaxation occurring at concentrations of 100 nM, thus only control experiments from equivalent batches were used when comparisons were made with different treatments. Whilst results from studies using AS as the donor compound are not directly comparable to those using IPA/NO, the minor differences between the two compounds means IPA/NO is certainly a useful alternative to AS as a donor of HNO.

The hyperpolarization generated by AS in this study was similar to that in the study by Yuill et al. (2011). In their study, sharp microelectrode recordings of rat mesenteric artery SMC showed a hyperpolarization of 7.3 ± 2.0 mV to 10μM AS and patch clamp recordings revealed a hyperpolarization of 17 ± 1 mV, meaning that our result of 13.2 ± 3.1 mV, to 10 μM AS, is comparable to their findings. The larger hyperpolarization generated in our sharp microelectrode studies, compared to their results, could potentially be due to the presence of

carboxy-PTIO in their study, which may have affected their recordings by lowering resting Em. In our hands, carboxy-PTIO repeatedly caused sharp microelectrode recordings to 'drift' once in a cell, this lowered the observed resting membrane potential and thus affected the recordings generated (results not shown). Whether the more negative membrane potential was real or an artefact has yet to be investigated further, however, given that the resting membrane potential in the Yuill et al. (2011) study was -57.6 ± 2.5 mV, compared to -49.3 ± 1.0 mV in our study, it is possible that the presence of carboxy-PTIO does affect membrane potential. Similar results were observed by Favaloro and Kemp-Harper (2009), where the resting membrane potential was recorded as approximately -62 mV and the addition of 10 μM AS hyperpolarized the cell by 6.1 ± 1 mV in the presence of carboxy-PTIO (200 μM) and EDTA (26 μM). It should also be noted that the experimental conditions of these studies differed from the current study, in that no-L-NAME was present and carbogen was used to bubble the bath solution. In our hands, the resting Em of smooth muscle cells becomes more positive in the presence of L-NAME, therefore the lower Em recorded by Yuill et al (2011) and Favaloro and Kemp-Harper (2009) could be explained by this experimental condition. Carbogen, a mixture of 95% O_2 and 5% CO_2, is close to the O_2 concentration present in blood and has a significantly higher concentration of O_2 in comparison to the air mixture used in this study (21% O_2). It is possible that the difference could also affect how the arteries respond to different treatments.

The relaxation of mesenteric arteries to both HNO donors is consistent with the relaxation demonstrated in previous studies, with full relaxation occurring at ~1 μM of the respective HNO donor compound (Favaloro & Kemp-Harper,

2009; Irvine et al., 2003). The relaxation generated to HNO, in the presence of HNO/NO scavenging compounds L-cysteine and HXC, is similar in our study to that of Irvine et al. (2003) and Yuill et al. (2011) who used carboxy-PTIO as a scavenger of NO. As expected the response to AS was reduced in the presence of L-cysteine, but unaffected by HXC, which is comparable to the results generated using carboxy-PTIO. As with AS, the results for IPA/NO demonstrated no discernible effect of scavenging NO. Due to its effect on membrane potential, carboxy-PTIO was not used in sharp electrode recordings and was replaced by HXC as a scavenger of NO. As with the relaxation experiments, HXC had no effect on hyperpolarization to IPA/NO, but L-cysteine significantly reduced the hyperpolarization response. It is clear from our results that HNO is the main component, released from IPA/NO and AS, responsible for the observed hyperpolarization.

In line with previous studies using AS the sGC inhibitor, ODQ, significantly inhibited the relaxation response to IPA/NO, with complete block achieved for concentrations below 10 μM (Favaloro & Kemp-Harper, 2009; Irvine et al., 2003; Wanstall et al., 2001). In addition, the relaxation response to IPA/NO in arteries pre-constricted with 123 mM K^+ Krebs was comparable to that observed by Irvine et al. (2003) when taking into consideration the lower concentration of K^+ used in their study (30 mM). In our study, at higher concentrations of IPA/NO (>10 μM) the effect of ODQ was overcome, however, the combination of ODQ and high K^+ completely blocked the response to IPA/NO, as previously reported by Irvine et al. (2003), who attributed the response to a cGMP-independent mechanism of smooth muscle relaxation, namely voltage-gated K^+ (K_V) channels.

Given the tricky nature of sharp microelectrode experiments it was decided to examine the possibility of repeated exposure to HNO donors in order to increase the amount of data that could be generated from a single artery. Some studies explicitly state that only one concentration-response curve to HNO donors was obtained for each artery without reference to an explanation (Favaloro & Kemp-Harper, 2009; Irvine et al., 2003). Our results demonstrate that in experiments examining the relaxation to IPA/NO, dual exposure has no effect on the relaxation produced. This contrasts with the results obtained from resting membrane potential, where repeat exposure significantly attenuated the hyperpolarization to IPA/NO. Repeat exposure was also examined for AS, where it was found that both hyperpolarization and relaxation were affected visually but not significantly. Based on these findings, it is advisable not to repeat exposure to AS or IPA/NO in studies investigating the effects on membrane potential, or for studies employing the use of AS for relaxation. IPA/NO may be used repeatedly, with caution, for experiments solely examining relaxation and therefore offers an advantage over AS as a donor of HNO.

The next stages of this investigation would be to examine the involvement of K^+ channels at the higher concentrations of IPA/NO. As discussed earlier, Irvine et al. (2003) attributed the sGC/cGMP-independent mechanism to activation of K_V channels. Pilot studies in our lab have demonstrated that, in the presence of ODQ, iberiotoxin significantly inhibits the relaxation to IPA/NO compared to IPA/NO with ODQ alone, thus suggesting a role for BK_{Ca} channels. Irvine et al. (2003) initially discounted the involvement of BK_{Ca} due to no significant alteration in the relaxation to AS in arteries mounted in a wire-myograph. A later study by Yuill et al. (2011), employing the use of pressure myography and

sharp microelectrode recording, demonstrated that a combination of both BK_{Ca} and K_V channels contribute to both relaxation and hyperpolarization of rat mesenteric arteries. The discrepancy between the two studies could be due to the techniques employed in the studies; it may be that ODQ is required to 'unmask' the effect of K^+ channels in wire-mounted arteries and therefore this discrepancy between preparations warrants further investigation.

In future investigations, we may also characterize newer generations of NONOates, such as AcOM-IPA-NO, which offer longer half-lives and therefore present the opportunity to examine chronic, as opposed to acute, exposure to HNO.

3.5 Conclusion

In conclusion, we have demonstrated that the responses to IPA/NO in rat mesenteric arteries are similar to those of AS, thus presenting IPA/NO as a viable, and comparative, alternative to AS in organ bath studies. We have also confirmed that a sGC/cGMP-independent pathway exists and K^+ channels are the main component of this secondary pathway. Finally, we have demonstrated that it is possible to repeat exposure to IPA/NO in experiments examining relaxation, but is not advisable for examinations of membrane potential, or for the HNO donor AS.

Chapter 4

Neurovascular Involvement in the response to HNO

4.1 Introduction

In 2014 Eberhardt et al demonstrated that HNO, generated through the reaction of NO with H_2S, could directly activate TRPA1 channels expressed on the membrane of Chinese hamster ovary cells. The activation of TRPA1 by HNO was further confirmed in dorsal root ganglion (DRG) neurons from wild type mice, where an increase in Ca^{2+} to Angeli's salt (AS) correlated with the response to the TRPA1 agonist allyl isothiocyanate (AITC). They subsequently linked the activation of TRPA1 to the release of CGRP and resulting hypotensive/dilatory effect of HNO in both mice and rats. Following this publication, we wished to examine the role of the HNO-TRPA1-CGRP pathway in the response to IPA/NO.

4.1.I Transient receptor potential A1 (TRPA1) channels

Transient receptor potential ankyrin 1 (TRPA1) belongs to a family of receptors named transient receptor potential (TRP) channels. The family consists of 28 subunit genes, which are subdivided into 6 subfamilies: TRPA, TRPC, TRPM, TRPML, TRPP, and TRPV (Ramsey et al., 2006).

TRPA1 is a homotetramer, where the 4 subunits are arranged forming a pore at the central axis. Each subunit consists of 6 transmembrane α-helices (S1-S6), with both the N- and C-terminal domains located intracellularly and a selectivity filter located between the S5 and S6 transmembrane domains. The defining feature of TRPA1 is the long ankyrin repeat (between 14 and 18 repeats) located within the N-terminal domain, which gives the channel its name (**Figure 4.1.1**; Chen and Hackos (2015)). TRPA1 is highly permeable to Ca^{2+}, in

addition to other monovalent and divalent cations, meaning that upon activation TRPA1 can depolarize the membrane of the cells it is expressed in and can initiate Ca^{2+} signalling (Chen & Hackos, 2015; Doerner et al., 2007; Zurborg et al., 2007).

A large number of factors have been proposed to activate TRPA1, including temperature, mechanosensitivity and stimulation by a number of agonists, of both natural and industrial origin (reviewed by Zygmunt and Hogestatt (2014)). TRPA1 is particularly sensitive to 'danger' signals and has been implicated in pain sensation, cough in response to respiratory irritants and histamine-independent itch (reviewed by Chen and Hackos (2015); Viana (2016)).

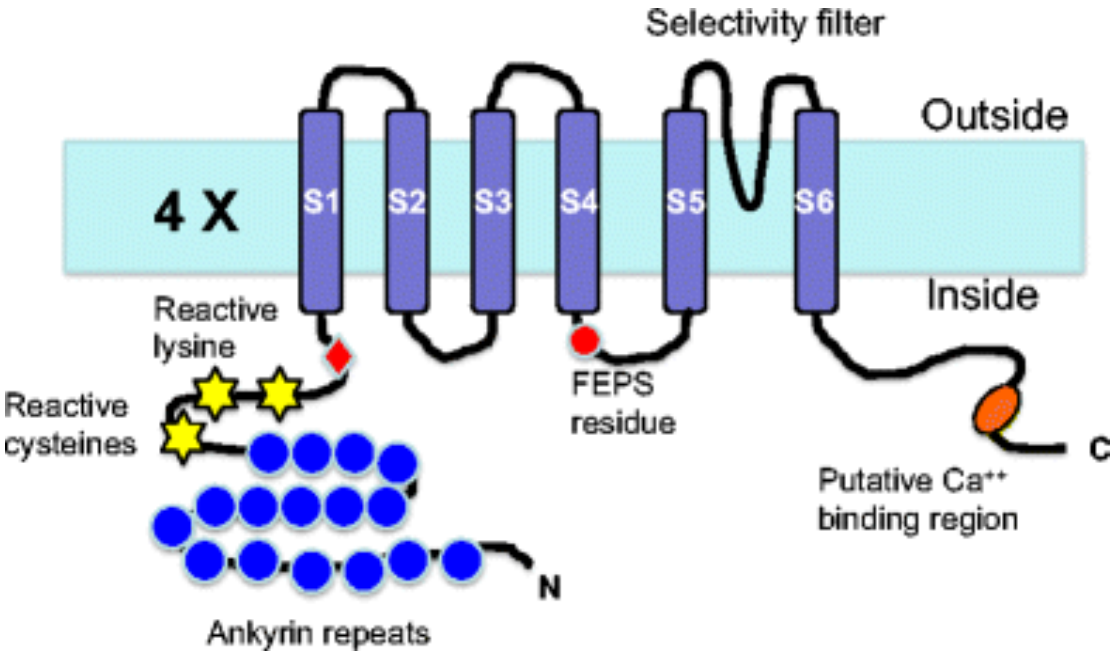


Figure 4.1.1: Structure of a single TPRA1 subunit.

Each subunit of the TRPA1 channel consists of 6 transmembrane α-helices, labelled S1-S6. The N- and C-termini are both located intracellularly, with the characteristic long chain of anyrin repeats located within the N-terminal domain. The reactive lysine and cysteine residues, where electrophilic agonists, such as AITC, form covalent adducts are also located within the N-terminal domain. The residues S5-S6 form the pore and selectivity filter of TRPA1, whilst the Ca^{2+} sensitive region attributed to channel regulation is located within the C-terminal domain. Taken from Chen and Hackos (2015).

4.1.II TRPA1 channel expression

TRPA1 is expressed in many different cell types of both neuronal and non-neuronal origin (Chen & Hackos, 2015; Zygmunt & Hogestatt, 2014). The channel is highly expressed in both Aδ- and C-fibre primary afferent somatosensory neurons of the DRG, trigeminal ganglia, and nodose ganglia and co-expression with TRPV1, a TRP channel sensitive to capsaicin, occurs in nearly all TRPA1 expressing DRG neurons (Bautista et al., 2006; Nagata et al., 2005). Non-neuronal cell types, where TRPA1 expression has been identified, include: lung fibroblasts and smooth muscle cells (Nassini et al., 2012), several skin cell types (Atoyan et al., 2009), beta islet cells of the pancreas (Cao et al., 2012), astrocytes (Shigetomi et al., 2012) and vascular endothelial cells (Earley, 2012).

4.1.III Aims

Eberhardt et al (2014) suggested HNO could potentially activate TRPA1 on perivascular nerves eliciting vasorelaxation. However, they provided no direct evidence of this process. Sullivan et al. (2015) demonstrated the presence of TRPA1 on the endothelium of cerebral arteries, but found no evidence of TRPA1 on the other vascular beds tested (mesenteric, renal and coronary). Therefore, the aim of this study was to clarify the observations and suppositions of Eberhardt *et al* (2014) in rat mesenteric arteries. In addition, we aim to confirm whether the finding of Sullivan et al (2015), i.e. a lack of TRPA1 on the endothelial cells of mesenteric arteries, is correct.

4.2 Materials & Methods

4.2.I Wire myography

Rat third order mesenteric arteries were pre-constricted with a sub-maximal concentration of phenylephrine (PE) or U46619 (~70% maximal tone). Except for L-NAME, all drugs were added directly to the bath and inhibitors were pre-incubated for a minimum of 30 minutes before dose response experiments were carried out. L-NAME (100 μM) was present throughout to prevent the basal and agonist-mediated release of nitric oxide (Dora et al., 2000).

For full details on the set up for wire myography studies please refer to **Methods & Materials section 2.2**.

4.2.II Sharp microelectrode studies of membrane potential

Rat third order mesenteric arteries were mounted and normalised to resting tension in an isometric wire myograph as previously described (**Methods & Material section 2.1 & 2.2**). The resting membrane potential (Em) of a single smooth muscle cell was examined by impalement with a sharp microelectrode back-filled with a 2M KCl solution. Inhibitors were added 30 minutes prior to impalement of the cell. Once a smooth muscle cell impalement had been successfully achieved (**Materials & Methods section 2.3.III**) increasing concentrations of IPA/NO, AS or CGRP were carefully added so as not to disturb the recording. All drugs were mixed through bubbling in the chamber. In common with the wire myography experiments L-NAME (100 μM) was present throughout all experiments.

For full details on the set up for sharp microelectrode studies please refer to **Methods & Materials section 2.3**.

4.2.III Immunohistochemistry

Rat third order mesenteric arteries were pressurized (**Materials & Methods 2.4.I**) or pinned (**Materials & Methods 2.4.II**) as required before being fixed and blocked on Day 1 and imaged and/or additional antibodies added on subsequent days as described in **Materials & Methods 2.4.III**.

4.3 Results

The location of TRPA1 in rat small mesenteric arteries

Prior to functional experimentation, the location of TRPA1 on mesenteric arteries was identified. TRPA1 staining was observed in the adventitia in addition to the presence of cell bodies (**Figure 4.3.1**). Some co-localisation with neurofilament light chain (NF-L) was also observed (**Figure 4.3.2**). These observations suggest that TRPA1 may be present on afferent sensory nerves. The endothelium was also examined for the presence of TRPA1. In pressurised arteries the results were unclear with no or very faint staining observed (**Figures 4.3.1B & 4.3.3A**). In contrast TRPA1-positive labelling was observed in the endothelium of en-face prepared pinned arteries (**Figure 4.3.3B**).

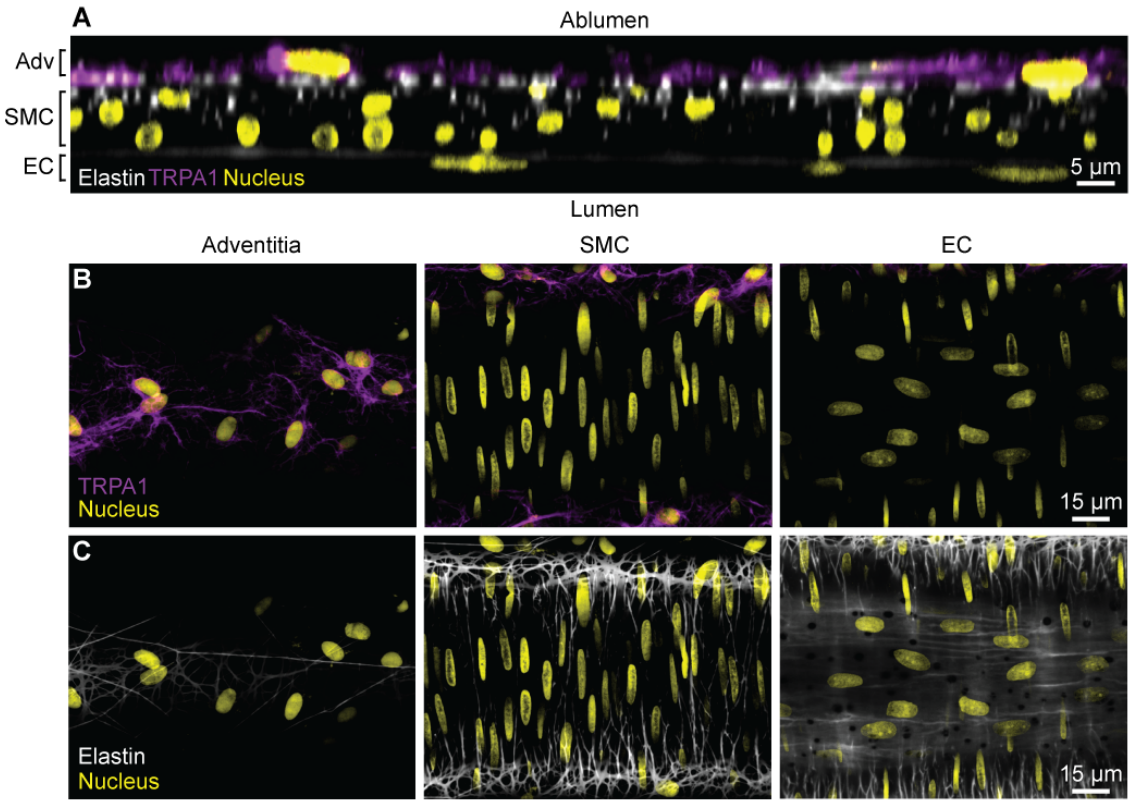


Figure 4.3.1: TRPA1 labelling in rat mesenteric arteries.

(A) Cross-section through the wall of a rat mesenteric artery demonstrating the presence of TRPA1 in the adventitia (Adv). Nuclei of endothelial cells (EC), smooth muscle cells (SMC) and cells in the adventitia are clearly labelled in their respective locations. The internal elastic lamina (IEL) is located above the EC layer and can be seen by the line of faint elastin staining. (B-C) Multiple sections were merged to give a clear indication of the location of TRPA1 in each arterial layer. (B) The TRPA1 staining indicated in the adventitia in (A) corresponds to labelling of TRPA1 on afferent neurons, with no demonstrable presence of TRPA1 in the SMC or EC layers. (C) The curvature of the artery is indicated by the elastin staining which is present between SMC and the IEL located between the SMC and EC layers. Perforations in the IEL can be identified where junctions between SMC and EC occur.

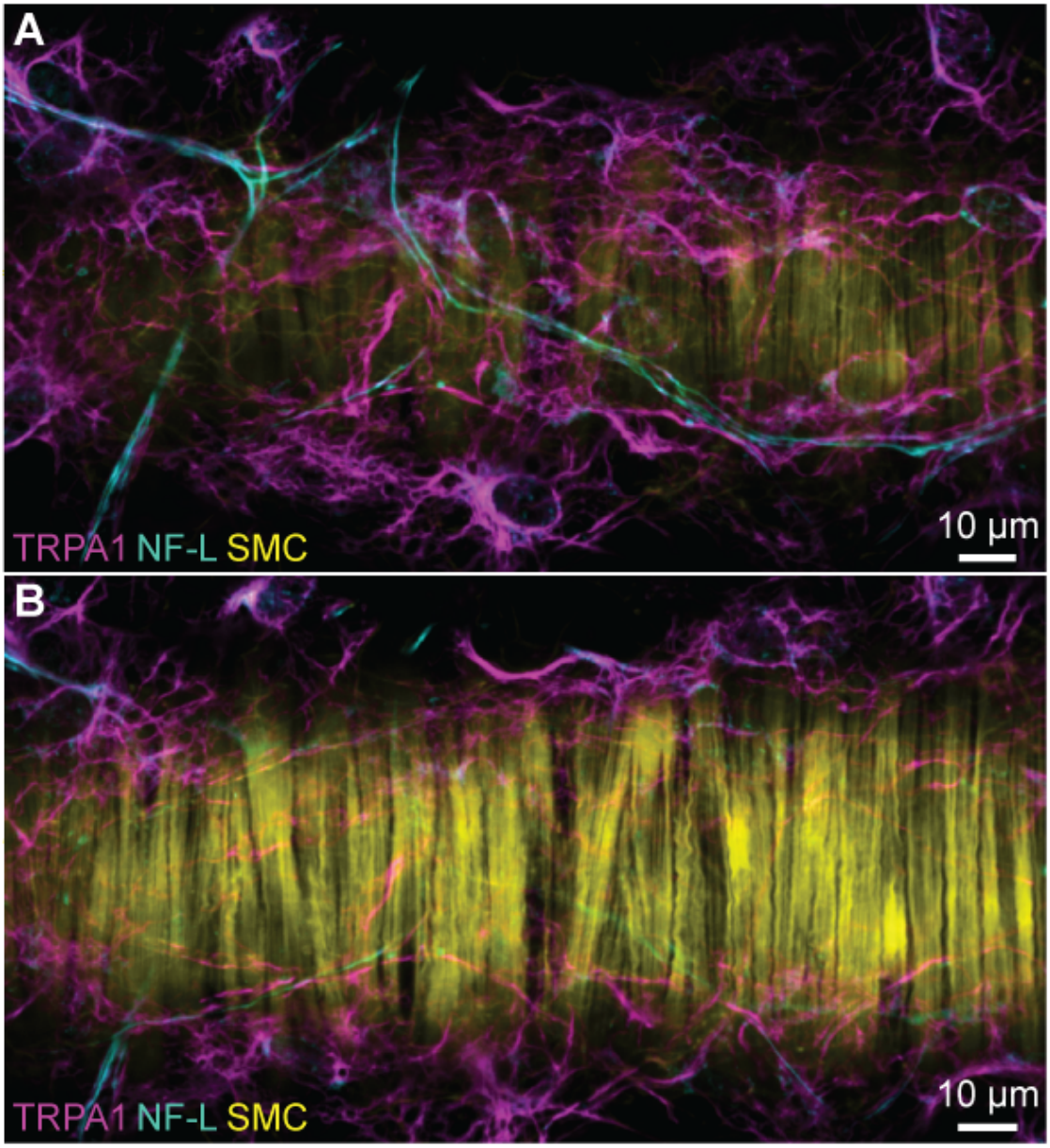


Figure 4.3.2: The presence of TRPA1 and neurofilament light chain in adventitia.

(A) TRPA1 labelling is clear in the adventitia of mesenteric arteries and is adjacent to neurofilament light chain (NF-L) in some afferents. (B) Phalloidin staining clearly identifies smooth muscle cells (SMC) where no TRPA1 or NF-L staining is present.

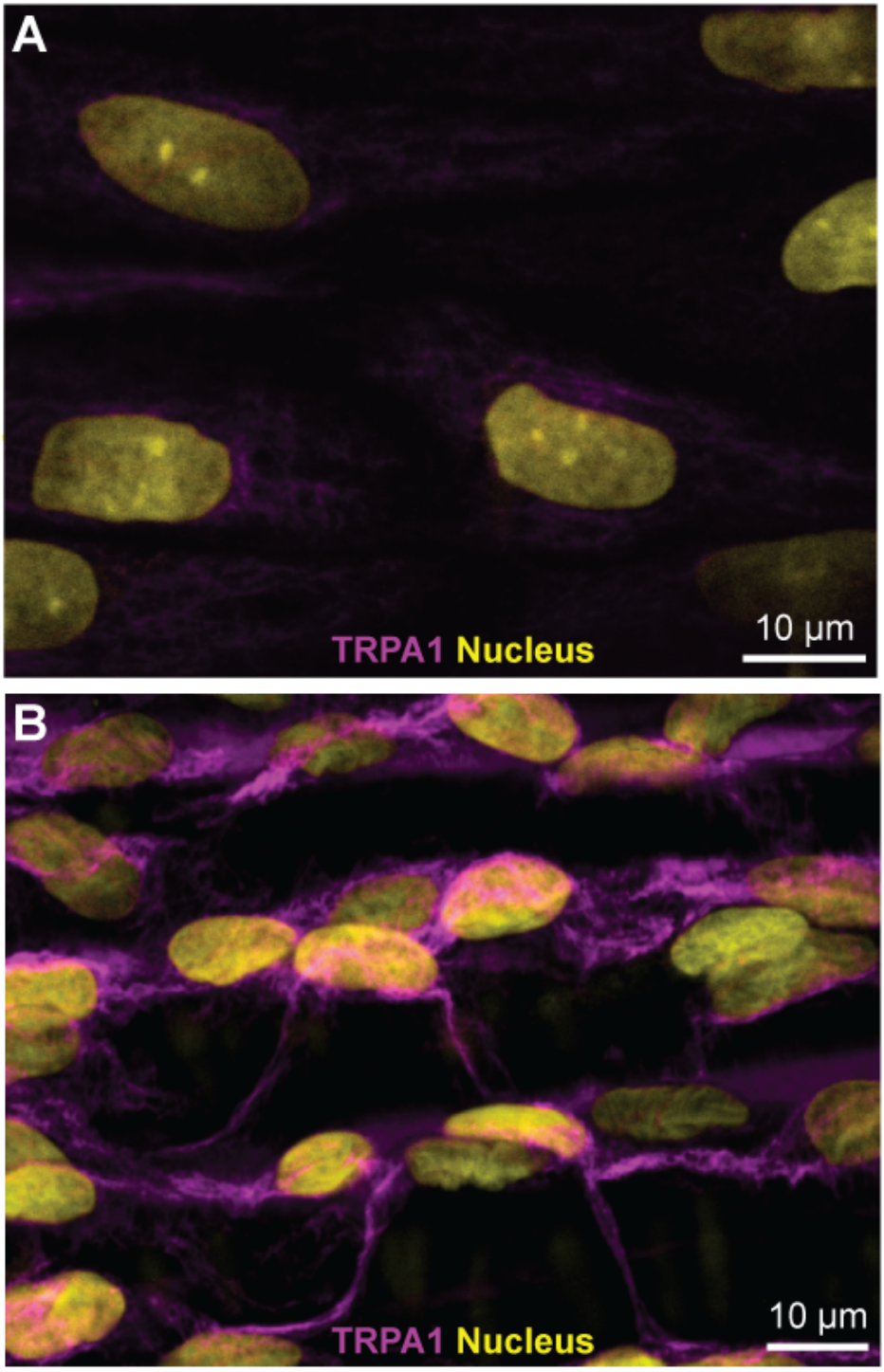


Figure 4.3.3: Identifying TRPA1 in the endothelium of mesenteric arteries.

(A) Staining for TRPA1 in the endothelium of pressurised arteries is unclear, however (B) TRPA1 staining was stronger in endothelium of en-face prepared pinned arteries. The presence of TRPA1 in the endothelium remains unconfirmed.

Functional response of mesenteric arteries to TRPA1 activation

Prior to examination of the role of TRPA1 in the response to HNO donors in mesenteric arteries, the effect of the TRPA1 activator AITC was examined. AITC was found to both hyperpolarize mesenteric arteries from resting membrane potential, and fully relax pre-constricted arteries. Pre-treatment with capsaicin, to deplete CGRP stores in sensory nerves, significantly attenuated the relaxation in response to AITC. The TRPA1 antagonist HC030031 (50 μM) also significantly reduced the relaxation to AITC. A single examination on the effect of HC030031 on hyperpolarization to AITC demonstrates that block of TRPA1 also affects changes in Em. (**Figure 4.3.4**).

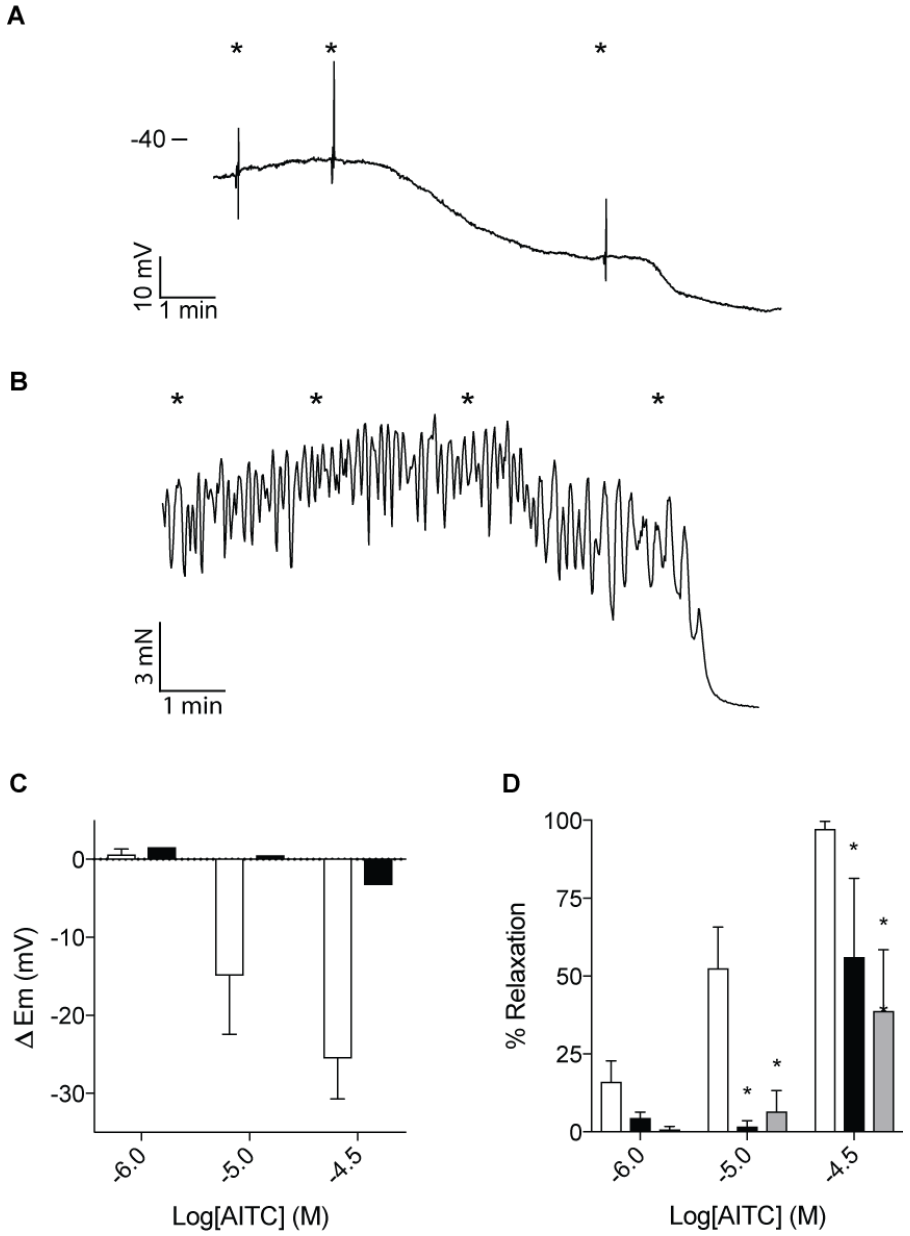


Figure 4.3.4: Examination into the effect of AITC in mesenteric arteries.

Increasing concentrations of AITC (A) hyperpolarize arteries from resting membrane potential (1 μM, 10 μM, 30 μM) and (B) relax pre-constricted arteries (1 μM, 3 μM, 10 μM, 30 μM). (C) Summary data, demonstrating the hyperpolarization produced by AITC (n=3) and inhibitory effect of the TRPA1 antagonist HC030031 (n=1). (D) Summary data for relaxation produced by AITC (n=7) and inhibition by HC030031 (n=4) and capsaicin pre-treatment (n=4). L-NAME was present throughout. Control (white), HC030031 (50 μM; black), capsaicin (1 μM; grey) * $P<0.05$ vs control using 2way ANOVA with Bonferroni multiple comparisons test.

Examination of the role of TRPA1 in the response to HNO

As discussed in **Chapter 3** the HNO donors AS and IPA/NO can relax pre-constricted arteries and produce hyperpolarization from resting membrane potential. The addition of the TRPA1 antagonist, HC030031 (50 μM; relaxation pEC50 = 7.95; hyperpolarization pEC50 = 5.86), had no effect on the relaxation produced in response to IPA/NO (relaxation pEC50 = 7.17; hyperpolarization pEC50 = 5.93), but significantly inhibited the hyperpolarization response. Mesenteric arteries depleted of CGRP through prior exposure to capsaicin (1μM; relaxation pEC50 = 7.40; hyperpolarization pEC50 = 5.74) were also examined. As with HC030031, the relaxation to IPA/NO was unchanged, whilst the hyperpolarization was significantly reduced at the higher concentrations of the HNO donor compounds (**Figure 4.3.5**).

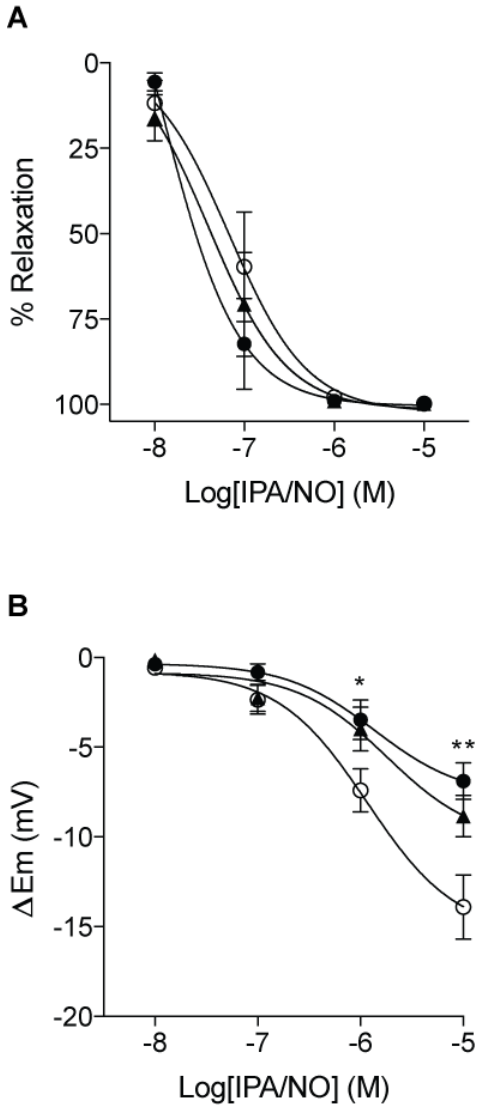


Figure 4.3.5: The role of TRPA1 in the response to HNO donors.

(A) The relaxation produced in response to isopropylamine NONOate (IPA/NO; ○ ; n=7) was unaffected by the addition of the TRPA1 antagonist HC030031 (● ; n=5). Pre-treatment of the arteries with capsaicin (▲; n=5) to deplete CGRP stores also had no effect on relaxation to IPA/NO. (B) Hyperpolarization in response to IPA/NO (n=7) was, however, significantly reduced by the addition of HC030031 (n=4) and capsaicin pre-treatment (n=6). * P<0.5 HC030031 vs control. ** P<0.05 HC030031 or capsaicin Vs control using 2way ANOVA with Bonferroni multiple comparisons test. L-NAME was present throughout. Curves were fitted using the three-parameter equation. Partial data sets were completed by Hamish Lemmey or Christopher Garland.

Examination of the role of CGRP in the relaxation and hyperpolarization of mesenteric arteries

The addition of CGRP (100 fM—30 nM) to pre-constricted mesenteric arteries produced full relaxation at 1 nM. CGRP also elicited a concentration-dependent hyperpolarization from resting membrane potential (**Figure 4.3.6**).

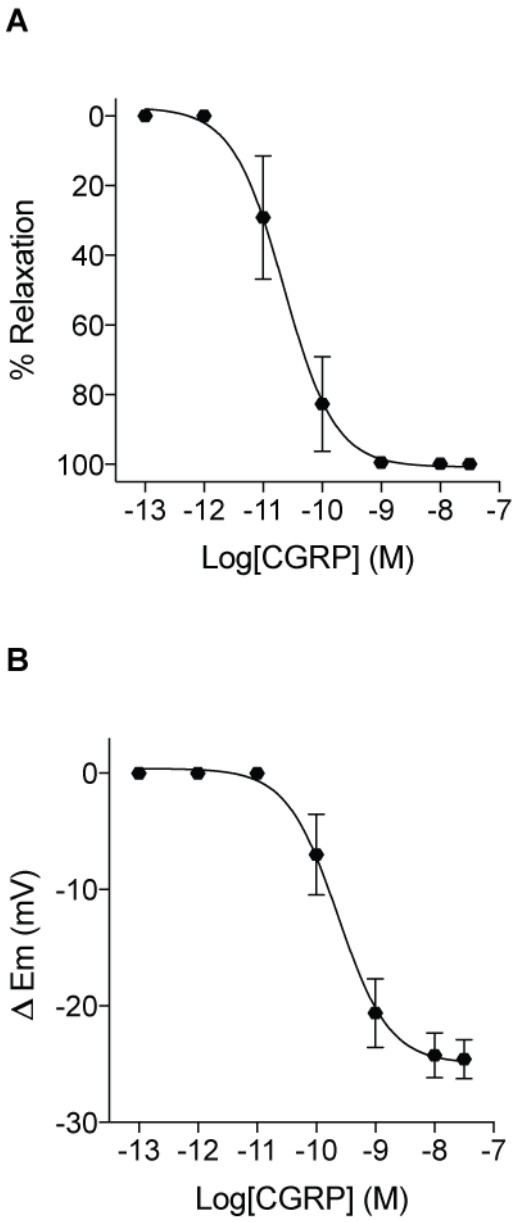


Figure 4.3.6: The effect of CGRP on mesenteric arteries.

(A) CGRP fully relaxed pre-constricted arteries (n=5; pEC50 = 10.65) and could also (B) hyperpolarize arteries from resting membrane potential (n=5; pEC50 = 9.63). Curves were fitted using the three-parameter equation. Data sets were acquired by Christopher Garland.

4.4 Discussion and future work

This chapter demonstrates the role of TRPA1 and CGRP in the response to HNO. Following the work by Eberhardt et al. (2014) who demonstrated that HNO may activate TRPA1 on perivascular nerves and postulated that subsequent CGRP release may be a key component in HNO induced vascular relaxation; we have demonstrated a role for the HNO-TRPA1-CGRP pathway in rat mesenteric arteries.

Immunohistochemistry demonstrated that TRPA1 was present in adventitial nerve fibres of rat mesenteric arteries, identified by the presence of cell bodies and co-localisation with NF-L. This finding is supported by a number of previous studies, such as that by Bautista et al. (2005) who demonstrated the presence of TRPA1 in ~22% of rat DRG neurons. They also found that TRPV1 was present in all TRPA1 expressing DRG neurons and that most TRPV1/TRPA1 positive cells also expressed CGRP. In relevance to our study they demonstrated the presence of TRPA1 and CGRP localised on adventitial nerve fibres of rat mesenteric arteries, thus indicating that TRPA1 is present on a subset of peptidergic sensory neurons.

Interestingly, positive staining for TRPA1 on mesenteric artery endothelial cells, in our study, was dependent on how the tissue was prepared. Pressurized arteries, luminally perfused with both primary and secondary antibodies showed no perceptible presence of TRPA1, however, pinned arteries that had been cut open in an en-face preparation showed strong staining for TRPA1. TRPA1 has been located in the endothelial cells of other vascular beds. Sullivan et al. (2015) and Earley et al. (2009) have demonstrated the presence of TRPA1 in

the endothelial cells of the cerebral vasculature and have also demonstrated a functional role of endothelial TRPA1 in vasodilation. Sullivan et al. (2015) also examined the presence of TRPA1 in mesenteric endothelial cells, using the same TRPA1 antibody as utilised in our study, and reported no presence of TRPA1. Due to the variability of TRPA1-staining in endothelial cells from our study it is still unclear whether TRPA1 is really present in our preparation. Further examination should therefore be carried out into a) the reliability of the TRPA1 antibody utilised and b) whether the TRPA1-staining in some preparations of mesenteric endothelial cells is real. This could be achieved by using an alternative TRPA1 antibody to confirm the staining seen with the Alomone antibody, or the endothelial cells could be isolated and stained separately. RT-PCR could also be carried out on both intact arteries and endothelial tubes, although this technique is reliant on enough genetic material being present in the samples taken to generate a read-out.

Functional experiments demonstrated no discernible role for the HNO-TRPA1-CGRP pathway, proposed by Eberhardt et al. (2014), in relaxation to donors of HNO, where no alterations to relaxation were observed when the HNO-TRPA1-CGRP pathway was inhibited. However, experiments examining the role of the HNO-TRPA1-GCRP pathway in hyperpolarization to HNO suggest that the release of CGRP, via TRPA1 activation, has some degree of importance.

A number of studies have examined the mechanism of CGRP mediated vascular relaxation, and can be related to the hyperpolarizing effects of CGRP that we have observed. The current consensus points towards a NO and

endothelium independent pathway, where CGRP directly activates CGRP receptors present on vascular smooth muscle; however, some tissues have been shown to require the presence of intact endothelium for relaxation to occur (Brain & Grant, 2004). The proposed endothelium-independent pathway, suggests that CGRP directly activates CGRP receptors on SMCs leading to an increase in cAMP, therefore suggesting the response to CGRP is mediated through adenylate cyclase (Hirata et al., 1988; Kubota et al., 1985). The increased levels of cAMP activate PKA which may open K_{ATP} and BK_{Ca} channels via phosphorylation (Dunn et al., 2003; Hong et al., 1996; Nelson et al., 1990). Whilst we have demonstrated that CGRP release has some role in the hyperpolarization to HNO, neither HC030031 nor CGRP depletion, through capsaicin pretreatment, completely abolished the response to HNO. It is therefore possible that the remaining hyperpolarization is driven by direct activation of K^+ channels such as K_{ATP} and K_V that have already been implicated in the vascular response to HNO dependent on vascular bed (Favaloro & Kemp-Harper, 2007; Irvine et al., 2003; Yuill et al., 2011).

In future, investigations into the remaining components of the HNO induced hyperpolarization could be carried out, however, given our observation that HNO induced hyperpolarization is not a driving factor in relaxation to HNO, attention may be best spent examining the effects of HNO in pre-constricted arteries as this may be more physiologically relevant. Other vascular beds, such as the cerebral vasculature could be investigated to determine if the HNO-TRPA1-CGRP pathway is relevant in HNO induced relaxation.

4.5 Conclusion

In conclusion, we have demonstrated a role for the HNO-TRPA1-CGRP pathway, as proposed by Eberhardt et al. (2014), in rat mesenteric arteries. Activation of TRPA1, by HNO, releases CGRP from perivascular sensory nerves, which then hyperpolarizes SMCs from resting membrane potential. We have seen no demonstrable role for the pathway in relaxation to HNO and therefore the clinical relevance of the pathway is questionable in mesenteric arteries. We have also provided further evidence for the presence of TRPA1 in perivascular nerves and have potentially seen evidence for TRPA1 in mesenteric endothelial cells, which warrants further investigation.

Chapter 5

An examination into the role of NO and HNO in vasomotion

5.1 Introduction

Vascular smooth muscle cells can spontaneously generate rhythmical contractions, which leads to oscillations of tone along significant lengths of arteries. This rhythmic oscillatory behaviour is termed ‘vasomotion’ (Nicoll & Webb, 1955; Nilsson & Aalkjaer, 2003) and was first observed in the bat wing in 1852 (Jones, 1852).

Since its initial observation over 160 years ago, vasomotion has been observed in a variety of vascular beds using many experimental techniques, ranging from myography and electrophysiology to intracellular ion imaging (Matchkov, 2010). Experimental limitations, such as the unpredictability of vasomotion, mean that it is often hard to draw reliable and/or reproducible conclusions from any results gained. Thus, there is continued scientific debate over both the mechanisms that underlie vasomotion and the physiological consequences of the oscillatory behaviour (Nilsson & Aalkjaer, 2003).

A number of theories pertaining to the physiological function of vasomotion have been proposed. It has been suggested that vasomotion may be beneficial in the regulation of blood flow. Using a mathematical model, Meyer et al. (2002) suggested that the oscillations of vasomotion result in a higher conductance of the vessel, and therefore blood flow, when compared to a vessel with the same average width and no oscillatory behaviour. It has also been suggested that vasomotion may be important in the regulation of tissue oxygenation. A model, developed by Tsai and Intaglietta (1993), suggests low frequencies of oscillation increases the ability of oxygen to diffuse to the capillaries and penetrate the surrounding tissue, thus oxygen becomes more evenly

distributed. This finding is supported by the work of Rucker et al. (2000) who studied vasomotion in the rat hindlimb. It was found that a reduction in perfusion triggered the development of vasomotion in most preparations; but more importantly, they demonstrated that vasomotion was an important factor in the redistribution of blood flow from muscle to neighbouring tissue, thus maintaining appropriate tissue oxygenation in surrounding tissues under conditions of reduced perfusion.

Whilst the physiological importance of vasomotion has not yet been fully elucidated, the mechanisms that underlie its development have begun to be unravelled and are discussed below.

5.1.I Mechanisms of vasomotion

With the improved understanding of the various cellular mechanisms that form the foundation for vasomotion, three different cellular oscillators have been proposed and will be outlined below (reviewed by Aalkjaer and Nilsson (2005)).

Two main types of cellular oscillators have been defined by Berridge and Rapp (1979), membrane oscillators and cytosolic oscillators. Membrane oscillators are determined by the generation of oscillations at the membrane, i.e. through transporters or fluctuations in permeability, whilst cytosolic oscillators are driven by intracellular mechanisms, such as calcium release. The third type of oscillator model described by Aalkjaer and Nilsson (2005), is a metabolic oscillator, which is also cytosolic in origin.

The proposed cytosolic oscillator responsible for vasomotion is a repetitive fluctuation in calcium. It has been well established that levels of intracellular

calcium can oscillate (Weissberg et al., 1989) and form waves that radiate along the long axis of smooth muscle cells (reviewed by Lee et al. (2002)). These waves are generated through release of calcium from the sarcoplasmic reticulum (SR) and require re-uptake of calcium to maintain the oscillations (Iino et al., 1994; Miriel et al., 1999; Ruehlmann et al., 2000). Activation of IP_3 receptors has been determined as the driving force underlying initiation of calcium waves, although other channels such as an IP_3-sensitive channel, a ryanodine or caffeine-sensitive channel, or a nicotinic acid adenine dinucleotide phosphate (NAADP)-sensitive channel may be involved in the calcium-induced calcium release that propagates the waves (Aalkjaer & Nilsson, 2005; Boittin et al., 2002; Boittin et al., 1999; McCarron et al., 2004a; McCarron et al., 2004b; Peng et al., 2001). The declining phase of the calcium waves is driven by a combination of the refractoriness of calcium release channels and/or refractoriness to IP_3, leading to a reduction in calcium release and active removal of calcium from the cytosol (Lee et al., 2001; McCarron et al., 2004a). In order for an oscillation to develop, a phase shift (where the feedback signal becomes out of phase with the initiating event) needs to occur. A phase shift can be generated by inertia in one of the steps of the feedback loops described above, such as slow refilling of the SR after calcium release which underlies the generation of calcium waves (Aalkjaer & Nilsson, 2005).

An oscillator of metabolic origin was proposed by Siegel and the concept summarised by Aalkjaer and Nilsson (2005). The metabolic oscillator is suggested to be driven by oscillations in glycolysis, which may lead to oscillations in concentrations of ATP. The fluctuations in concentration of ATP

may alter the activity of the Na,K-pump causing it to also oscillate, ultimately driving oscillations in membrane potential (Aalkjaer & Nilsson, 2005).

The evidence for a membrane oscillator derives from studies where oscillations have been observed after calcium-induced calcium release has been inhibited (Aalkjaer & Nilsson, 2005). Experiments by Omote *et al.* (1992; 1993; 1993) demonstrated that oscillations could still be generated in rabbit arteries after inhibition of SR Ca^{2+}-ATPase or ryanodine-sensitive receptors. The remaining oscillations could be inhibited by charybdotoxin and iberiotoxin, suggesting the involvement of both BK_{Ca} and voltage gated potassium channels (K_V). IP_3 receptors may also be stimulated by increased concentrations of calcium (Taylor & Tovey, 2010). However, it is yet to be investigated whether inhibition of IP_3 receptors, in combination with inhibition of both SR Ca^{2+}-ATPase and ryanodine-sensitive receptors would inhibit the observed oscillations. Interestingly, high concentrations of the SR Ca^{2+}-ATPase inhibitor, cyclopiazonic acid, inhibited all oscillatory behaviour, thus demonstrating that the SR is important in maintaining membrane driven oscillations (Griffith & Edwards, 1997). For this reason, the membrane and cytosolic oscillators should be considered in conjunction with one another (Aalkjaer & Nilsson, 2005).

It has been suggested by Griffith et al. (2009) that chaos theory may be applied to the generation of vasomotion. In an earlier review, Griffith (1996) suggested four key dominant control variables that may underlie the generation of chaotic vasomotion: cytosolic Ca^{2+}, Ca^{2+} located in the SR, membrane potential, and outward flux of K^+ across the cell membrane, thus both membrane and cytosolic oscillators are implicated when chaos theory is applied to vasomotion. An

important aspect of chaos theory is that a small change in one of the underlying variables of vasomotion leads to dramatic changes in the vasomotion produced, such as the dysregulation observed in the absence of NO (see **Figure 5.3.1**).

The oscillations of vasomotion are not limited to individual smooth muscle cells, but are in fact synchronous along millimetre lengths of arteries. Due to this characteristic, it is highly likely that electrical communication between cells is an essential feature of vasomotion (Nilsson & Aalkjaer, 2003). Another key feature of vasomotion is the underlying fluctuation in membrane potential, which oscillates with the same frequency, but in advance of, the oscillations in tension (Hill et al., 1999).

For vasomotion to occur, it has been suggested that entrainment of the calcium oscillations, driven by the SR, needs to occur throughout the length of the artery. Peng et al. (2001) proposed that the intermittent calcium release from the SR activates a depolarizing current. The depolarizing current then radiates out to other smooth muscle cells, initiating calcium influx into these cells. This synchronous influx of calcium, through voltage-dependent calcium channels, increases the likelihood of synchronised calcium release from the SR, and thus synchronised calcium oscillations and the initiation of vasomotion.

5.1.II Alteration of vasomotion in disease

Several disease states have been implicated in the alteration of vasomotion. Whilst the role of vasomotion in these conditions is still to be clarified, it is interesting to note the effects of disease on normal arterial function.

In diabetic patients, it has been observed that vasomotion is less prevalent. Stansberry et al. (1996) concluded that vasomotion was impaired in up to 75% of diabetics. Multiple studies have also shown that, in *in vivo* animal models of diabetes, vasomotion is significantly suppressed, but can be enhanced by metformin, a treatment used in the management of non-insulin dependent diabetes (Bouskela et al., 1997; Renaudin et al., 1999).

Vasomotion is also altered in hypertension. In contrast to diabetes, hypertension enhances the prevalence of vasomotion in multiple rat models, whilst treatment with ACE inhibitors reduces the prevalence of vasomotion (Bandick & Sparks, 1970; Holloway & Bohr, 1973; Lamb & Webb, 1989; Sada et al., 1990; Watts et al., 1994).

Given that there is so much yet to still resolve regarding the mechanisms and physiological importance of vasomotion, it is important that further research attention is given to the phenomenon.

5.1.III Aims

Given the lack of clarity with regards to the generation of vasomotion, in this study we will attempt to begin to address how vasomotion is affected under conditions of reduced NO bioavailability, which is a common occurrence in diseased arteries.

5.2 Methods & Materials

5.2.I Wire myography

Rat third order mesenteric arteries were used to examine the effects of increasing concentrations of phenylephrine (PE). All inhibitors or scavengers were pre-incubated for a minimum of 20 minutes before dose response experiments were undertaken. Both L-cysteine and L-NAME were prepared as working-concentration solutions in Krebs because of the effect on pH when added directly to the bath (see **section 3.2.i**).

For full details on the set up for wire myography studies please refer to **Methods & Materials section 2.2**.

5.2.II Sharp microelectrode studies of membrane potential

Rat third order mesenteric arteries were mounted and normalised to resting tension in an isometric wire myograph as previously described (**Methods & Materials 2.1 & 2.2**). The resting membrane potential (Em) of a single smooth muscle cell was examined by impalement with a sharp microelectrode back-filled with a 2M KCl solution. Inhibitors were added at least 20 minutes prior to impalement of the cell. Once a smooth muscle cell impalement was established (**Methods & Materials section 2.3.iii**) increasing concentrations of PE were applied, with and without the presence of inhibitors and scavengers. All drugs were applied carefully, to not disturb the recording, and were mixed through bubbling of the chamber.

5.3 Results

The effect of L-NAME on membrane potential in rat smooth muscle cells

In previous studies from our group the addition of L-NAME alters the membrane potential of rat smooth muscle cells when constricted with PE. The absence of NO, or one of its redox variants, leads to the generation of spikes at the peaks of the fluctuations in membrane potential that underlie vasomotion (**Figure 5.3.1**).

Examination of the development of spikes

Initial work was undertaken to examine the development of spike generation over increasing concentrations of PE (**Figure 5.3.2**). It was consistently found that at high concentrations of PE the spikes diminished. Following these observations, a range between 500 nM and 700 nM PE was determined as suitable to use for subsequent experiments examining Em spikes.

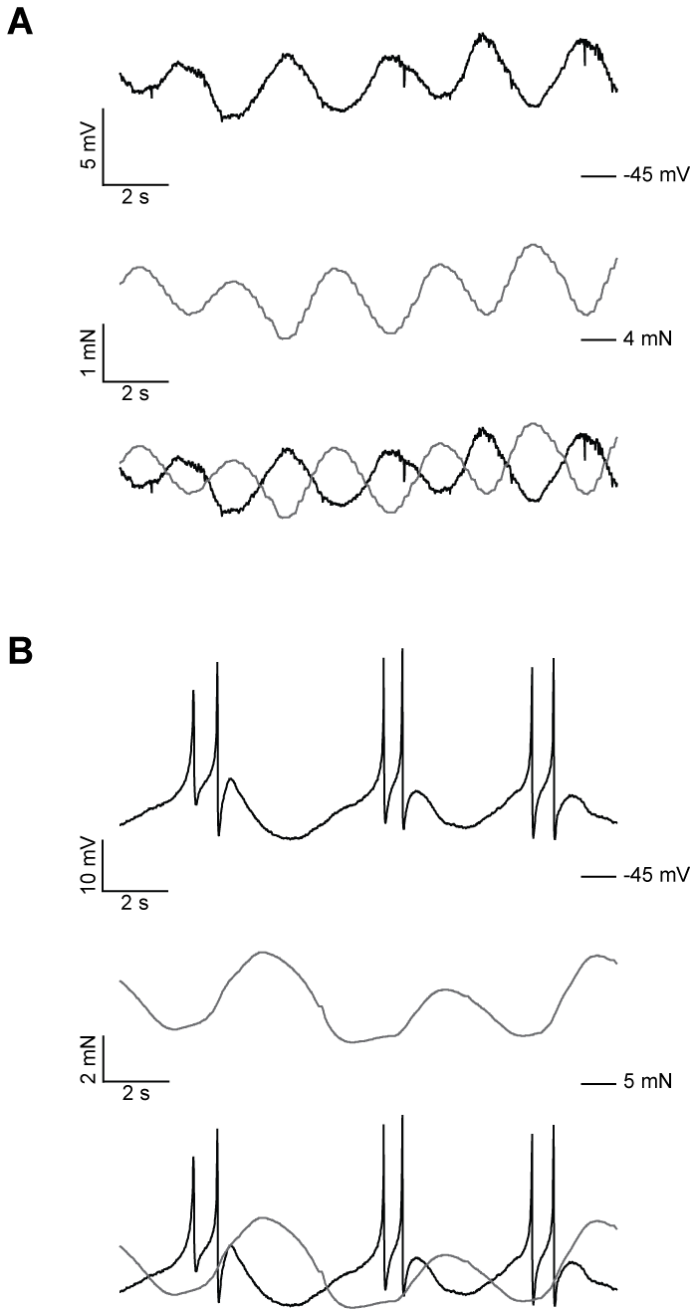


Figure 5.3.1: Simultaneous recording of membrane potential (Em) and tension

(A) recording of membrane potential and tension in rat mesenteric arteries constricted with phenylephrine (1 μM). Fluctuations in Em precede the fluctuations in tension. (B) recording of membrane potential and tension in rat mesenteric arteries constricted with phenylephrine (500 nM) and in the presence of L-NAME. Spikes develop and increase the fluctuations in tension that follow the underlying changes in Em.

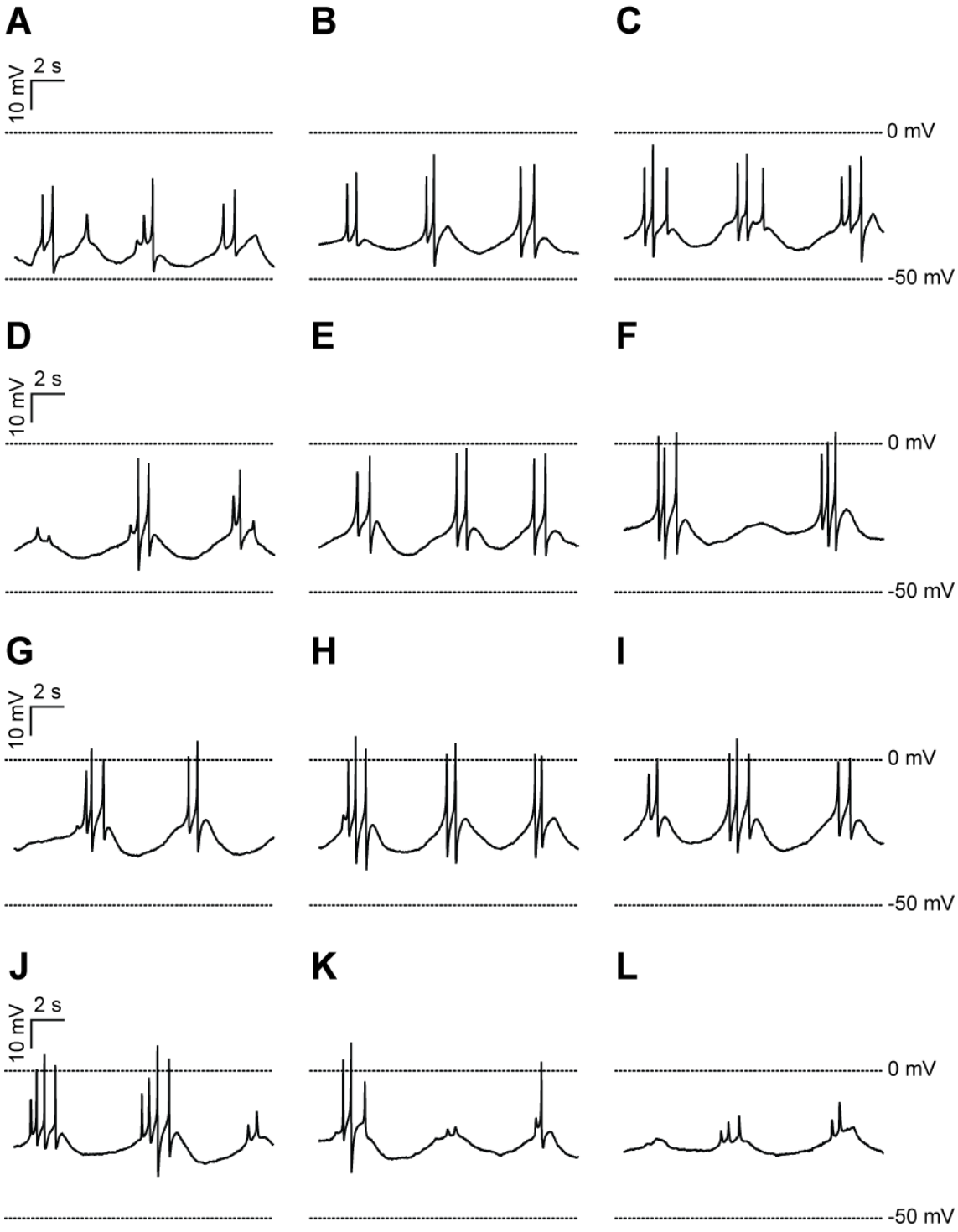


Figure 5.3.2: Generation of spikes at increasing concentrations of PE

Increasing concentrations of PE were added to rat mesenteric arteries pre-incubated with 100 μM L-NAME. Dashed line indicates Em = 0 mV or -50 mV as indicated (A) 100 nM (B) 200 nM (C) 300 nM (D) 400 nM (E) 500 nM (F) 600 nM (G) 700 nM (H) 800 nM (I) 900 nM (J) 1 μM (K) 1.5 μM (L) 2 μM.

The effect of NO and HNO scavengers on vasomotion and spike generation

Following our initial observations, that the addition of L-NAME induced membrane potential spike generation, we aimed to determine which redox variant of NO was responsible for spike suppression in untreated arteries. Early attempts were made to inhibit spikes in arteries treated with L-NAME by directly applying IPA/NO to the bath. This method was unsuccessful as relaxation and then hyperpolarization occurred before any spike suppression was observed. This method was therefore developed. In the revised method SNOG, a donor of NO, and IPA/NO were applied prior to vessel constriction with PE. This method was slightly more successful, but not surprisingly required a higher concentration of PE to elicit constriction (~1 μM). Results using this method remain unclear due to difficulty sustaining a recording during constriction.

As an alternative to direct spike examination, cumulative concentration-response experiments for PE, recording tension, were carried out in the presence of either L-NAME (100 μM), hydroxocobalamin (HXC; 100 μM), L-cysteine (3 mM), or NAC (3 mM). Experiments were not paired. As anticipated L-NAME caused a significant left shift in the response to PE. HXC significantly increased the response to PE at 1 μM, but not to the extent of L-NAME (**Figure 5.3.3a**). Neither L-Cysteine nor NAC had any effect on the response to PE (**Figure 5.3.3b**).

Additional analysis was undertaken to examine the change in amplitude of vasomotion over increasing concentrations of PE and at increased tension. Using data obtained from the cumulative concentration-response experiments displayed in **Figure 5.3.3**, a comparison between PE concentration and

amplitude of the fluctuations in tension was undertaken using inbuilt LabChart analysis software. An additional comparison was made between % constriction and amplitude of the fluctuations in tension, also using LabChart software. The analysis demonstrated that vasomotion was reduced at higher concentrations of PE. The same result was seen with increased constriction (**Figure 5.3.4**).

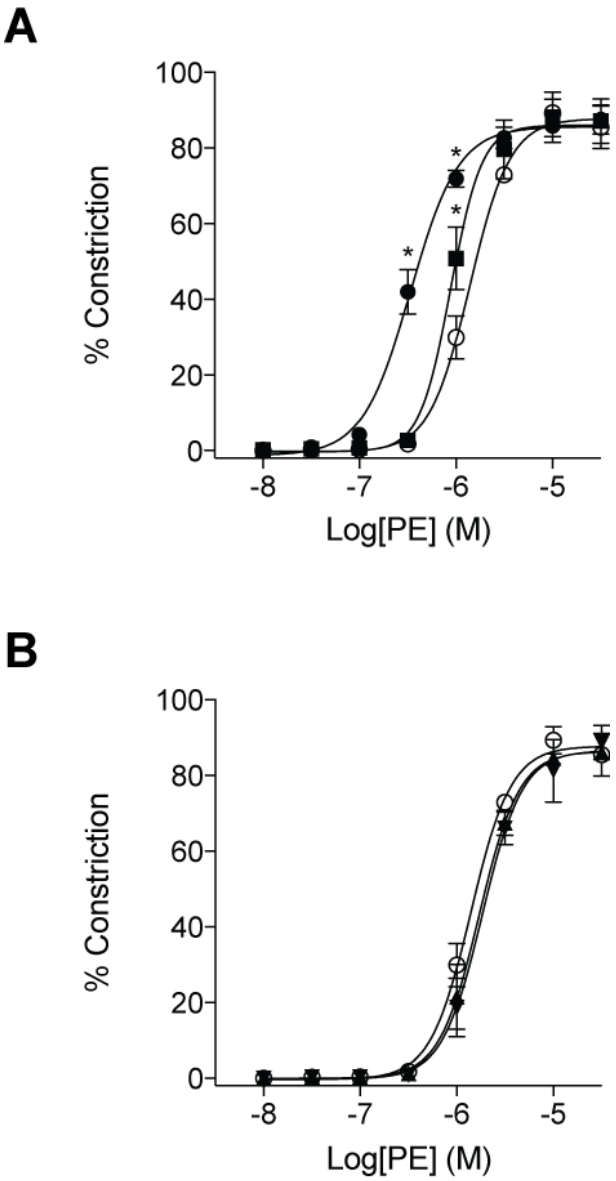


Figure 5.3.3: The effect of HNO and NO on the response to phenylephrine in rat mesenteric arteries.

(A) 100 μM L-NAME (●; pEC50 = 6.47) and 100 μM HXC alone (■; pEC50 = 6.05), a NO scavenger, significantly enhanced the response to PE (○; pEC50 = 5.86). (B) L-cysteine (3 mM; ▲; pEC50 = 5.77), a scavenger of HNO, and NAC (3 mM; ▼; pEC50 = 5.74), a cell permeant scavenger of HNO, had no effect on the response to PE (○). Curves were fitted using the four-parameter equation. * = $p<0.05$ using 2way ANOVA with Bonferroni multiple comparison test. n=4 for each treatment.

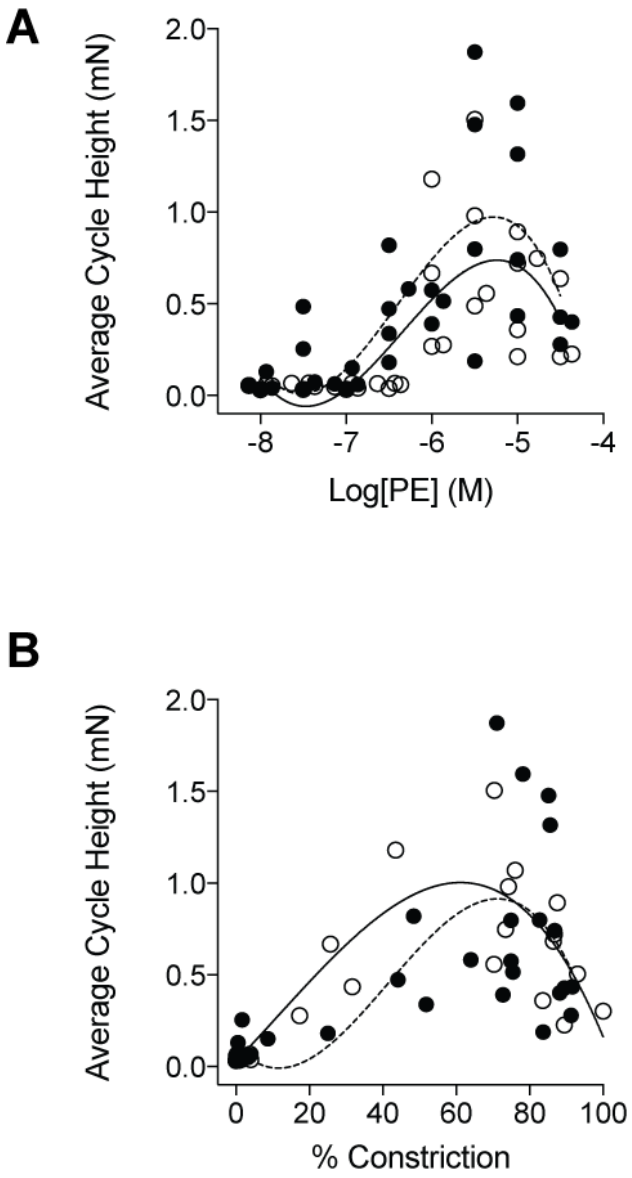


Figure 5.3.4: The effect of increasing constriction and concentration of PE on amplitude of vasomotion

(A) The amplitude of oscillations in control arteries (○) and arteries treated with L-NAME (●) was plotted against the concentration of phenylephrine (PE). Average cycle height was calculated using inbuilt LabChart analysis software. The concentration data was then converted to a % of maximal artery constriction and plotted in (B). Data consists of a 30 s sample taken at increasing concentrations of PE. n=4 for each treatment and all data are displayed. Curves were fitted using the equation for a centred third order polynomial [Y=B0 + B1*(X - MeanX) +B2*((X - MeanX)^2) + B3*((X - MeanX)^3)].

5.4 Discussion and future work

We have shown, for the first time, the formation of membrane potential spikes (i.e. rapid depolarization of Em in smooth muscle cells, similar to an action potential) in rat mesenteric arteries treated with L-NAME, that occur out of phase by 180º with the oscillations in tension. It was also noted that the presence of L-NAME, and therefore spikes, altered the appearance of the oscillations in tension, from regular waveforms to irregular waveforms. We are, however, not the first to observe the generation of arterial smooth muscle cell action potentials.

Lamb and Webb (1989) examined changes in membrane potential and tension of tail arteries from both Wistar-Kyoto (WKY) rats and spontaneously hypertensive rats-stroke prone strain (SHRSP). They found that arteries from the SHRSP rats spontaneously developed spikes associated with the rising phase of vasomotion when using norepinephrine as a constricting agent. Interestingly the arteries from WKY rats developed neither membrane potential spikes, nor vasomotion.

Gokina et al. (1996) have also observed spontaneous spike activity in vascular smooth muscle from human pial arteries, taken from patients undergoing surgery to resection brain tumours. Gokina et al. (1996) commented that the spikes occurred when the smooth muscle cells were depolarized to around -40 mV. This finding is similar to the development of spikes that we have observed.

In comparison to our experiments, where the presence of L-NAME was required to induce the development of spikes, both these studies required no inhibitors and in the case of the pial arteries no constricting agent was needed for the development of spikes. The arteries in these studies did, however, come from potentially diseased tissue. Gokina et al. (1996) note that, due to the age of the patients in the study, the presence of vascular disease cannot be ruled out and the SHRSP rats in the Lamb and Webb (1989) study are known to have lower bioavailability of NO, which may relate to a defect in the activation pathways of eNOS (Hamilton et al., 2006). Therefore, it could be suggested that the spikes seen in these studies could be related to a reduced bioavailability of NO, consistent with our observation that loss of NO, by inhibition of eNOS with L-NAME leads to spike generation in mesenteric arteries. Given these observations, it could therefore be suggested that generation of membrane potential spikes, in phase with vasomotion, is a marker for vascular disease where there is reduced bioavailability of NO.

Also of interest is the observation that as the smooth muscle cells become more depolarized the prevalence of spikes decreases and those that do fire are depressed. This correlates with an overall decrease in the amplitude of vasomotion at higher concentrations of phenylephrine and increased tension. Further investigation is required to determine why spikes are not generated at higher tensions and, in addition to this, which underlying ionic currents drive spike generation. It is highly likely that calcium is the driving force in spike generation and therefore both L- and T-type channels should be investigated, as they are present in smooth muscle cells and have been associated with action potential generation in these cells (Brueggemann et al., 2005). Gokina et

al. (1996) have already determined that removal of calcium from the bath solution inhibited spike generation in human pial arteries and that the L-type calcium channel blocker, nifedipine, was able to block the spikes. Therefore, as a starting point, we should examine if this finding is consistent in rat mesenteric arteries.

As mentioned above, the oscillations in Em and tension occur out of phase with one another by approximately 180°. As discussed in **Section 5.1.I**, it is likely that both the membrane oscillator and cytosolic oscillator are involved in conjunction with one another to drive the changes in membrane potential and tension. Omote *et al.* (1992; 1993; 1993) demonstrated that membrane oscillations may occur in the absence of calcium-induced calcium-release, whilst both BK_{Ca} and K_V channels have been implicated in maintaining the membrane oscillator, thus it is possible that flux of potassium ions across the membrane is responsible for the changes in membrane potential, independent to the oscillation of tension observed. Changes in Em can alter the permeability of calcium channels, such as the L-type and T-type voltage dependent calcium channels, which activate during depolarization of the membrane (Catterall et al., 2017). Inward flux of calcium activates IP_3 and/or ryanodine receptors on the sarcoplasmic reticulum, which in turn drives the calcium-induced calcium release that underlies the cytosolic oscillator, as described in **Section 5.1.I**. The fluctuations in calcium can activate calcium activated potassium channels, such as BK_{Ca}, on the membrane leading to an efflux of potassium and subsequent hyperpolarization of the cell. Therefore, it is difficult to determine without further experimentation whether it is the membrane oscillator driving the cytosolic oscillator, or the cytosolic oscillator driving the membrane oscillator, but it is

probable that the oscillations in Em and tension are out of phase due to the membrane and cytosolic oscillators not oscillating in synchrony with one another.

Finally, we wished to determine which redox variant of NO is responsible for spike suppression in untreated, healthy arteries. Maintaining membrane potential recordings in oscillating arteries is technically very difficult and therefore we had limited success in directly observing whether addition of NO and HNO donor compounds had any effect on spike generation. It appears as if the addition of SNOG may suppress spike generation for a short period of time, before spikes reappear, but the recording gained was poor and not enough observations have been made to confirm that this is the case. In the examination of vasomotion alone, our group have demonstrated that addition of SNOG can reverse the dysregulation that occurs in the presence of L-NAME (Joshua Smith, unpublished observations) suggesting that spike activity may be limited.

To address the technical difficulties of membrane potential recording, it was decided to examine the effects of NO and HNO scavengers on responses to PE. It is known that the presence of L-NAME augments the response to PE due to inhibition of both indirect and PE stimulated release of NO from endothelial cells (Dora et al., 2000). Our current findings are consistent with this, as scavengers for HNO had no effect on the dose response curve of PE, yet the NO scavenger, HXC, significantly augmented the response to PE at 1 μM. Thus, these observations suggest that NO is the most likely form of NO responsible for spike inhibition in healthy arteries.

Further electrophysiological experiments are required to confirm whether addition of an NO donor can inhibit the generation of spikes in L-NAME treated arteries. If it remains too difficult to gather usable traces using this method, an alternative approach where HXC is applied in place of L-NAME should be considered. This would demonstrate whether spikes are uncovered through the removal of NO, or whether L-NAME may have a direct effect on a channel underlying spike generation.

5.5 Conclusion

In summary, we have determined that the presence of L-NAME elicits the generation of membrane potential spikes in rat mesenteric arteries and that the redox form of NO responsible for spike suppression in untreated arteries is most likely NO, however further experiments are required to clarify this theory.

Chapter 6

Summary and future directions

This thesis examines the role of NO and its redox variants, in the regulation of vascular SMC membrane potential and relaxation of rat mesenteric arteries. Specifically it examines the response to donors of HNO, the reduced and protonated form of NO, which has been proposed as a viable alternative to NO donors in the treatment of cardiovascular disorders.

In **Chapter 3** we have demonstrated that the HNO donor IPA/NO is comparable to the more frequently used AS and therefore is a viable alternative to AS in organ bath studies.

Using IPA/NO we confirmed the presence of a sGC/cGMP-independent pathway, of which K^+ channels are the primary component. Whilst Irvine et al. (2003) attributes the sGC/cGMP-independent pathway to K_v channels, pilot data from our lab has implicated BK_{Ca} in this pathway. Further investigation is therefore required as the role of BK_{Ca} is only revealed at the highest of IPA/NO concentrations and therefore may not be physiologically relevant.

We also demonstrated that IPA/NO could be used repeatedly for experiments examining the relaxation in response to IPA/NO. However, secondary exposure significantly reduced hyperpolarization in studies examining membrane potential therefore, repeat applications in membrane potential experiments is not advised. It is possible that the discrepancy between repeat exposure for hyperpolarization and relaxation is due to the depletion of CGRP. We showed, in **Chapter 4**, how depletion of CGRP stores using capsaicin could significantly decrease the hyperpolarization in response to IPA/NO, but had no effect on relaxation. This should therefore be examined further.

We also demonstrated in **Chapter 4** that the HNO-TRPA1-CGRP pathway proposed by Eberhardt et al. (2014) is present in rat mesenteric arteries, but given that the addition of HC030031, a TRPA1 blocker, and CGRP depletion has no effect on the relaxation to IPA/NO, it is unlikely that this pathway has any significant physiological relevance as a target for the treatment of hypertension.

As expected, we demonstrated the presence of TRPA1 in the perivascular nerves of mesenteric arteries. Unexpectedly, we also noted the apparent presence of TRPA1 on endothelial cells, dependent on the method of preparation. To address this discrepancy our lab has conducted Western blot and PCR experiments on endothelial tubes, however so far these have proven inconclusive. Additional immunohistochemistry should therefore be carried out using alternative TRPA1 antibodies.

It would also be useful to conduct experiments, examining the HNO-TRPA1-CGRP pathway in other vascular beds. It is possible that other arteries may be more sensitive to CGRP. Therefore, relaxation in response to HNO, may be affected.

Finally in **Chapter 5** we addressed the effect of the absence of NO and its redox variants on vasomotion in rat mesenteric arteries. We showed, for the first time, that the addition of L-NAME and therefore the loss of NO, induced the development of membrane potential spikes. We suggest that membrane potential spikes are representative of endothelial dysfunction, due to the previous observations of membrane spike potentials by Lamb and Webb (1989) and Gokina et al. (1996) who examined arteries from spontaneously

hypertensive rats and human pial arteries where cardiovascular disease was likely to be present.

Due to the difficulty in maintaining membrane potential recordings in constricted arteries where vasomotion is present, little additional work has been carried out to examine the underlying ion fluxes that generate the spike potentials. It is most likely that both L- and T-type channels are involved and this should therefore be the primary focus in understanding the spike generation in rat mesenteric arteries. It would also be interesting to use spontaneously hypertensive rats to confirm the observations of Lamb and Webb (1989) and also to determine if the addition of NO or HNO to the system would inhibit any spikes generated.

From our initial work examining the effects of NO and HNO scavengers on relaxation to phenylephrine, it is most likely that NO is the primary redox variant of NO responsible for supressing spikes in healthy arteries. Initial work has begun to examine whether the addition of a NO donor to the organ bath suppresses spikes, however, due to the technical difficulty of maintaining membrane potential recordings, nothing conclusive has been observed.

The theme of this thesis, examining the role of NO and its redox variants in the regulation of vascular smooth muscle tone, is being continued by other members of the lab, who are investigating the role of NO in the modulation of vasomotion. One of the hardest aspects of studying vasomotion is reliable analysis, due to the variance in the waveforms observed day-to-day and between arteries. For this reason protocols have been developed by other members of the lab, which generate more consistent vasomotion. In addition to

this, an autoanalysis program is being developed by Joshua Smith, which will provide a more reliable analysis of the waveforms and frequency of vasomotion and alterations of vasomotion after different treatments are applied. This program is also being adapted to analyse the changes in spike potentials meaning more information can be drawn from the data besides casual observations.

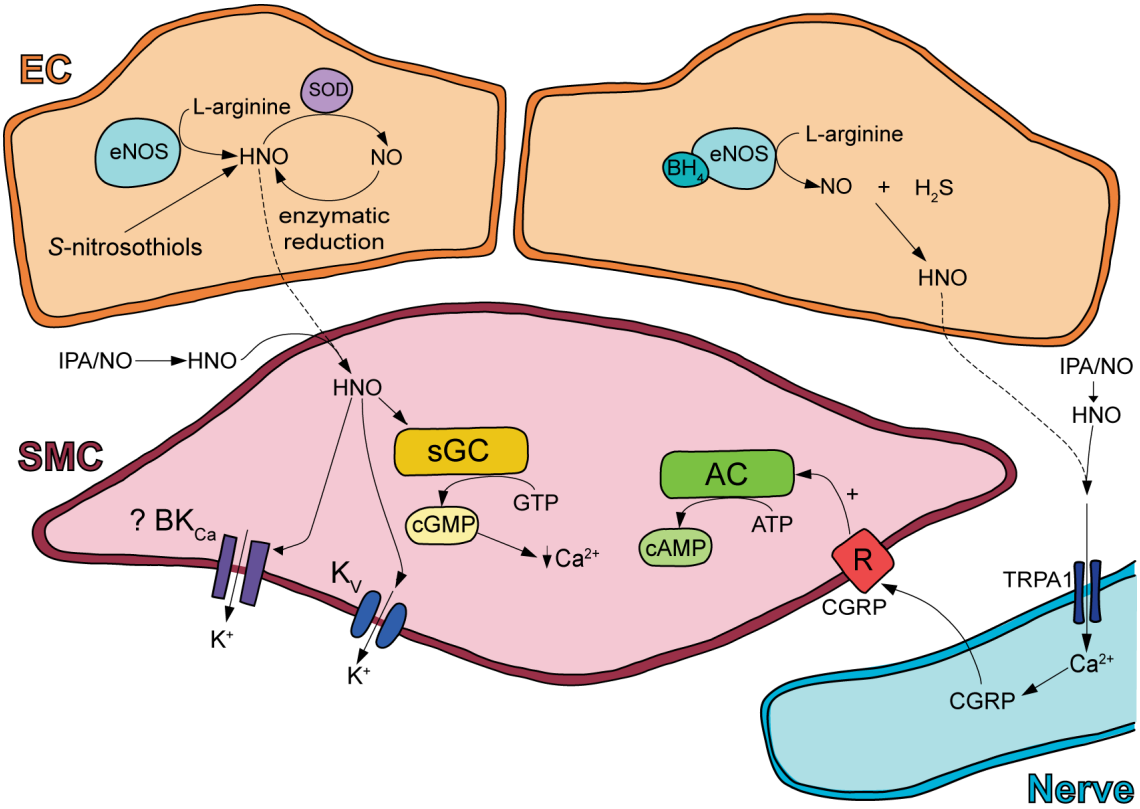


Figure 6.1: Summary schematic detailing the signaling pathways confirmed in this study.

Endogenous HNO can be formed as described in **Figure 1.5.2**. HNO (endogenous or released from a donor molecule) is proposed to diffuse into vascular smooth muscle cells (SMC) and interact with soluble guanylyl cyclase (sGC). Activated sGC converts guanosine triphosphate (GTP) to cyclic guanosine monophosphate (cGMP), which (primarily via protein kinase G (PKG)) leads to a decrease in intracellular calcium and SMC relaxation as described in **Figure 1.5.1**. HNO may also directly activate large conductance Ca^{2+}-cativated potassium channels (BK_{Ca}) and voltage-gated potassium channels (K_v) leading to K^+ efflux and hyperpolarization, which leads to vasorelaxation. HNO also activates transient receptor potential A1 (TRPA1) channels, which triggers the release of calcitonin gene-related peptide (CGRP) from sensory nerves. CGRP activates CGRP receptors (R) on SMC, promoting the activation of adenylyl cyclase (AC) and subsequent increase in cyclic adenosine monophosphate (cAMP) which leads to hyperpolarization, but not vasorelaxation.

References

Aalkjaer C, & Nilsson H (2005). Vasomotion: cellular background for the oscillator and for the synchronization of smooth muscle cells. Br J Pharmacol 144**:** 605-616.

Adak S, Wang Q, & Stuehr DJ (2000). Arginine conversion to nitroxide by tetrahydrobiopterin-free neuronal nitric-oxide synthase. Implications for mechanism. J Biol Chem 275**:** 33554-33561.

Andrei D, Salmon DJ, Donzelli S, Wahab A, Klose JR, Citro ML*, et al.* (2010). Dual mechanisms of HNO generation by a nitroxyl prodrug of the diazeniumdiolate (NONOate) class. J Am Chem Soc 132**:** 16526-16532.

Andrews KL, Irvine JC, Tare M, Apostolopoulos J, Favaloro JL, Triggle CR*, et al.* (2009). A role for nitroxyl (HNO) as an endothelium-derived relaxing and hyperpolarizing factor in resistance arteries. Br J Pharmacol 157**:** 540-550.

Arcaro A, Lembo G, & Tocchetti CG (2014). Nitroxyl (HNO) for treatment of acute heart failure. Curr Heart Fail Rep 11**:** 227-235.

Arnelle DR, & Stamler JS (1995). NO^+, $NO^\cdot$, and NO^- donation by S-nitrosothiols: implications for regulation of physiological functions by S-nitrosylation and acceleration of disulfide formation. Arch Biochem Biophys 318**:** 279-285.

Atoyan R, Shander D, & Botchkareva NV (2009). Non-neuronal expression of transient receptor potential type A1 (TRPA1) in human skin. J Invest Dermatol 129**:** 2312-2315.

Bandick NR, & Sparks HV (1970). Contractile response of vascular smooth muscle of renal hypertensive rats. Am J Physiol 219**:** 340-344.

Bates JN, Baker MT, Guerra R, Jr., & Harrison DG (1991). Nitric oxide generation from nitroprusside by vascular tissue. Evidence that reduction of the nitroprusside anion and cyanide loss are required. Biochem Pharmacol 42 Suppl**:** S157-165.

Bautista DM, Jordt SE, Nikai T, Tsuruda PR, Read AJ, Poblete J*, et al.* (2006). TRPA1 mediates the inflammatory actions of environmental irritants and proalgesic agents. Cell 124**:** 1269-1282.

Bautista DM, Movahed P, Hinman A, Axelsson HE, Sterner O, Hogestatt ED*, et al.* (2005). Pungent products from garlic activate the sensory ion channel TRPA1. Proc Natl Acad Sci USA 102**:** 12248-12252.

Benjamin N, O'Driscoll F, Dougall H, Duncan C, Smith L, Golden M*, et al.* (1994). Stomach NO synthesis. Nature 368**:** 502.

Beny JL, & Schaad O (2000). An evaluation of potassium ions as endothelium-derived hyperpolarizing factor in porcine coronary arteries. Br J Pharmacol 131**:** 965-973.

Berridge MJ, & Rapp PE (1979). A comparative survey of the function, mechanism and control of cellular oscillators. J Exp Biol 81**:** 217-279.

Bevan JA, & Osher JV (1972). A direct method for recording tension changes in the wall of small blood vessels in vitro. Agents Actions 2**:** 257-260.

Boittin FX, Galione A, & Evans AM (2002). Nicotinic acid adenine dinucleotide phosphate mediates Ca2+ signals and contraction in arterial smooth muscle via a two-pool mechanism. Circ Res 91**:** 1168-1175.

Boittin FX, Macrez N, Halet G, & Mironneau J (1999). Norepinephrine-induced Ca(2+) waves depend on InsP(3) and ryanodine receptor activation in vascular myocytes. Am J Physiol 277**:** C139-151.

Bolotina VM, Najibi S, Palacino JJ, Pagano PJ, & Cohen RA (1994). Nitric oxide directly activates calcium-dependent potassium channels in vascular smooth muscle. Nature 368**:** 850-853.

Bolton TB, Lang RJ, & Takewaki T (1984). Mechanisms of action of noradrenaline and carbachol on smooth muscle of guinea-pig anterior mesenteric artery. J Physiol 351**:** 549-572.

Bonner FT, & Ravid B (1975). Thermal decomposition of oxyhyponitrite (sodium trioxodinitrate(II)) in aqueous solution. Inorg Chem 14**:** 558-563.

Bouskela E, Cyrino FZ, & Wiernsperger N (1997). Effects of insulin and the combination of insulin plus metformin (glucophage) on microvascular reactivity in control and diabetic hamsters. Angiology 48**:** 503-514.

Brain SD, & Grant AD (2004). Vascular actions of calcitonin gene-related peptide and adrenomedullin. Physiol Rev 84**:** 903-934.

Bredt DS, & Snyder SH (1990). Isolation of nitric oxide synthetase, a calmodulin-requiring enzyme. Proc Natl Acad Sci U S A 87**:** 682-685.

Brien JF, Peachey JE, Rogers BJ, & Loomis CW (1978). A study of the calcium carbimide-ethanol interaction in man. Eur J Clin Pharmacol 14**:** 133-141.

Brueggemann LI, Martin BL, Barakat J, Byron KL, & Cribbs LL (2005). Low voltage-activated calcium channels in vascular smooth muscle: T-type channels and AVP-stimulated calcium spiking. Am J Physiol Heart Circ Physiol 288**:** H923-935.

Burnstock G (2009). Purinergic regulation of vascular tone and remodelling. Auton Autacoid Pharmacol 29**:** 63-72.

Campbell WB, & Fleming I (2010). Epoxyeicosatrienoic acids and endothelium-dependent responses. Pflugers Arch 459**:** 881-895.

Cao DS, Zhong L, Hsieh TH, Abooj M, Bishnoi M, Hughes L*, et al.* (2012). Expression of transient receptor potential ankyrin 1 (TRPA1) and its role in insulin release from rat pancreatic beta cells. PLoS One 7**:** e38005.

Catterall WA, Perez-Reyes E, Snutch TP, Striessnig J (2017) *Voltage-gated calcium channels, introduction.* [Online] Available from http://guidetopharmacology.org/GRAC/FamilyIntroductionForward?familyId=80. [Accessed: 11 March 2018]

Chen G, Suzuki H, & Weston AH (1988). Acetylcholine releases endothelium-derived hyperpolarizing factor and EDRF from rat blood vessels. Br J Pharmacol 95**:** 1165-1174.

Chen J, & Hackos DH (2015). TRPA1 as a drug target--promise and challenges. Naunyn Schmiedebergs Arch Pharmacol 388**:** 451-463.

Doerner JF, Gisselmann G, Hatt H, & Wetzel CH (2007). Transient receptor potential channel A1 is directly gated by calcium ions. J Biol Chem 282**:** 13180-13189.

Dora KA (2001). Cell-cell communication in the vessel wall. Vasc Med 6**:** 43-50.

Dora KA, & Garland CJ (2001). Properties of smooth muscle hyperpolarization and relaxation to K+ in the rat isolated mesenteric artery. Am J Physiol Heart Circ Physiol 280**:** H2424-2429.

Dora KA, Hinton JM, Walker SD, & Garland CJ (2000). An indirect influence of phenylephrine on the release of endothelium-derived vasodilators in rat small mesenteric artery. Br J Pharmacol 129**:** 381-387.

Dora KA, Sandow SL, Gallagher NT, Takano H, Rummery NM, Hill CE*, et al.* (2003). Myoendothelial gap junctions may provide the pathway for EDHF in mouse mesenteric artery. J Vasc Res 40**:** 480-490.

Dudzinski DM, Igarashi J, Greif D, & Michel T (2006). The regulation and pharmacology of endothelial nitric oxide synthase. Annu Rev Pharmacol Toxicol 46**:** 235-276.

DuMond JF, & King SB (2011). The chemistry of nitroxyl-releasing compounds. Antioxid Redox Signal 14**:** 1637-1648.

Dunn WR, Hardy TA, & Brock JA (2003). Electrophysiological effects of activating the peptidergic primary afferent innervation of rat mesenteric arteries. Br J Pharmacol 140**:** 231-238.

Earley S (2012). TRPA1 channels in the vasculature. Br J Pharmacol 167**:** 13-22.

Earley S, Gonzales AL, & Crnich R (2009). Endothelium-dependent cerebral artery dilation mediated by TRPA1 and Ca^{2+}-Activated K^+ channels. Circ Res 104**:** 987-994.

Eberhardt M, Dux M, Namer B, Miljkovic J, Cordasic N, Will C*, et al.* (2014). H2S and NO cooperatively regulate vascular tone by activating a neuroendocrine HNO-TRPA1-CGRP signalling pathway. Nat Commun 5**:** 4381.

Edvinsson L, Ekblad E, Hakanson R, & Wahlestedt C (1984). Neuropeptide Y potentiates the effect of various vasoconstrictor agents on rabbit blood vessels. Br J Pharmacol 83**:** 519-525.

Edwards G, Dora KA, Gardener MJ, Garland CJ, & Weston AH (1998). K^+ is an endothelium-derived hyperpolarizing factor in rat arteries. Nature 396**:** 269-272.

Edwards G, Feletou M, Gardener MJ, Glen CD, Richards GR, Vanhoutte PM*, et al.* (2001). Further investigations into the endothelium-dependent hyperpolarizing effects of bradykinin and substance P in porcine coronary artery. Br J Pharmacol 133**:** 1145-1153.

Edwards G, Feletou M, & Weston AH (2010). Endothelium-derived hyperpolarising factors and associated pathways: a synopsis. Pflugers Arch 459**:** 863-879.

Favaloro JL, & Kemp-Harper BK (2007). The nitroxyl anion (HNO) is a potent dilator of rat coronary vasculature. Cardiovasc Res 73**:** 587-596.

Favaloro JL, & Kemp-Harper BK (2009). Redox variants of NO ($NO^{\cdot}$ and HNO) elicit vasorelaxation of resistance arteries via distinct mechanisms. Am J Physiol Heart Circ Physiol 296**:** H1274-1280.

Forstermann U, Closs EI, Pollock JS, Nakane M, Schwarz P, Gath I*, et al.* (1994). Nitric oxide synthase isozymes. Characterization, purification, molecular cloning, and functions. Hypertension 23**:** 1121-1131.

Forstermann U, Gorsky LD, Pollock JS, Ishii K, Schmidt HH, Heller M*, et al.* (1990). Hormone-induced biosynthesis of endothelium-derived relaxing factor/nitric oxide-like material in N1E-115 neuroblastoma cells requires calcium and calmodulin. Mol Pharmacol 38**:** 7-13.

Friebe A, & Koesling D (2003). Regulation of nitric oxide-sensitive guanylyl cyclase. Circ Res 93**:** 96-105.

Fukuto JM, Dutton AS, & Houk KN (2005). The chemistry and biology of nitroxyl (HNO): a chemically unique species with novel and important biological activity. Chembiochem 6**:** 612-619.

Fukuto JM, Hobbs AJ, & Ignarro LJ (1993). Conversion of nitroxyl (HNO) to nitric oxide (NO) in biological systems: the role of physiological oxidants and relevance to the biological activity of HNO. Biochem Biophys Res Commun 196**:** 707-713.

Furchgott RF, & Zawadzki JV (1980). The obligatory role of endothelial cells in the relaxation of arterial smooth muscle by acetylcholine. Nature 288**:** 373-376.

Galley HF, & Webster NR (2004). Physiology of the endothelium. Br J Anaesth 93**:** 105-113.

Garland CJ, Hiley CR, & Dora KA (2011). EDHF: spreading the influence of the endothelium. Br J Pharmacol 164**:** 839-852.

Garland CJ, & McPherson GA (1992). Evidence that nitric oxide does not mediate the hyperpolarization and relaxation to acetylcholine in the rat small mesenteric artery. Br J Pharmacol 105**:** 429-435.

Gladwin MT, Schechter AN, Kim-Shapiro DB, Patel RP, Hogg N, Shiva S*, et al.* (2005). The emerging biology of the nitrite anion. Nat Chem Biol 1**:** 308-314.

Gokina NI, Bevan RD, Walters CL, & Bevan JA (1996). Electrical activity underlying rhythmic contraction in human pial arteries. Circ Res 78**:** 148-153.

Griffith TM (1996). Temporal chaos in the microcirculation. Cardiovasc Res 31**:** 342-358.

Griffith TM, & Edwards DH (1997). Ca^{2+} sequestration as a determinant of chaos and mixed-mode dynamics in agonist-induced vasomotion. Am J Physiol 272**:** H1696-1709.

Griffith TM, Parthimos D, & Edwards DH (2009). Vasomotion: the case for chaos. J Biorheol 23**:** 11-23.

Griffiths MJ, & Evans TW (2005). Inhaled nitric oxide therapy in adults. N Engl J Med 353**:** 2683-2695.

Guimaraes S, & Moura D (2001). Vascular adrenoceptors: an update. Pharmacol Rev 53**:** 319-356.

Gutterman DD (1999). Adventitia-dependent influences on vascular function. Am J Physiol 277**:** H1265-1272.

Haas TL, & Duling BR (1997). Morphology favors an endothelial cell pathway for longitudinal conduction within arterioles. Microvasc Res 53**:** 113-120.

Hamilton CA, Groves S, Carswell HV, Brosnan MJ, Graham D, & Dominiczak AF (2006). Estrogen treatment enhances nitric oxide bioavailability in normotensive but not hypertensive rats. Am J Hypertens 19**:** 859-866.

Heberlein KR, Straub AC, & Isakson BE (2009). The myoendothelial junction: breaking through the matrix? Microcirculation (New York, NY : 1994) 16**:** 307-322.

Hill CE, Eade J, & Sandow SL (1999). Mechanisms underlying spontaneous rhythmical contractions in irideal arterioles of the rat. J Physiol 521 Pt 2**:** 507-516.

Hill CE, Phillips JK, & Sandow SL (2001). Heterogeneous control of blood flow amongst different vascular beds. Med Res Rev 21**:** 1-60.

Hirata Y, Takagi Y, Takata S, Fukuda Y, Yoshimi H, & Fujita T (1988). Calcitonin gene-related peptide receptor in cultured vascular smooth muscle and endothelial cells. Biochem Biophys Res Commun 151**:** 1113-1121.

Hobbs AJ, Fukuto JM, & Ignarro LJ (1994). Formation of free nitric oxide from l-arginine by nitric oxide synthase: direct enhancement of generation by superoxide dismutase. Proc Natl Acad Sci USA 91**:** 10992-10996.

Holloway ET, & Bohr DF (1973). Reactivity of vascular smooth muscle in hypertensive rats. Circ Res 33**:** 678-685.

Hong KW, Yoo SE, Yu SS, Lee JY, & Rhim BY (1996). Pharmacological coupling and functional role for CGRP receptors in the vasodilation of rat pial arterioles. Am J Physiol 270**:** H317-323.

Huang QQ, Fisher SA, Brozovich (2004). Unzipping the role of myosin light chain phosphatase in smooth muscle cell relaxation. J Biol Chem 279: 597-603

Ignarro LJ, Buga GM, Wood KS, Byrns RE, & Chaudhuri G (1987a). Endothelium-derived relaxing factor produced and released from artery and vein is nitric oxide. Proc Natl Acad Sci USA 84**:** 9265-9269.

Ignarro LJ, Byrns RE, Buga GM, & Wood KS (1987b). Endothelium-derived relaxing factor from pulmonary artery and vein possesses pharmacologic and chemical properties identical to those of nitric oxide radical. Circ Res 61**:** 866-879.

Iino M, Kasai H, & Yamazawa T (1994). Visualization of neural control of intracellular Ca2+ concentration in single vascular smooth muscle cells in situ. EMBO J 13**:** 5026-5031.

Irvine JC, Favaloro JL, & Kemp-Harper BK (2003). NO^{-} activates soluble guanylate cyclase and K_v channels to vasodilate resistance arteries. Hypertension 41**:** 1301-1307.

Irvine JC, Favaloro JL, Widdop RE, & Kemp-Harper BK (2007). Nitroxyl anion donor, Angeli's salt, does not develop tolerance in rat isolated aortae. Hypertension 49**:** 885-892.

Irvine JC, Kemp-Harper BK, & Widdop RE (2011). Chronic administration of the HNO donor Angeli's salt does not lead to tolerance, cross-tolerance, or endothelial dysfunction: comparison with GTN and DEA/NO. Antioxid Redox Signal 14**:** 1615-1624.

Irvine JC, Ritchie RH, Favaloro JL, Andrews KL, Widdop RE, & Kemp-Harper BK (2008). Nitroxyl (HNO): the Cinderella of the nitric oxide story. Trends Pharmacol Sci 29**:** 601-608.

Isakson BE, & Duling BR (2005). Heterocellular contact at the myoendothelial junction influences gap junction organization. Circ Res 97**:** 44-51.

Jones TW (1852). Discovery that the veins of the bat's wing (which are furnished with valves) are endowed with rhythmical contractility, and that onward flow of blood is accelerated by each contraction. Phil Trans R Soc Lond 142**:** 131-136.

Keefer LK (2003). Progress toward clinical application of the nitric oxide-releasing diazeniumdiolates. Annu Rev Pharmacol Toxicol 43**:** 585-607.

Kemp-Harper BK, Horowitz JD, & Ritchie RH (2016). Therapeutic potential of nitroxyl (HNO) donors in the management of acute decompensated heart failure. Drugs 76**:** 1337-1348.

Klabunde RE (2012) *Cardiovascular Pharmacology Concepts: Nitrodilators.* [Online] Available from http://www.cvpharmacology.com/vasodilator/nitro. [Accessed: 1 Dec 2017].

Komarova Y, & Malik AB (2010). Regulation of endothelial permeability via paracellular and transcellular transport pathways. Annu Rev Physiol 72**:** 463-493.

Kruger O, Plum A, Kim JS, Winterhager E, Maxeiner S, Hallas G*, et al.* (2000). Defective vascular development in connexin 45-deficient mice. Development 127**:** 4179-4193.

Kubota M, Moseley JM, Butera L, Dusting GJ, MacDonald PS, & Martin TJ (1985). Calcitonin gene-related peptide stimulates cyclic AMP formation in rat aortic smooth muscle cells. Biochem Biophys Res Commun 132**:** 88-94.

Kuriyama H, & Suzuki H (1978). The effects of acetylcholine on the membrane and contractile properties of smooth muscle cells of the rabbit superior mesenteric artery. Br J Pharmacol 64**:** 493-501.

Lamb FS, & Webb RC (1989). Regenerative electrical activity and arterial contraction in hypertensive rats. Hypertension 13**:** 70-76.

Lee CH, Poburko D, Kuo KH, Seow CY, & van Breemen C (2002). $Ca^{(2+)}$ oscillations, gradients, and homeostasis in vascular smooth muscle. Am J Physiol Heart Circ Physiol 282**:** H1571-1583.

Lee CH, Poburko D, Sahota P, Sandhu J, Ruehlmann DO, & van Breemen C (2001). The mechanism of phenylephrine-mediated [$Ca^{(2+)}$](i) oscillations underlying tonic contraction in the rabbit inferior vena cava. J Physiol 534**:** 641-650.

Li H, & Forstermann U (2000). Nitric oxide in the pathogenesis of vascular disease. J Pathol 190**:** 244-254.

Lima B, Forrester MT, Hess DT, & Stamler JS (2010). S-nitrosylation in cardiovascular signaling. Circ Res 106**:** 633-646.

Lin YF, Raab-Graham K, Jan YN, & Jan LY (2004). NO stimulation of ATP-sensitive potassium channels: Involvement of Ras/mitogen-activated protein kinase pathway and contribution to neuroprotection. Proc Natl Acad Sci USA 101**:** 7799-7804.

Little TL, Beyer EC, & Duling BR (1995). Connexin 43 and connexin 40 gap junctional proteins are present in arteriolar smooth muscle and endothelium in vivo. Am J Physiol 268**:** H729-739.

Lundberg JO, Weitzberg E, Cole JA, & Benjamin N (2004). Nitrate, bacteria and human health. Nat Rev Microbiol 2**:** 593-602.

Lundberg JO, Weitzberg E, Lundberg JM, & Alving K (1994). Intragastric nitric oxide production in humans: measurements in expelled air. Gut 35**:** 1543-1546.

Luo W, Liu B, & Zhou Y (2016). The endothelial cyclooxygenase pathway: Insights from mouse arteries. Eur J Pharmacol 780**:** 148-158.

Maragos CM, Morley D, Wink DA, Dunams TM, Saavedra JE, Hoffman A*, et al.* (1991). Complexes of .NO with nucleophiles as agents for the controlled biological release of nitric oxide. Vasorelaxant effects. J Med Chem 34**:** 3242-3247.

Matchkov VV (2010). Mechanisms of cellular synchronization in the vascular wall. Mechanisms of vasomotion. Dan Med Bull 57**:** B4191.

McCarron JG, Bradley KN, MacMillan D, Chalmers S, & Muir TC (2004a). The sarcoplasmic reticulum, Ca^{2+} trapping, and wave mechanisms in smooth muscle. News Physiol Sci 19**:** 138-147.

McCarron JG, MacMillan D, Bradley KN, Chalmers S, & Muir TC (2004b). Origin and mechanisms of Ca^{2+} waves in smooth muscle as revealed by localized photolysis of caged inositol 1,4,5-trisphosphate. J Biol Chem 279**:** 8417-8427.

Meyer C, de Vries G, Davidge ST, & Mayes DC (2002). Reassessing the mathematical modeling of the contribution of vasomotion to vascular resistance. J Appl Physiol 92**:** 888-889.

Miller MR, & Megson IL (2007). Recent developments in nitric oxide donor drugs. Br J Pharmacol 151**:** 305-321.

Miller TW, Cherney MM, Lee AJ, Francoleon NE, Farmer PJ, King SB*, et al.* (2009). The effects of nitroxyl (HNO) on soluble guanylate cyclase activity: interactions at ferrous heme and cysteine thiols. J Biol Chem 284**:** 21788-21796.

Miranda KM (2005). The chemistry of ntiroxyl (HNO) and implications in biology. Coordin Chem Rev 249**:** 433-455.

Miranda KM, Dutton AS, Ridnour LA, Foreman CA, Ford E, Paolocci N*, et al.* (2005a). Mechanism of aerobic decomposition of Angeli's salt (sodium trioxodinitrate) at physiological pH. J Am Chem Soc 127**:** 722-731.

Miranda KM, Katori T, Torres de Holding CL, Thomas L, Ridnour LA, McLendon WJ*, et al.* (2005b). Comparison of the NO and HNO donating properties of diazeniumdiolates: primary amine adducts release HNO in Vivo. J Med Chem 48**:** 8220-8228.

Miranda KM, Yamada K, Espey MG, Thomas DD, DeGraff W, Mitchell JB*, et al.* (2002). Further evidence for distinct reactive intermediates from nitroxyl and peroxynitrite: effects of buffer composition on the chemistry of Angeli's salt and synthetic peroxynitrite. Arch Biochem Biophys 401**:** 134-144.

Miriel VA, Mauban JR, Blaustein MP, & Wier WG (1999). Local and cellular Ca^{2+} transients in smooth muscle of pressurized rat resistance arteries during myogenic and agonist stimulation. J Physiol 518 (Pt 3)**:** 815-824.

Mistry DK, & Garland CJ (1998). Nitric oxide (NO)-induced activation of large conductance Ca^{2+}-dependent K^+ channels ($BK_{(Ca)}$) in smooth muscle cells isolated from the rat mesenteric artery. Br J Pharmacol 124**:** 1131-1140.

Moncada S, Gryglewski R, Bunting S, & Vane JR (1976). An enzyme isolated from arteries transforms prostaglandin endoperoxides to an unstable substance that inhibits platelet aggregation. Nature 263**:** 663-665.

Moncada S, Herman AG, Higgs EA, & Vane JR (1977). Differential formation of prostacyclin (PGX or PGI2) by layers of the arterial wall. An explanation for the anti-thrombotic properties of vascular endothelium. Thromb Res 11**:** 323-344.

Mulvany MJ, & Halpern W (1977). Contractile properties of small arterial resistance vessels in spontaneously hypertensive and normotensive rats. Circ Res 41**:** 19-26.

Murad F (1986). Cyclic guanosine monophosphate as a mediator of vasodilation. J Clin Invest 78**:** 1-5.

Murphy ME, & Brayden JE (1995). Nitric oxide hyperpolarizes rabbit mesenteric arteries via ATP-sensitive potassium channels. J Physiol 486 (Pt 1)**:** 47-58.

Nagasawa HT, DeMaster EG, Redfern B, Shirota FN, & Goon DJ (1990). Evidence for nitroxyl in the catalase-mediated bioactivation of the alcohol deterrent agent cyanamide. J Med Chem 33**:** 3120-3122.

Nagata K, Duggan A, Kumar G, & Garcia-Anoveros J (2005). Nociceptor and hair cell transducer properties of TRPA1, a channel for pain and hearing. J Neurosci 25**:** 4052-4061.

Nassini R, Pedretti P, Moretto N, Fusi C, Carnini C, Facchinetti F*, et al.* (2012). Transient receptor potential ankyrin 1 channel localized to non-neuronal airway cells promotes non-neurogenic inflammation. PLoS One 7**:** e42454.

Nelli S, Wilson WS, Laidlaw H, Llano A, Middleton S, Price AG*, et al.* (2003). Evaluation of potassium ion as the endothelium-derived hyperpolarizing factor (EDHF) in the bovine coronary artery. Br J Pharmacol 139**:** 982-988.

Nelson MT, Huang Y, Brayden JE, Hescheler J, & Standen NB (1990). Arterial dilations in response to calcitonin gene-related peptide involve activation of K^+ channels. Nature 344**:** 770-773.

Nicoll PA, & Webb RL (1955). Vascular patterns and active vasomotion as determiners of flow through minute vessels. Angiology 6**:** 291-308.

Niketic V, Stojanovic S, Nikolic A, Spasic M, & Michelson AM (1999). Exposure of Mn and FeSODs, but not Cu/ZnSOD, to NO leads to nitrosonium and nitroxyl

ions generation which cause enzyme modification and inactivation: an in vitro study. Free radic Biol Med 27**:** 992-996.

Nilsson H, & Aalkjaer C (2003). Vasomotion: mechanisms and physiological importance. Mol Interv 3**:** 79-89, 51.

Omote M, Kajimoto N, & Mizusawa H (1992). Phenylephrine induces endothelium-independent rhythmic contraction in rabbit mesenteric arteries treated with ryanodine. Acta Physiol Scand 145**:** 295-296.

Omote M, Kajimoto N, & Mizusawa H (1993). The ionic mechanism of phenylephrine-induced rhythmic contractions in rabbit mesenteric arteries treated with ryanodine. Acta Physiol Scand 147**:** 9-13.

Omote M, & Mizusawa H (1993). Phenylephrine-induced rhythmic activity in the rabbit ear artery. Jpn J Physiol 43**:** 511-520.

Paolocci N, Jackson MI, Lopez BE, Miranda K, Tocchetti CG, Wink DA*, et al.* (2007). The pharmacology of nitroxyl (HNO) and its therapeutic potential: not just the Janus face of NO. Pharmacol Ther 113**:** 442-458.

Paolocci N, Katori T, Champion HC, St John ME, Miranda KM, Fukuto JM*, et al.* (2003). Positive inotropic and lusitropic effects of HNO/NO- in failing hearts: independence from beta-adrenergic signaling. Proc Natl Acad Sci USA 100**:** 5537-5542.

Parkington HC, Coleman HA, & Tare M (2004). Prostacyclin and endothelium-dependent hyperpolarization. Pharmacol Res 49**:** 509-514.

Peng H, Matchkov V, Ivarsen A, Aalkjaer C, & Nilsson H (2001). Hypothesis for the initiation of vasomotion. Circ Res 88**:** 810-815.

Pepke-Zaba J, Higenbottam TW, Dinh-Xuan AT, Stone D, & Wallwork J (1991). Inhaled nitric oxide as a cause of selective pulmonary vasodilatation in pulmonary hypertension. Lancet 338**:** 1173-1174.

Piper S, & McDonagh T (2014). The role of intravenous vasodilators in acute heart failure management. Eur J Heart Fail 16**:** 827-834.

Poderoso JJ, Carreras MC, Schopfer F, Lisdero CL, Riobo NA, Giulivi C*, et al.* (1999). The reaction of nitric oxide with ubiquinol: kinetic properties and biological significance. Free Radic Biol Med 26**:** 925-935.

Qian J, & Fulton D (2013). Post-translational regulation of endothelial nitric oxide synthase in vascular endothelium. Front Physiol 4**:** 347.

Racchi H, Irarrazabal MJ, Howard M, Moran S, Zalaquett R, & Huidobro-Toro JP (1999). Adenosine 5'-triphosphate and neuropeptide Y are co-transmitters in conjunction with noradrenaline in the human saphenous vein. Br J Pharmacol 126**:** 1175-1185.

Ramsey IS, Delling M, & Clapham DE (2006). An introduction to TRP channels. Annu Rev Physiol 68**:** 619-647.

Renaudin C, Michoud E, Lagarde M, & Wiernsperger N (1999). Impaired microvascular responses to acute hyperglycemia in type I diabetic rats. J Diabetes Complications 13**:** 39-44.

Rubino A, & Burnstock G (1996). Capsaicin-sensitive sensory-motor neurotransmission in the peripheral control of cardiovascular function. Cardiovasc Res 31**:** 467-479.

Rucker M, Strobel O, Vollmar B, Roesken F, & Menger MD (2000). Vasomotion in critically perfused muscle protects adjacent tissues from capillary perfusion failure. Am J Physiol Heart Circ Physiol 279**:** H550-558.

Ruehlmann DO, Lee CH, Poburko D, & van Breemen C (2000). Asynchronous Ca(2+) waves in intact venous smooth muscle. Circ Res 86**:** E72-79.

Sabbah HN, Tocchetti CG, Wang M, Daya S, Gupta RC, Tunin RS*, et al.* (2013). Nitroxyl (HNO): A novel approach for the acute treatment of heart failure. Circ Heart Fail 6**:** 1250-1258.

Sada T, Koike H, Ikeda M, Sato K, Ozaki H, & Karaki H (1990). Cytosolic free calcium of aorta in hypertensive rats. Chronic inhibition of angiotensin converting enzyme. Hypertension 16**:** 245-251.

Saleem M, & Ohshima H (2004). Xanthine oxidase converts nitric oxide to nitroxyl that inactivates the enzyme. Biochem Biophys Res Commun 315**:** 455-462.

Salmon DJ, Torres de Holding CL, Thomas L, Peterson KV, Goodman GP, Saavedra JE*, et al.* (2011). HNO and NO release from a primary amine-based diazeniumdiolate as a function of pH. Inorg Chem 50**:** 3262-3270.

Sampson LJ, Plane F, & Garland CJ (2001). Involvement of cyclic GMP and potassium channels in relaxation evoked by the nitric oxide donor, diethylamine

NONOate, in the rat small isolated mesenteric artery. Naunyn Schmiedebergs Archiv Pharmacol 364**:** 220-225.

Sharpe MA, & Cooper CE (1998). Reactions of nitric oxide with mitochondrial cytochrome c: a novel mechanism for the formation of nitroxyl anion and peroxynitrite. Biochem J 332 (Pt 1)**:** 9-19.

Shigetomi E, Tong X, Kwan KY, Corey DP, & Khakh BS (2012). TRPA1 channels regulate astrocyte resting calcium and inhibitory synapse efficacy through GAT-3. Nat Neurosci 15**:** 70-80.

Shirota FN, Goon DJ, DeMaster EG, & Nagasawa HT (1996). Nitrosyl cyanide, a putative metabolic oxidation product of the alcohol-deterrent agent cyanamide. Biochem Pharmacol 52**:** 141-147.

Singh A, Laribi S, Teerlink JR, & Mebazaa A (2017). Agents with vasodilator properties in acute heart failure. Eur Heart J 38**:** 317-325.

Stamler JS, Singel DJ, & Loscalzo J (1992). Biochemistry of nitric oxide and its redox-activated forms. Science 258**:** 1898-1902.

Stansberry KB, Shapiro SA, Hill MA, McNitt PM, Meyer MD, & Vinik AI (1996). Impaired peripheral vasomotion in diabetes. Diabetes Care 19**:** 715-721.

Storkebaum E, & Carmeliet P (2011). Paracrine control of vascular innervation in health and disease. Acta Physiol (Oxf) 203**:** 61-86.

Stuehr DJ, Cho HJ, Kwon NS, Weise MF, & Nathan CF (1991). Purification and characterization of the cytokine-induced macrophage nitric oxide synthase: an FAD- and FMN-containing flavoprotein. Proc Natl Acad Sci USA 88**:** 7773-7777.

Sullivan MN, Gonzales AL, Pires PW, Bruhl A, Leo MD, Li W*, et al.* (2015). Localized TRPA1 channel Ca^{2+} signals stimulated by reactive oxygen species promote cerebral artery dilation. Sci Signal 8**:** ra2.

Taylor CW, & Tovey SC (2010). IP(3) receptors: toward understanding their activation. Cold Spring Harb Perspect Biol 2**:** a004010.

Taylor SG, & Weston AH (1988). Endothelium-derived hyperpolarizing factor: a new endogenous inhibitor from the vascular endothelium. Trends Pharmacol Sci 9**:** 272-274.

Tennant M, & McGeachie JK (1990). Blood vessel structure and function: a brief update on recent advances. Aust N Z J Surg 60**:** 747-753.

Thomson C, & Loudon J (2014). Medicines for your heart. British Heart Foundation, London, UK.

Townsend N, Bhatnagar P, Wilkins E, Wickramasinghe K, & Rayner M (2015) *Cardiovascular Disease Statistics 2015*. British Heart Foundation, London, UK.

Tsai AG, & Intaglietta M (1993). Evidence of flowmotion induced changes in local tissue oxygenation. Int J Microcirc Clin Exp 12**:** 75-88.

van Faassen E, & Vanin AF (2007). Nitric oxide radicals and their reactions. In Radicals for Life: The Various Forms of Nitric Oxide. eds van Faassen E., & Vanin A.F. Elsevier: Amsterdam, The Netherlands, pp 3-13.

Viana F (2016). TRPA1 channels: molecular sentinels of cellular stress and tissue damage. J Physiol 594**:** 4151-4169.

Waldron GJ, & Garland CJ (1994). Contribution of both nitric oxide and a change in membrane potential to acetylcholine-induced relaxation in the rat small mesenteric artery. Br J Pharmacol 112**:** 831-836.

Wanstall JC, Jeffery TK, Gambino A, Lovren F, & Triggle CR (2001). Vascular smooth muscle relaxation mediated by nitric oxide donors: a comparison with acetylcholine, nitric oxide and nitroxyl ion. Br J Pharmacol 134**:** 463-472.

Watts SW, Traub O, & Webb RC (1994). Effects of ramipril on contractile oscillations in arteries from genetically hypertensive rats. Clin Exp Hypertens 16**:** 881-898.

Webb AJ, Patel N, Loukogeorgakis S, Okorie M, Aboud Z, Misra S*, et al.* (2008). Acute blood pressure lowering, vasoprotective, and antiplatelet properties of dietary nitrate via bioconversion to nitrite. Hypertension 51**:** 784-790.

Weissberg PL, Little PJ, & Bobik A (1989). Spontaneous oscillations in cytoplasmic calcium concentration in vascular smooth muscle. Am J Physiol 256**:** C951-957.

Wever RM, van Dam T, van Rijn HJ, de Groot F, & Rabelink TJ (1997). Tetrahydrobiopterin regulates superoxide and nitric oxide generation by recombinant endothelial nitric oxide synthase. Biochem Biophys Res Commun 237**:** 340-344.

Wong PS, Hyun J, Fukuto JM, Shirota FN, DeMaster EG, Shoeman DW*, et al.* (1998). Reaction between S-nitrosothiols and thiols: generation of nitroxyl (HNO) and subsequent chemistry. Biochemistry 37**:** 5362-5371.

Yeh HI, Rothery S, Dupont E, Coppen SR, & Severs NJ (1998). Individual gap junction plaques contain multiple connexins in arterial endothelium. Circ Res 83**:** 1248-1263.

Yuill KH, Yarova P, Kemp-Harper BK, Garland CJ, & Dora KA (2011). A novel role for HNO in local and spreading vasodilatation in rat mesenteric resistance arteries. Antioxid Redox Signal 14**:** 1625-1635.

Zhao Y, Vanhoutte PM, & Leung SW (2015). Vascular nitric oxide: Beyond eNOS. J Pharmacol Sci 129**:** 83-94.

Zheng Z, Shimamura K, Anthony TL, Travagli RA, & Kreulen DL (1997). Nitric oxide is a sensory nerve neurotransmitter in the mesenteric artery of guinea pig. J Auton Nerv Syst 67**:** 137-144.

Zurborg S, Yurgionas B, Jira JA, Caspani O, & Heppenstall PA (2007). Direct activation of the ion channel TRPA1 by Ca2+. Nat Neurosci 10**:** 277-279.

Zygmunt PM, & Hogestatt ED (1996). Role of potassium channels in endothelium-dependent relaxation resistant to nitroarginine in the rat hepatic artery. Br J Pharmacol 117**:** 1600-1606.

Zygmunt PM, & Hogestatt ED (2014). Trpa1. Handb Exp Pharmacol 222**:** 583-630.